

Staphylococci of the Skin: Consequences for Host Health

by

Veda D. Khadka

B.A., Biology
Swarthmore College, 2016

Submitted to the Microbiology Graduate Program
in partial fulfillment of the requirements for the Degree of

Doctor of Philosophy

at the

MASSACHUSETTS INSTITUTE OF TECHNOLOGY

May 2024

© Veda D. Khadka, 2024. All rights reserved.

The author hereby grants MIT a nonexclusive, worldwide, irrevocable, royalty-free license to exercise any and all rights under copyright, including to reproduce, preserve, distribute, and publicly display copies of the thesis or release the thesis under an open-access license.

Signature of Author
Microbiology Graduate Program
May 16, 2024

Certified by
Tami Lieberman, Thesis Supervisor
Associate Professor, Civil Engineering

Accepted by
Jacquin C. Niles
Professor of Biological Engineering

Staphylococci of the Skin: Consequences for Host Health

by
Veda D. Khadka

Submitted to the Microbiology Graduate Program
on May 16, 2024, in Partial Fulfillment of the Requirements for the Degree of
Doctor of Philosophy

ABSTRACT

The skin is the body's largest barrier organ, and as such hosts roughly one million bacteria per square centimeter over its 1.8m^2 surface area. As a barrier organ, the skin not only provides a physical layer of defense against these microbes but an immunological one as well. Immune cells present in deeper layers of skin are in constant dialogue with the microbes present on the surface, and these interactions have far-reaching consequences for host health. Here, I interrogate the dynamics of the skin microbiome and consequences of host-microbe interactions when the skin barrier is damaged.

The skin as an external organ is subject to frequent stressors encountered in daily life, and can also be compromised due to genetic factors that weaken the barrier and predispose the host to inflammatory skin diseases. On healthy adults with an intact skin barrier, the skin microbiome is relatively diverse and stable. When the skin barrier is disrupted – either by daily stressors or genetic factors – the composition of the microbiome abruptly shifts to a less diverse state with an abundance of Staphylococci. Staphylococci have been shown to be important modulators of the host immune response and can improve host barrier repair from damage by wounding or parasitic infection during health. Much less is known about immune interactions with skin resident microbes like Staphylococci during barrier damage, however.

In this work, I investigate the skin microbiome dynamics underlying a common inflammatory skin disease, atopic dermatitis (AD). During flares of AD, the pathogen *Staphylococcus aureus* rises to dominate the skin microbiome, and I show that relative abundance of *S. aureus* decreases in patients who are treated with a combination of conventional therapies and dilute bleach baths. Next, I use an animal model to interrogate how the host responds to skin resident microbes when the skin barrier is damaged. Although the protective effect of skin resident microbes like *S. epidermidis* during health have made members of the skin microbiome attractive targets for development into probiotic therapies, I show that common skin microbes ubiquitously delay skin barrier repair.

Together, these works suggest a mechanism by which the skin microbiome can exacerbate disease during barrier damage, such as during AD, and describe the underlying dynamics of the skin microbiome during treatment for AD.

Thesis Supervisor: Tami Lieberman
Title: Associate Professor, Civil Engineering

Acknowledgments

Before I begin, I would like to acknowledge all the lives I took in the preparation of this thesis. Over 1,000 mice gave their lives so that I could complete this work and my degree. That debt is a heavy one to repay, but I would like to try by beginning this section with my mice in mind.

I have so many wonderful, kind, supportive and lovely people to thank for assisting in the creation of this work.

My advisor, Tami Lieberman, and my super-human collaborator, co-author, and mentor Laura Markey. Tami was brave enough to take a chance on my interest in host-microbe interactions in the skin microbiome, and always pushed me to be better, more rigorous, and more thoughtful in my experiments and analysis. My collaborator Laura, in addition to teaching me some of her mouse-wizardry, was also a voice of patience, reason, and support these past few years, and I would not have been able to produce this work without her invaluable contributions. I also must thank all the other members of the Lieberman lab who have contributed to scientific discussions of this work over the years.

I have to also thank the members of my Thesis Advisory Committee and Defense Advisory Committees: Alex Shalek, Michael Birnbaum, Eric Alm, Erin Chen, and Isaac Chiu, for their insights and useful critique of my work.

I have been incredibly fortunate to have had generous and thoughtful academic collaborators who have contributed to my research throughout graduate school: Isaac Chiu, and Kimbria Blake, Liwen Deng, and Samantha Choi in his lab; Maria Theresa Garcia-Romero; and Jeff Yu. I have also received considerable academic support from other sources: Brian Lagace and Magalie Boucher at DCM, who helped us with our mouse work, as well as Mike Waring, the Director of the Flow Cytometry Core at the Ragon Institute. Mike was an amazing resource as I learned the basics of flow cytometry – and was kind, patient, and understanding in the process.

I would not have even considered attending graduate school had it not been for the concerted efforts of some truly exceptional mentors, who all saw my interest in microbiology and invested their time and energy into shaping that interest into something more meaningful. Amy Vollmer at Swarthmore College opened my eyes to the amazing world of microbes – and changed my perception of Biology and the natural world in the process. Alan Wolfe at Loyola University set my standards for mentorship incredibly high as he has continued to take the time to mentor me through my career in academia even though I had only been a research intern in his lab for a single summer. Henry Cheng, Stephen Popper, and Fiona Strouts all invested their time into my development: teaching me to code (a heroic task), training me in DNA extractions, and providing invaluable lessons on collaboration. I have already mentioned Laura but I will do so again: for her lessons in diplomacy, mouse work, host-microbe interactions, and just being an overall amazing human being. There is no one else with whom I could have survived 14-hr days, cramped in a single biosafety hood in the sweltering mouse house, working elbow to elbow in the heat of that COVID summer.

My friends in Boston kept me sane through graduate school (mostly sane), and all the members of the Microbiome Club and the work we did together helped to remind me that hard work can and does pay off, and that you can indeed have fun in the process.

I owe perhaps some of my biggest thank-yous to my friends/ co-sufferers / muddy crew, my cohort. I still cannot believe we were lucky enough to all find one another in this cohort and life. I could perhaps write a whole separate thesis on how these amazing women stuck together to

support, uplift, and grit their way through these trying years. Thank you Annex (Annika) for always contributing the smartest, most rational take on whatever turmoil I was going through, for being a beacon of calm through our symposium planning, and for showing me how to take everything in stride. Thank you Irene, for always being there to listen, for your wonderful quips, for Johannes, and for showing me how to keep moving forward even when things seemed to be going off the rails. Thank you Jade for our many, many conversations as we both were learning to navigate our lives and futures, for your amazing burgers I dream of every summer, for throwing the best parties, for reminding me that it was possible to still love science through it all, and for showing me how to speak my mind and mean it. Finally, I have to thank Mandy. So, so many thank-yous for Mandy. Thank you Mandy, for being such a wonderful, true friend, for our free therapy sessions, for reminding me I was cared for when times got so dark, for the gatorade and books you brought me when I was ill, for introducing me to your amazing mom, for our walkos and the ship and Roy and giving me the joy of sush and spring rolls, for our spontaneous trips to Newbury, for indulging me in my delusions, and for showing me every day the power of persistence.

I began my graduate degree far away from my family, who live thousands of miles away. Incredibly, I found a new family in so many kind people: my friends so close they could be siblings, Adriana, Sarah, and Bill; the generous, loving Babinski family, who opened their doors to me almost every Thanksgiving I spent in the states and gave me a home when I needed one; Emilie and the Cameras, who have provided such levity and riotous fun when things were bleak; Mandy and her mom, who continually look out for me; and of course, my own Bassignana family, who ground my place in the world.

When I faltered in my ability to believe in myself – and I faltered often – there was often a single voice of reason. Alex, thank you. Thank you for seeing me as I needed to be seen. For believing in me, whether it was driving a dune buggy, riding a motorbike, writing my paper, or this thesis, or surviving through each day. Thank you for being my home, and giving me Enzo, who keeps our lives delightfully furry.

Most importantly, I have to thank my parents, but especially my mom. My father always taught me to have ambition, to work hard, and then harder, and to be proud of where I'm from. My mother, however, raised me, taught me to love science and to love learning, read poetry to me every night, and always worked tirelessly to help me achieve whatever I could. My mom has been my mentor, advisor, editor, travel companion, pun-buddy, fellow salami-lover, confidant – and she has been my Mom. This thesis, this degree, exists only because of her. This is for her.

Contents

List of Figures	9
1 Introduction	11
The skin and its microbiome	11
Etiologies of inflammatory skin diseases	12
Staphylococci in skin disease	14
Probiotic strategies for treating inflammatory skin diseases	14
References	17
2 The skin microbiome of patients with atopic dermatitis normalizes gradually during treatment	21
Abstract	22
Introduction	23
Materials and Methods	23
Patient enrollment	24
Study procedure	24
DNA extraction and sequencing	25
16S rRNA data processing and ASV classification using QIIME2	26
Statistical Analyses	26
Results	27
<i>S. aureus</i> dominates the microbiome on lesional sites and correlates with AD severity.	27
Treatment gradually shifts bacterial community composition in patients with AD towards that of healthy controls	27
Lower relative abundance of <i>S. aureus</i> in patients treated with DBB at the final visit	29
Discussion	31
Acknowledgements	32
References	34
Supplementary Tables	36
Supplementary Figures	36
3 Commensal skin bacteria exacerbate inflammation and delay skin barrier repair	41
Abstract	42
Introduction	43
Results	44
Perturbation of the skin microbiome affects recovery from barrier repair	44

Additional commensal skin bacteria do not improve skin healing following mechanical damage	45
Multiple isolates of <i>S. epidermidis</i> delay healing when applied during damage	46
Application of <i>S. epidermidis</i> after damage induces an inflammatory innate response	47
<i>S. epidermidis</i> prolongs expression of epithelial proliferation pathways	48
Discussion	51
Methods	52
Animals	52
Animal experiments study design	53
Statistical analysis	53
Tape-stripping Barrier Damage Model	53
Application of bacteria or vehicle control	54
Bacterial growth and preparation	54
Bacterial inactivation	54
Bacterial gene expression analysis	54
Bacterial enumeration from murine skin	55
Antibiotic treatment	55
Tissue dissociation and flow cytometry	55
DNA extraction and 16S sequencing	55
Microbiome analysis	56
RNA isolation and cDNA library synthesis	56
RNA sequencing and differential expression analysis	56
Histology / pathology	57
Immunoassay for skin cytokine protein quantification	57
Data and materials availability	58
Acknowledgements	58
References	59
Supplementary Figures	62
4 Conclusions and Future Perspectives	73
References	76
Appendix I: Conventional probiotics and pre-exposure to <i>S. epidermidis</i> do not improve healing outcomes	78
Abstract	80
A conventional gut probiotic does not significantly improve healing from barrier damage .	81
Topical or oral pre-exposure to <i>L. reuteri</i> does not improve barrier repair	81
<i>Staphylococcus epidermidis</i> delays barrier repair in a <i>Staphylococcus</i> -naive mouse model .	83
Methods	85
ASF mice	85
Bacterial cultures	85
Topical pre-exposure	85
Oral pre-exposure	85
References	88

List of Figures

Chapter 2. The skin microbiome of patients with atopic dermatitis normalizes gradually during treatment	20
Figure 1: Longitudinal unblinded study of standard treatment vs standard treatment + dilute bleach baths (DBB) in children with Atopic Dermatitis (AD)	25
Figure 2: Atopic Dermatitis (AD) sites are dominated by <i>Staphylococcus aureus</i>)	27
Figure 3: Treatment gradually shifts microbiomes of children with AD towards healthy-like microbiota	29
Figure 4: <i>S. aureus</i> abundance but not SCORAD is lower in patients after DBB treatment	29
Table 1: Demographic and clinical characteristics of healthy controls and patients included in the study	32
Supplementary Figures	36
Supplementary Figure 1: Flowchart of patient enrollment and clinical data analysis . . .	36
Supplementary Figure 2: Differences in composition and diversity between treatment groups	37
Supplementary Figure 3: Health-like staphylococci are inversely correlated with disease severity	38
Supplementary Figure 4: Community composition underlying <i>S. aureus</i> dominance is similarly diverse in patients and controls	39
Chapter 3. Commensal skin bacteria exacerbate inflammation and delay skin barrier repair	40
Figure 1: Perturbation of the native skin microbiome by depletion or supplementation delays healing	45
Figure 2: Human skin commensals including <i>S. epidermidis</i> delay barrier repair	47
Figure 3: Application of <i>S. epidermidis</i> following barrier damage induces an innate inflammatory immune response	48
Figure 4: <i>S. epidermidis</i> application after barrier damage increases and prolongs expression of epithelial cell proliferation pathways	48
Supplementary Figures	62
Supplementary Figure 1: <i>S. epidermidis</i> induced inflammation and delayed barrier repair at multiple timepoints	62
Supplementary Figure 2: Oral antibiotic treatment depleted the skin microbiome with minimal impact on gut microbiome	73

Supplementary Figure 3: Multiple strains of <i>S. epidermidis</i> colonize tape-stripped skin, express ecpA and delay healing	73
Supplementary Figure 4: Mice exposed to <i>S. aureus</i> after tape-stripping do not heal 4 days post-damage	73
Supplementary figure 5: Application of <i>S. epidermidis</i> to intact skin had no effect on skin barrier function or subsequent response to tape-stripping damage	73
Supplementary Figure 6: <i>S. epidermidis</i> applied after damage induces T cell response . .	73
Supplementary Figure 7: <i>S. epidermidis</i> increased IL-17A protein and broadly upregulated innate immune response in the skin	73
Supplementary Figure 8: Flow cytometry gating strategy for innate immune cell populations in skin	73

Appendix I: Conventional probiotics and pre-exposure to *S. epidermidis* do not improve healing outcomes **78**

Figure 1: Exposure to conventional probiotic <i>L. reuteri</i> during barrier abrasion does not improve skin healing	81
Figure 2: Pre-exposure to conventional probiotic <i>L. reuteri</i> does improve healing	83
Figure 3: Pre-exposure to <i>S. epidermidis</i> does not improve healing in a Staphylococcus-naive mouse model	85

1. Introduction

The skin supports an abundance of microbes across its surface. On healthy adults with an intact skin barrier, the skin microbiome is partitioned by ecological niche (moist, dry, sebaceous) and remains relatively diverse and stable. Though composition varies by niche, Staphylococci, Corynebacteria, and Cutibacteria represent the dominant genera present on the skin. However, the skin is prone to damage, either through frequent stressors encountered in daily life such as abrasions, UV damage, scrapes and scratches, or inflammatory diseases. When the skin is damaged, Staphylococci dominate the skin microbiome, and the development of probiotics to curtail this loss in diversity is an active area of research.

The skin and its microbiome

The skin, the body's largest organ, is the host's first line of defense against external threats. In addition to being a formidable physical barrier, the skin is a hostile environment that is desiccated, acidic, saline, and hostile to most microbes that may land on its surface [1]. Like other barrier sites in the body, the skin also serves as a zone of engagement between these microbes and the host immune cells that reside in the deeper layers of skin. The outcome of this host-microbe crosstalk is influenced by the integrity of the skin, and can have long-term consequences for host health.

Intact skin consists of three layers: the epidermis, the dermis, and the hypodermis. The outermost layer of the epidermis, the stratum corneum, is a layer of dead, cornified skin cells (keratinocytes). Underneath, the epidermis and dermis are layers of active growth consisting predominantly of keratinocytes. The dermis houses neurons, blood vessels, and immune cells. Blood and lymphatic vessels are housed in the deepest layer of skin, the dermis [2], and they play an important role in the body's inflammatory response by circulating adaptive and immune cells capable of responding to microbial threats [3]. The dermis also contains its own residential immune cells, and often in association with a hair follicle and associated sweat or sebaceous gland. These immune cells consist of both innate (Langerhans cells) and adaptive immune cells (T-cells) and are thought to be important regulators of homeostasis in the skin [4].

Immune cells that reside in the dermis are capable of responding both to microbes that survive or reside on the skin surface, and to any microbes that invade the deeper layers of skin. Recent studies have shown that microbes on the skin surface are capable of penetrating the skin, down to deeper layers of the dermis, and may survive there [5]. Additional work has shown that hair follicles associated with sebaceous glands (pilosebaceous follicles, or pores on the face) are often colonized by a single bacteria capable of growth on secreted fatty acids as a carbon source [6, 7].

The microbes that exist on the surface of the skin vary in composition across the different ecologic niches of the skin, which can be categorized as: moist, dry, and sebaceous (oily). Sebaceous sites such as the face and back are colonized by lipophilic Cutibacterium species (largely *Cutibacterium acnes*),

while moist sites such as toe webs and inguinal creases (groin) are dominated by Staphylococci and Corynebacteria. As such, the four most dominant phyla are Actinobacteria, Firmicutes, Proteobacteria and Bacteroidetes [8]. The skin also supports a rich diversity of fungi, parasites, and viruses, though their impact on host immunity has not been as well characterized. Bacteria are also thought to exist at high densities on the skin: sebaceous sites host large numbers of bacteria that live in close conjunction with pilosebaceous follicles [9], and amplicon sequencing data suggests that the skin overall supports an estimated 1 million bacteria per cm^2 [10], though recent work has shown that most bacteria detected by sequencing on non-sebaceous skin sites may not be viable [11]. Regardless, the skin microbiome of distinct skin sites in adults is stable at the species level (and for some species, at the strain level) [12], which suggests that the host immune system often encounters the same key players over time.

Of particular interest are Staphylococcal species on the skin, which have emerged as a focus of study in understanding host-microbe interactions on the skin. Coagulase-negative species, such as *Staphylococcus epidermidis*, *Staphylococcus hominis* and *Staphylococcus lugdunensis* have gained notoriety as model commensal species, thought to colonize the skin while providing an overall benefit to the host – be it through displacing pathogens by colonization resistance [13], disarming pathogens by microbial warfare [14–17], or boosting host immune responses to invading pathogens [18]. Conversely, *Staphylococcus aureus* has long been studied as a model pathogen on the skin, capable of causing life-threatening skin and soft tissue infections and exploiting weaknesses in the skin barrier to cause localized infections [19].

When the skin barrier is intact, the model commensal *S. epidermidis* can boost host immunity by engaging specific arms of the adaptive immune response. Additionally, the intact skin barrier serves its protective purpose: the model pathogen *S. aureus* is incapable of causing disease [20, 21] on skin that is not damaged. However, as an external barrier tissue, the skin is subject to near-constant levels of superficial damage, either via UV exposure, mechanical abrasion (scratching, etc.). These breaches in the barrier leave the host vulnerable to attack by pathogens like *S. aureus*, making model commensals like *S. epidermidis* an attractive candidate for probiotic therapies.

However, it is unclear what the consequences of colonization with commensal bacteria are when the skin barrier is damaged, such as during disease or superficial abrasion. This work presents an exploration of colonization dynamics when the skin barrier is weakened through inflammatory skin disease, and the role of commensal microbes in influencing host response when the skin barrier is subjected to mechanical damage.

Etiologies of inflammatory skin diseases

Inflammatory skin diseases, such as atopic dermatitis (AD), psoriasis, hidradentitis supparativa, and acne present quite different clinically, but have in common a complex etiology arising from host genetic and immune factors, environmental factors, and culminating in a weakened skin barrier that supports an aberrant skin microbiome. Although there is a well-established correlation between the overgrowth of pathogens (such as *S. aureus*) and a weakened skin barrier [22], the precise underlying causative role of one over the other in causing disease is not understood. This link has been perhaps best studied in AD (eczema), due to its fairly high prevalence in children (20%, [23]).

Most commonly developed during childhood, AD presents as a recurring flare of itchy, blistering, inflamed, red lesions that occur on the face, hands, antecubital and popliteal fossa. These flares can occur periodically (although in severe cases flares do not resolve) and subside with age.

Risk factors for AD include both heritable genetic factors as well as environmental factors (urban environments, and dry climates with little UV exposure), though the latter are still poorly supported by data. One of the best studied genetic risk factors for AD is a mutation in the FLG gene, which results in a decrease in the expression of filaggrin in the skin [24]. Filaggrin is an important protein in the formation of the cornified cell envelope of keratinocytes in the epidermis, and defects in this gene have been experimentally shown to result in a weakened skin barrier [25, 26], though the mechanisms by which this occurs are not yet understood. Surprisingly, despite the extensive work done on Filaggrin mutations in AD, only 20% of AD patients harbor FLG mutations [27], and the majority of individuals with mutations do not develop AD [23]. The inability of heritable filaggrin mutations to explain the development of AD makes it a compelling disease to study in the context of the microbiome. Interestingly, patients with AD often present with allergic comorbidities such as food allergies, asthma and allergic rhinitis, suggesting an altered immune state. Additionally, AD tends to recur in elderly patients, affecting 1-3% of elderly populations [28], with some reports claiming that these cases have been found to be gradually increasing [29]. Aging populations experience immunosenescence in the skin (in addition to other body sites), and this deregulation of the body's immune response could play a crucial role in cutaneous impairment and resulting microbial inflammation that underlies AD [30]. Understanding how epidermal barrier dysfunction, dysregulated [23] immune responses, and the skin microbiome together can cause disease is an active area of research.

Studies attempting to elucidate the mechanistic underpinnings of AD have often resorted to animal models, which provide a more holistic measurement of disease over less invasive cell-culture methods. Animal models either attempt to elicit skin barrier damage through chemical or mechanical abrasion of the skin, or by inducing genetic defects in animals that mimic the loss of skin barrier integrity in patients with AD. While it is beyond the scope of this work to list all possible animal models (for a review, see Jin et al. 2009, [31]), it is worth noting that there is a large variety in animal model, skin type, and genetic strain of animal used. Although mice are commonly used, porcine skin has been found to be much more similar to human skin and is emerging as a model of interest. A common issue with murine skin is the presence of a dense fur coat, which must either be removed (which limits the duration of the experimental process), or genetically engineered to be removed. Hairless mice often present with a multitude of immune deficiencies [32], and so ear skin is used as a proxy in mice with fur, although it is quite different in its composition than dorsal skin [33]. Comparisons across studies are therefore quite difficult to do given the immunological and skin composition differences across different strains of mice (for a discussion of cytokine profile differences between commonly used strains of mice, see Trunova et al. 2011 [34]), different models of barrier damage, and different animals altogether, and researchers must be wary of drawing conclusions around AD skin from a single model.

The altered skin microbiome of patients with AD has become a focus in recent years. In particular, the skin of patients with AD often displays lower species richness (alpha-diversity) and an increase in the abundance of the skin pathogen *S. aureus*. In AD patients, the prevalence of *S. aureus* on the skin varies from 30% - 100% [35], whereas in healthy individuals the prevalence is roughly 20% [23]. *S. aureus* is well-characterized as a pathogen capable of driving skin inflammation and further loss of integrity when the skin barrier is weakened, but whether it is responsible for driving the pathology of an AD flare or simply a well-positioned opportunist remains an open question. Despite this, given the association between *S. aureus* prevalence and worse clinical disease, therapies such as antibiotics and dilute bleach baths have been administered in conjunction with corticosteroids to

some success. In my second chapter, I investigate how the use of dilute bleach baths can curb the abundance of *S. aureus* on the skin and improve severity scores in children with AD.

Staphylococci in skin disease

A well-studied pathogen, *S. aureus* hosts an impressive array of virulence factors, such as adhesion factors, proteases, toxins, mechanisms by which to evade the host immune system [36], and other factors that modulate the host environment to be more conducive to infection. Adhesion factors such as clumping factor B (ClfB) and fibronectin-binding proteins (FnBP) allow the bacteria to attach efficiently to AD skin specifically [37, 38]. Inflammation in response to *S. aureus* is driven by the damage of keratinocytes by α -toxin [39], mast cell degranulation by δ -toxin [40], and the secretion of pro-inflammatory phenol-soluble modulins [41]. In addition to inducing inflammation, *S. aureus* can disarm host defenses through the secretion of proteases staphopain and aureolysin [42, 43], which cleave the antimicrobial peptides that contribute to host skin immunity. Lastly, but not exhaustively, expression of the host polysaccharide capsule allows the bacterium to “cloak” its antigenic proteins in the cell wall and resist opsonization and phagocytic killing [44].

Treatments for inflammatory skin diseases with a microbial component like AD must thus be two-pronged: they must treat defects in the host skin barrier, and they must decrease the relative abundance of *S. aureus* on the skin. Conventional treatments deal largely with the former and include a combination of emollients (moisturizers), topical anti-inflammatory corticosteroids, and immunosuppressants/immune inhibitors. While infection with *S. aureus* could be treated through the use of antibiotics, studies have shown that the antibiotics offer no benefit over conventional treatments [45]. These data, in addition to concerns over growing antibiotic resistance, make antibiotics a weak choice. Alternative treatments, such as the use of dilute bleach baths in conjunction with conventional treatment, remain in use in the USA and other countries [36], and are supported by a growing number of studies. There is, however, a clear lack of therapies that effectively target *S. aureus* without off-target effects on the skin microbiome, and as such the development of such therapies represents a hotbed of research.

Although *S. aureus* represents an attractive pathogen target for treating AD, other staphylococcal species have also been found to be enriched in lesional skin. While the pathogen *Staphylococcus argenteus* has been found on AD skin, the model commensal *S. epidermidis* has also been linked to flares in AD [46], as have the other coagulase-negative staphylococcal species (CoNS) *Staphylococcus capitis*, *Staphylococcus hominis*, and *Staphylococcus lugdunensis* [47]. These findings were somewhat surprising, as CoNS on the skin had been studied in a therapeutic capacity for their ability to deter *S. aureus* growth, either through colonisation resistance (*S. epidermidis*) or more sophisticated means: the CoNS *S. lugdunensis* and *S. hominis* have been studied for their ability to produce an antibiotic that inhibits the growth of *S. aureus* (lugdumin) and their ability to interfere with *S. aureus* virulence gene regulatory networks respectively. Despite their correlation with AD on the skin, the success of these organisms’ ability to inhibit *S. aureus* has led to an interest in the development of live microbial topical therapeutics (probiotics) for inflammatory skin diseases.

Probiotic strategies for treating inflammatory skin diseases

There has long been an interest in the development of orally delivered probiotics to improve inflammatory skin diseases [48, 49]. Much of this interest has centered around the genus *Lactobacillus*,

a naturally occurring rod-shaped gram-positive organism that is commonly found in fermented products. The positive association of host health and lactobacilli in the gut dates back to 1905, when Elie Metchnikoff published his theory of longevity in a Bulgarian population and their consumption of certain lactobacilli in yogurt [50]. By 1922, the first human study on the use of *Lactobacillus acidophilus* to improve eczema had been performed [51]. In the 2000s there was an exponential rise in the number of clinical trials for probiotic use for a variety of ailments [52] including AD: either through regulation of the host immune system, improvement of host barrier integrity, or the production of antimicrobials [53]. However, these studies (both in human and animal subjects) resulted in no clear benefit of colonization of the host with lactobacilli [54], and the development of oral probiotics for AD remains an active, if somewhat dubious, area of research today.

Notably, recent work utilizing oral probiotics to prevent disease via pathogen decolonisation appears to hold some promise. The most frequent source of infection with *S. aureus* is self-infection as a result of asymptomatic colonization [55] in the nares, which act as a major reservoir of *S. aureus* in the body [56]. Other work, however, has shown that *S. aureus* can persist in the intestine at a colonization frequency of roughly 20% [57], which can act as a reservoir for outbreaks of infection [58]. Recently, it was found that *Bacillus* species in the gut are capable of producing lipopeptides which are able to inhibit gene regulatory networks in *S. aureus*, and that *B. subtilis* spores were able to completely abrogate the *S. aureus* intestinal colonization in a murine model [59].

More recently, the development of topical probiotics for AD therapy has gained traction. The rationale that the skin's own native commensals are (1) capable of ousting pathogenic bacteria through an array of defense mechanisms, (2) beneficial to the host in other ways (improvement of barrier integrity, etc.) and (3) the natural colonizers of a healthy host, make them a very attractive target for development into therapies.

To this end, Nakatsuji et al. put forward the idea that commensal CoNS species such as *S. epidermidis* and *S. hominis* could produce antimicrobial peptides that selectively killed *S. aureus*, and could decrease *S. aureus* burden on patients with AD [14]. In particular, they found that a commensal strain of *S. hominis* interfered with *S. aureus* quorum sensing to downregulate key virulence factors contributing to skin barrier disease [15]. However, when this strain of *S. hominis* was applied to patients in a Phase I clinical trial, *S. aureus* abundance was significantly decreased but disease severity was not reduced [60]. These data suggest that replacement of *S. aureus* on the skin via commensal "probiotics" may not be efficacious enough to warrant their use.

Many other studies have focused on the protective benefits of *S. epidermidis*, studying its early education of the host immune system to develop tolerance and importance as a microbiome constituent in wound healing and parasitic infections. As a topical probiotic in AD, Zheng et al. found that application of *S. epidermidis* in a mouse model of damaged skin improved barrier integrity by promoting the host production of ceramides [61]. Other studies have shown that the monocolonization of germ-free mice with *S. epidermidis* improved healing from leishmaniasis and candidiasis via the promotion of IL-17A producing CD8+ T-cells [18, 62]. This elicitation of the adaptive immune response (specifically, CD8+ T-cells) by *S. epidermidis*, has also been shown to improve wound healing in mice with a complete microbiome (not germ-free) [63], suggesting the use of *S. epidermidis* as a topical probiotic when the skin barrier is damaged.

However, other studies have shown that *S. epidermidis* may also increase the burden of *S. aureus* colonization [64] and thus host disease, and is associated with more severe disease in AD [65]. Skin-associated coagulase negative staphylococcal species like *S. epidermidis* have often been implicated in nosocomial infections of indwelling devices and heart valves [19], making them potentially

unattractive candidates for live topical therapeutics. *S. epidermidis* is capable of colonizing the damaged skin barrier as well, as evidenced by its presence in AD [46], dandruff [66, 67], rosacea [68, 69] and seborrhoeic dermatitis [70, 71]. Like its cousin *S. aureus*, *S. epidermidis* genomes encode virulence factors, adhesins, and proteases [72] that all contribute to its dual lifestyle as commensal and pathogen [73].

It is thus unclear what role commensal staphylococci may play in the exacerbation or amelioration of inflammatory skin disease, and whether there is a viable route to their development as topical probiotics. In this work I present an analysis of the skin microbiome during conventional treatment for AD, as well as an experimental investigation into the development of skin commensal bacteria as probiotics during skin barrier breach.

References

1. Grice, E. A. & Segre, J. A. The Skin Microbiome. en. *Nature Reviews. Microbiology* **9**, 244–53 (2011).
2. Yousef, H., Alhajj, M. & Sharma, S. et. in *StatPearls. Treasure Island* (StatPearls Publishing, FL, 2022).
3. Zraggen, S., Ochsenbein, A. M. & Detmar, M. An Important Role of Blood and Lymphatic Vessels in Inflammation and Allergy. en. *Journal of Allergy*. January): 672381. (2013).
4. Belkaid, Y. & Tamoutounour, S. The Influence of Skin Microorganisms on Cutaneous Immunity. en. *Nature Reviews. Immunology* **16**, 353–66 (2016).
5. Nakatsuji, T. et al. The Microbiome Extends to Subepidermal Compartments of Normal Skin. en. *Nature Communications* **4**, 1431 (2013).
6. Conwill, A. et al. Anatomy Promotes Neutral Coexistence of Strains in the Human Skin Microbiome. en. *Cell Host & Microbe* **30**, 171–82 7 (2022).
7. Zouboulis, C. C. Acne and Sebaceous Gland Function. en. *Clinics in Dermatology* **22**, 360–66 (2004).
8. Grice, E. A. et al. Topographical and Temporal Diversity of the Human Skin Microbiome. en. *Science* **324**, 1190–92 (2009).
9. Leyden, J. J., McGinley, K. J., Mills, O. H. & Kligman, A. M. Propionibacterium levels in patients with and without acne vulgaris. *Journal of Investigative Dermatology* **65**, 382–384 (1975).
10. Grice, E. A. et al. A Diversity Profile of the Human Skin Microbiota. en. *Genome Research* **18**, 1043–50 (2008).
11. Acosta, E. M. et al. *Bacterial DNA on the Skin Surface Overrepresents the Viable Skin Microbiome* en. eLife 12 (June). 2023. <https://doi.org/10.7554/eLife.87192>..
12. Oh, J., Byrd, A. L., Morgan Park, N. S. P., Kong, H. H. & Segre, J. A. Temporal Stability of the Human Skin Microbiome. en. *Cell* **165**, 854–66 (2016).
13. Wei, M. et al. *Harnessing Diversity and Antagonism within the Pig Skin Microbiota to Identify Novel Mediators of Colonization Resistance to Methicillin-Resistant* en. 2023.
14. Nakatsuji, T. et al. Antimicrobials from Human Skin Commensal Bacteria Protect against Staphylococcus Aureus and Are Deficient in Atopic Dermatitis. en. *Science Translational Medicine* **9**. <https://doi.org/10.1126/scitranslmed.aah4680>. (2017).
15. Williams, M. R. et al. Quorum Sensing between Bacterial Species on the Skin Protects against Epidermal Injury in Atopic Dermatitis. af. et al **5**. <https://doi.org/10.1126/scitranslmed.aat8329>. (2019).
16. Canovas, J. et al. Cross-Talk between Staphylococcus Aureus and Other Staphylococcal Species via the Agr Quorum Sensing System. en. *Frontiers in Microbiology* **7**, 223156 (2016).
17. Paharik, A. E. et al. Coagulase-Negative Staphylococcal Strain Prevents Staphylococcus Aureus Colonization and Skin Infection by Blocking Quorum Sensing. en. *Cell Host & Microbe* **22**, 746–56 5 (2017).
18. Naik, S. et al. Commensal-Dendritic-Cell Interaction Specifies a Unique Protective Skin Immune Signature. en. *Nature* **520**, 104–8 (2015).
19. Brown, M. M. & Horswill, A. R. Staphylococcus Epidermidis-Skin Friend or Foe? et. *PLoS Pathogens* **16**, 1009026 (2020).
20. Kazakova, S. V. et al. A Clone of Methicillin-Resistant Staphylococcus Aureus among Professional Football Players. en. *The New England Journal of Medicine* **352**, 468–75 (2005).
21. Singh, G., Marples, R. & Kligman, A. Experimental Staphylococcus Aureus Infections in Humans. en. *The Journal of Investigative Dermatology* **57**, 149–62 (1971).
22. Jinnestål, C. L., Belfrage, E., Bäck, O., Schmidtchen, A. & Sonesson, A. Skin Barrier Impairment Correlates with Cutaneous Staphylococcus Aureus Colonization and Sensitization to Skin-Associated Microbial Antigens in Adult Patients with Atopic Dermatitis. en. *International Journal of Dermatology* **53**, 27–33 (2014).
23. Weidinger, S., Beck, L. A., Bieber, T., Kabashima, K. & Irvine, A. D. Atopic Dermatitis. id. *Nature Reviews. Disease Primers* **4**, 1 (2018).
24. Irvine, A. D., McLean, W. & Leung, D. Y. Filaggrin Mutations Associated with Skin and Allergic Diseases. en. *The New England Journal of Medicine* **365**, 1315–27 (2011).
25. Mildner, M. et al. Knockdown of Filaggrin Impairs Diffusion Barrier Function and Increases UV Sensitivity in a Human Skin Model. en. *The Journal of Investigative Dermatology* **130**, 2286–94 (2010).

26. Gruber, R. *et al.* Filaggrin Genotype in Ichthyosis Vulgaris Predicts Abnormalities in Epidermal Structure and Function. en. *The American Journal of Pathology* **178**, 2252–63 (2011).
27. Baurecht, H. *et al.* Toward a Major Risk Factor for Atopic Eczema: Meta-Analysis of Filaggrin Polymorphism Data. en. *The Journal of Allergy and Clinical Immunology* **120**, 1406–12 (2007).
28. Takeuchi, S., Esaki, H. & Furue, M. Epidemiology of atopic dermatitis in Japan. en. *The Journal of dermatology* **41**, 200–204 (2014).
29. Bocheva, G., Slominski, R. & Slominski, A. Immunological aspects of skin aging in atopic dermatitis. en. *International journal of molecular sciences* **22**, 5729 (2021).
30. Martinis, M., Sirufo, M. & Ginaldi, L. Allergy and aging: an old/new emerging health issue. en. *Aging and disease* **8**, 162 (2017).
31. Jin, H., He, R., Oyoshi, M. & Geha, R. S. Animal models of atopic dermatitis. *Journal of Investigative Dermatology* **129**, 31–40 (2009).
32. Benavides, F., Oberyzyzn, T., VanBuskirk, A., Reeve, V. & Kusewitt, D. The hairless mouse in skin research. en. *Journal of dermatological science* **53**, 10–18 (2009).
33. Martins Cardoso, R., Absalah, S., Eck, M. & Bouwstra, J. Barrier lipid composition and response to plasma lipids: A direct comparison of mouse dorsal back and ear skin. en. *Experimental Dermatology* **29**, 548–555 (2020).
34. Trunova, G. *et al.* Morphofunctional characteristic of the immune system in BALB/c and C57BL/6 mice. en. *Bulletin of experimental biology and medicine* **151**, 99–102 (2011).
35. Tauber, M. *et al.* Staphylococcus Aureus Density on Lesional and Nonlesional Skin Is Strongly Associated with Disease Severity in Atopic Dermatitis. en. *The Journal of Allergy and Clinical Immunology* **137**, 1272–74 3 (2016).
36. Geoghegan, J. A., Irvine, A. D. & Foster, T. J. Staphylococcus Aureus and Atopic Dermatitis: A Complex and Evolving Relationship. en. *Trends in Microbiology* **26**, 484–97 (2018).
37. Fleury, O. M. *et al.* Clumping Factor B Promotes Adherence of Staphylococcus Aureus to Corneocytes in Atopic Dermatitis. en. *Infection and Immunity* **85**. <https://doi.org/10.1128/IAI.00994-16>. (2017).
38. Cho, S., Strickland, I., Boguniewicz, M. & Leung, D. Fibronectin and Fibrinogen Contribute to the Enhanced Binding of Staphylococcus Aureus to Atopic Skin. en. *The Journal of Allergy and Clinical Immunology* **108**, 269–74 (2001).
39. Brauweiler, A. M., Goleva, E. & Leung, D. Y. Th2 Cytokines Increase Staphylococcus Aureus Alpha Toxin-Induced Keratinocyte Death through the Signal Transducer and Activator of Transcription 6 (STAT6). en. *The Journal of Investigative Dermatology* **134**, 2114–21 (2014).
40. Nakamura, Y. *et al.* Staphylococcus δ -Toxin Induces Allergic Skin Disease by Activating Mast Cells. en. *Nature* **503**, 397–401 (2013).
41. Nakagawa, S. *et al.* Staphylococcus Aureus Virulent PSM α Peptides Induce Keratinocyte Alarmin Release to Orchestrate IL-17-Dependent Skin Inflammation. en. *Cell Host & Microbe* **22**, 667–77 5 (2017).
42. Sonesson, A. *et al.* Identification of Bacterial Biofilm and the Staphylococcus Aureus Derived Protease, Staphopain, on the Skin Surface of Patients with Atopic Dermatitis. en. *Scientific Reports* **7**, 8689 (2017).
43. Sieprawska-Lupa, M. *et al.* Degradation of Human Antimicrobial Peptide LL-37 by Staphylococcus Aureus-Derived Proteinases. en. *Antimicrobial Agents and Chemotherapy* **48**, 4673–79 (2004).
44. O’Riordan, K. & Lee, J. C. Staphylococcus Aureus Capsular Polysaccharides. en. *Clinical Microbiology Reviews* **17**, 218–34 (2004).
45. Francis, N. A. *et al.* Oral and Topical Antibiotics for Clinically Infected Eczema in Children: A Pragmatic Randomized Controlled Trial in Ambulatory Care. en. *Annals of Family Medicine* **15**, 124–30 (2017).
46. Byrd, A. L. *et al.* And Strain Diversity Underlying Pediatric Atopic Dermatitis. en. *Science Translational Medicine* **9**. <https://doi.org/10.1126/scitranslmed.aal4651>. (2017).
47. Edslev, S. M. *et al.* Staphylococcal Communities on Skin Are Associated with Atopic Dermatitis and Disease Severity. en. *Microorganisms* **9**. <https://doi.org/10.3390/microorganisms9020432>. (2021).
48. Kechagia, M. *et al.* Health Benefits of Probiotics: A Review. en. *ISRN Nutrition*. January): 481651. (2013).
49. Lunjani, N., Ahearn-Ford, S., Dube, F. S., Hlela, C. & O’Mahony, L. Mechanisms of Microbe-Immune System Dialogue within the Skin. en. *Genes and Immunity* **22**, 276–88 (2021).

50. Metchnikoff, I. I. *The Prolongation of Life: Optimistic Studies* zu (Springer Publishing Company, 2004).
51. Rettger, L. F. Bacillus Acidophilus and Its Therapeutic Application. en. *Archives of Internal Medicine* **29**, 357 (1922).
52. McFarland, L. V. From Yaks to Yogurt: The History, Development, and Current Use of Probiotics. en. *Clinical Infectious Diseases: An Official Publication of the Infectious Diseases Society of America* **60** **2**, 85–90 (2015).
53. Xie, A. *et al.* For the Treatment and Prevention of Atopic Dermatitis: Clinical and Experimental Evidence. en. *Frontiers in Cellular and Infection Microbiology* **13**, 1137275 (2023).
54. Rather, I. A., Bajpai, V. K., Kumar, S. & Lim, J. Probiotics and Atopic Dermatitis: An Overview. en. *Frontiers in Microbiology* **7** (2016).
55. Eiff, C., Becker, K., Machka, K., Stammer, H. & Peters, G. Nasal carriage as a source of Staphylococcus aureus bacteremia. en. *New England Journal of Medicine* **344**, 11–16 (2001).
56. Wertheim, H. F. The role of nasal carriage in Staphylococcus aureus infections. en. *The Lancet infectious diseases* **5**, 751–762 (2005).
57. Acton, D., Tempelmans Plat-Sinnige, M., Wamel, W., Groot, N. & Belkum, A. Intestinal carriage of Staphylococcus aureus: how does its frequency compare with that of nasal carriage and what is its clinical impact? en. *European journal of clinical microbiology & infectious diseases* **28**, 115–127 (2009).
58. Squier, C. *et al.* Staphylococcus aureus rectal carriage and its association with infections in patients in a surgical intensive care unit and a liver transplant unit. en. *Infection Control & Hospital Epidemiology* **23**, 495–501 (2002).
59. Piewngam, P. *et al.* Pathogen elimination by probiotic Bacillus via signalling interference. en. *Nature* **562**, 532–537 (2018).
60. Nakatsuji, T. *et al.* Development of a Human Skin Commensal Microbe for Bacteriotherapy of Atopic Dermatitis and Use in a Phase 1 Randomized Clinical Trial. en. *Nature Medicine* **27**, 700–709 (2021).
61. Zheng, Y. *et al.* Commensal Staphylococcus Epidermidis Contributes to Skin Barrier Homeostasis by Generating Protective Ceramides. en. *Cell Host & Microbe* **30**, 301–13 9 (2022).
62. Naik, S. *et al.* Compartmentalized Control of Skin Immunity by Resident Commensals. en. *Science* **337**, 1115–19 (2012).
63. Linehan, J. L. *et al.* Non-Classical Immunity Controls Microbiota Impact on Skin Immunity and Tissue Repair. en. *Cell* **172**, 784–96 18 (2018).
64. Burian, M., Bitschar, K., Dylus, B., Peschel, A. & Schitteck, B. The Protective Effect of Microbiota on S. Aureus Skin Colonization Depends on the Integrity of the Epithelial Barrier. en. *The Journal of Investigative Dermatology* **137**, 976–79 (2017).
65. Hon, K., Tsang, Y., Pong, N., Leung, T. & Ip, M. Exploring Staphylococcus Epidermidis in Atopic Eczema: Friend or Foe? en. *Clinical and Experimental Dermatology* **41**, 659–63 (2016).
66. Saxena, R. *et al.* Comparison of Healthy and Dandruff Scalp Microbiome Reveals the Role of Commensals in Scalp Health. en. *Frontiers in Cellular and Infection Microbiology* **8** (2018).
67. Xu, Z. *et al.* Dandruff Is Associated with the Conjoined Interactions between Host and Microorganisms. en. *Scientific Reports* **6**, 24877 (2016).
68. Woo, Y. R., Lee, S. H., Cho, S. H., Lee, J. D. & Kim, H. S. Characterization and Analysis of the Skin Microbiota in Rosacea: Impact of Systemic Antibiotics. en. *Journal of Clinical Medicine Research* **9**. <https://doi.org/10.3390/jcm9010185>. (2020).
69. Holmes, A. D. Potential Role of Microorganisms in the Pathogenesis of Rosacea. en. *Journal of the American Academy of Dermatology* **69**, 1025–32 (2013).
70. Sanders, M. G., Nijsten, T., Verlouw, J., Kraaij, R. & Pardo, L. M. Composition of Cutaneous Bacterial Microbiome in Seborrheic Dermatitis Patients: A Cross-Sectional Study. en. *PloS One* **16**, 0251136 (2021).
71. Tanaka, A. *et al.* Comprehensive Pyrosequencing Analysis of the Bacterial Microbiota of the Skin of Patients with Seborrheic Dermatitis. en. *Microbiology and Immunology* **60**, 521–26 (2016).
72. Cau, L. *et al.* Staphylococcus Epidermidis Protease EcpA Can Be a Deleterious Component of the Skin Microbiome in Atopic Dermatitis. en. *The Journal of Allergy and Clinical Immunology* **147**, 955–66 16 (2021).
73. Severn, M. M. & Horswill, A. R. Staphylococcus Epidermidis and Its Dual Lifestyle in Skin Health and Infection. en. *Nature Reviews. Microbiology* **21**, 97–111 (2023).

THIS PAGE INTENTIONALLY LEFT BLANK

2. The skin microbiome of patients with atopic dermatitis normalizes gradually during treatment

This work was published as Khadka, Veda D. & Key, Felix M., et al. "The skin microbiome of patients with atopic dermatitis normalizes gradually during treatment." *Frontiers in Cellular and Infection Microbiology* 11 (2021): 720674.

V. D. K. and F.M.K. contributed equally to this work.

Abstract

Background: Atopic dermatitis (AD) is characterized by an altered skin microbiome dominantly colonised by *S. aureus*. Standard treatment includes emollients, anti-inflammatory medications and antiseptics.

Objectives: To characterize changes in the skin microbiome during treatment for AD.

Methods: The skin microbiomes of children with moderate-to-severe AD and healthy children were investigated in a longitudinal prospective study. Patients with AD were randomized to receive either standard treatment with emollients and topical corticosteroids or standard treatment with the addition of dilute bleach baths (DBB) and sampled at four visits over a three-month period. At each visit, severity of AD was measured, swabs were taken from four body sites and the composition of the microbiome at those sites was assessed using 16S rRNA amplification.

Results: We included 14 healthy controls and 28 patients. We found high relative abundances of *S. aureus* in patients, which correlated with AD severity and reduced apparent alpha diversity. As disease severity improved with treatment, the abundance of *S. aureus* decreased, gradually becoming more similar to the microbiomes of healthy controls. After treatment, patients who received DBB had a significantly lower abundance of *S. aureus* than those who received only standard treatment.

Conclusions: There are clear differences in the skin microbiome of healthy controls and AD patients that diminish with treatment. After three months, the addition of DBB to standard treatment had significantly decreased the *S. aureus* burden, supporting its use as a therapeutic option. Further study in double-blinded trials is needed.

Introduction

Atopic dermatitis (AD) is the most common chronic inflammatory skin disease characterized by eczematous skin lesions and pruritus in specific body sites, affecting 10-30% children [1, 2]. Its complex and multifactorial etiology is driven by a combination of genetic, environmental, and immune factors that include epidermal abnormalities which lead to a defective stratum corneum; enhanced allergen penetration and immunoglobulin E (IgE) sensitization, hyperreactive immune responses; and an altered skin microbiota [2–6].

The relationship between an altered skin bacterial microbiome and AD is well recognized clinically. In recent years, new methods and techniques to study bacteria on and in skin have permitted investigation at the level of species and strains, allowing for more granular insight into the relationship between altered skin flora and disease.

Studies using traditional culturing, 16s rRNA gene sequencing, and shotgun metagenomics have demonstrated a significant increase in the absolute and relative abundance of the opportunistic pathogen *Staphylococcus aureus* during AD flares [7–10]. Studies using the latter two approaches have also shown a reduction in alpha diversity as assessed by standard microbiome alpha diversity metrics [7–9]. While diversity metrics are sensitive to blooms of bacteria (e.g. *S. aureus*) [11], there are reasons to think that a more diverse microbiota may play a role in mitigating AD severity. In particular, in vitro and in vivo experiments have shown that various species present on healthy skin, including the ubiquitous *Staphylococcus epidermidis*, can generate anti- *S. aureus* responses through microbe-microbe and microbe-host interactions, including modulation of host immune responses [12–14].

Targeting the skin bacterial community using antibiotic cocktails reduces the relative abundance of *S. aureus*, increases diversity, and improves eczematous lesions dramatically in mouse models [15]. In clinical studies, decreasing burden or colonisation of *S. aureus* using antimicrobial treatments has also been demonstrated to improve AD severity [15, 16]. However, sustained antibiotic use for AD management and prevention is not practical long-term, as it can result in undesirable effects on commensal skin bacteria, on the microbiota in the gut and other sites, and it can contribute to antibiotic resistance, an increasing public health problem [17]. For this reason, other anti-*S.aureus* therapeutic options are worth exploring, such as dilute bleach baths (DBB).

Standard treatment for AD includes the use of emollients to improve the skin barrier, varying combinations of topical or systemic corticosteroids, anti-inflammatory or immunosuppressive medications, antibiotics, and dilute sodium hypochlorite (house bleach) baths. The antibacterial properties of bleach are thought to be mediated by the generation of superoxide radicals by hypochlorous acid, which can cause oxidative injury and bacterial cell death [18]. DBB may offer a benefit to patients by other mechanisms of action as well [5, 6, 19, 20]. Several clinical studies have reported varying effects on disease severity, microbiome composition, and *S. aureus* abundance when standard AD treatment was supplemented with DBB, although these studies varied widely in their methodologies and assessment metrics [9, 19, 21–23].

Here, we used high-throughput sequencing to study the dynamics of the skin bacterial microbiome during the course of disease in pediatric AD patients with moderate-to-severe disease, to compare with healthy controls, and to better understand the effect of treatment with or without DBB.

Materials and Methods

Patient enrollment

This randomized non-blinded study was approved by the Institutional Review Board of the National Institute for Pediatrics, Mexico City (registration no. 042/2016) and Massachusetts Institute for Technology (MIT), Cambridge, and was conducted according to the Declaration of Helsinki principles. Patients with moderate to severe AD and age-matched healthy children who attended the Dermatology Clinic at the NIP were recruited. Children aged 5 to 18 years with the diagnosis of AD were included in this study if they had AD as defined by the modified Hanifin and Rajka criteria [24], had moderate or severe disease according to the SCORing Atopic Dermatitis (SCORAD) clinical tool score ≥ 25 , had not received topical or systemic antibiotics for the past month, and provided written consent to participate. Healthy controls were children aged 5 to 18 years without any systemic inflammatory or autoimmune diseases, who had not received topical or systemic antibiotics for the past month [7] and were not being currently treated with any systemic medication and provided written consent to participate. Exclusion criteria included later diagnosis of other inflammatory or autoimmune conditions, treatment with systemic immunomodulatory drugs or corticosteroids, and/or actual visit dates not within 30 days of the monthly planned visit schedule. Our sample size of a minimum of 12 subjects per group was determined due to convenience, comparability with the literature, and because this study was part of a more intensive effort of tracking *S. aureus* evolution on individual patients [25].

After providing written consent from parent(s) and assent by children older than 12 years of age, patients and healthy controls were enrolled between June 2017 and December 2018. Patients were sampled at four time-points (baseline during flare, and one, two, and three months later). Some deviation from this schedule occurred due to patients' schedules, as well the disruption caused by the earthquake in September 2017. Healthy controls were sampled once (Figure 1).

Study procedure

Disease severity in patients was measured using SCORAD. Patients were prescribed standard treatment with class II to VI topical corticosteroids (TCS) twice daily until improvement according to the location and severity of their AD, with or without DBB according to block randomization (ratio 1:1) using sequentially numbered envelopes previously generated by an independent individual and concealed to investigators who enrolled patients (MG-R and BC-C) and assigned to interventions (AM-G). Those randomized to the DBB condition were instructed to add 1 mL of 6% liquid house bleach per litre of bath water to achieve a concentration of 0.006%, and to soak twice weekly for 10-15 minutes. All patients were instructed to use mild soap for cleansing daily and to use bland emollients twice or thrice a day as part of the recommended skin routine for AD. Patients were instructed to avoid bathing for 24 hours prior to subsequent visits. Subjects were instructed not to take antibiotics during the study and were not instructed regarding probiotics.

Superficial samples were taken from four sites to represent the range of commonly affected and unaffected AD sites: right anterior forearm (as an unaffected non-lesional site), right antecubital and popliteal fossa (as commonly affected lesional AD sites) and an actively lesional AD site from patients (Figure 1). From subjects 1-4, bilateral samples were taken to understand variability, and

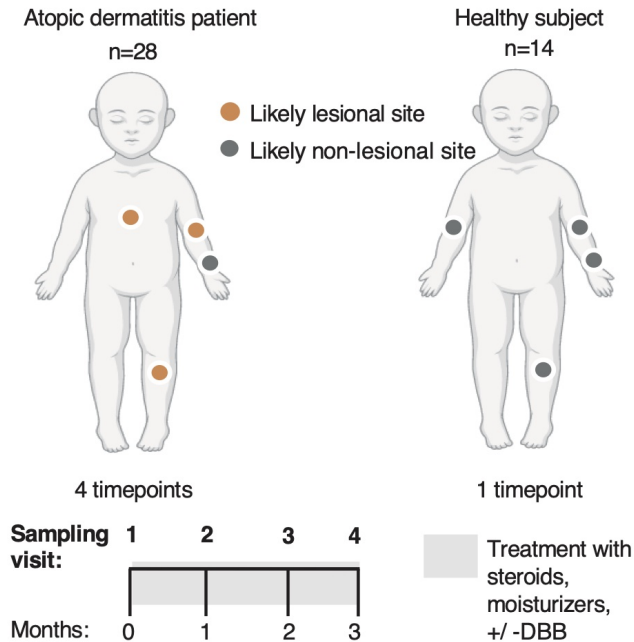


Figure 1: Longitudinal unblinded study of standard treatment vs standard treatment + dilute bleach baths (DBB) in children with Atopic Dermatitis (AD).

28 children with AD were sampled at four sites (right anterior forearm, right antecubital and popliteal fossa and another lesional site chosen to represent the area of worst active AD on that patient) across four visits, spanning three months. The forearm was determined to be a likely non-lesional site on AD patients. 14 healthy controls were also recruited and sampled similarly (both antecubital fossae, popliteal fossa and forearm) at a single visit. This figure was created with BioRender.com

replicate swabs were taken at each site. For each site, a new sterile applicator was moistened in sterile TES buffer (10mM Tris-HCl; 1mM EDTA; 100mM NaCl) and used to swab the skin at the specified site 40 times over a five cm² area, pressing firmly and twirling the swab to coat all surfaces. The applicator was then placed into a microtube with 0.5 mL of TES buffer and rotated against the side of the vial to release any biomaterial present. Immediately after sampling, samples were labeled and frozen at -20 °C until shipment and further processing.

At each subsequent visit SCORAD was measured, and samples were taken as above. If control of disease had been achieved, patients were instructed to continue using TCS twice weekly as proactive treatment in previously affected areas +/- DBB twice weekly as indicated. Granular information about each subject is included in Supplementary Table 1.

DNA extraction and sequencing

DNA was extracted in the collection buffer using ReadyLyse (Lucigen) at a final concentration of 1250 U/ul and incubated at room temperature for 12 hours. The V1-V3 region of the bacterial 16S rRNA gene was amplified for 36 cycles using 27F-plex (TCGTCGGCAGCGTCAGATGTGTATAAGAGACAGAGAGTTTGATCMTGGCTCAG) and 534R-plex (GTCTCGTGGGCTCGGAGATGTGTATAAGAGACAGATTACCGCGGCTGCTGG) the KAPA HiFi HotStart ReadyMix with an

annealing temperature of 54.5C. Two independent PCR replicates were performed and barcoded separately for each lysis product. Samples were cleaned using a bead-based approach beads [26] and a round of barcoding PCR was performed for 14 cycles using standard primers [27]. Samples were cleaned again and sequenced on an Illumina MiSeq with 300 paired-end sequencing to a median number of 16,007 reads (considering each replicate separately).

16S rRNA data processing and ASV classification using QIIME2

All data processed was done using QIIME2 (v2019.01) [28], including de-multiplexing and primer removal. Forward reads were filtered for a minimum base quality (default: $-p$ -min-quality 4) and truncated; and removed if the retained sequence was below $< 75\%$ (default) of the input sequence. Reverse reads were not used because the quality was too low to overlap read pairs. All sequences were denoised using the deblur algorithm [29] (trimmed to 209bp) to generate the feature (amplicon sequence variant (ASV)) table. ASVs with less than 10 representative reads were removed leading to 7,913 ASVs in total.

We built a custom classifier for ASVs based on a cleaned-up version of the SILVA database (version 132) [30]. We extracted target sequences from SILVA based on the primers used here and retained all sequences 100-700 bp. Erroneous taxonomic sequence labels in a 16S rRNA dataset can prevent species identification despite sufficient nucleotide information present in the amplified fragment of the 16S rRNA gene. Here, to ensure correct identification of species within the *Staphylococcus* genus, we removed: (i) 1 sequence with a non-species taxon assignment, (ii) 25 taxa that had ≤ 10 assigned sequences, or (iii) 12 taxa where $> 60\%$ of sequences were identical to another taxa. Critically, sequences with taxonomic misclassifications in the database were removed using the phylogeny-aware pipeline SATIVA [31]. SATIVA removed 69 sequences out of the 17,882 (0.39%) *Staphylococcus* sequences in the SILVA database. The filtered data was used to train the naive bayes classifier in QIIME2. The resulting ASVs were exported and taxa-level assignments used for further analysis.

Exported taxa from QIIME2 analyses were analyzed in R version 3.3.3. We identified potential contaminant sequences in these low biomass samples by looking for sequences that were specific to either sequencing replicate, as each replicate was run in an independent batch. We performed principal component analysis (PCA) to identify taxa that were segregated by batch: a high relative abundance of *Delftia* in one batch and *Pseudomonas* in another. These two genera are usually not associated with skin microbiome composition [32], and are known common contaminants [33]. We removed both taxa and an additional seven taxa that showed high covariance (> 0.34) with *Delftia* across all samples (*Serratia*, *Stenotrophomonas*, *Microbacterium*, *Ralstonia*, *Pelomonas*, *Microbacterium testaceum*, *Methylobacterium*). We also removed any *Cyanobacteria*. Samples were removed from downstream analysis if they had fewer than 500 reads after this filtering or if greater than 25% of reads matched the pool-based contaminants. We then merged samples across replicate pools if pools had a Bray-Curtis distance of less than 0.75 were merged; more divergent pools were deemed to be low quality and discarded (removed 17.13% of samples at this stage). Replicate swab samples from the more intensively sampled subjects were merged after this step. Critically, we did not evaluate outcomes when setting these quality thresholds to avoid p-value hacking.

Statistical Analyses

Subjects were included in the longitudinal analysis if their actual visit dates were within 30 days of the monthly planned visit schedule (timepoints excluded = 6). Data was analyzed using the intention-to-treat principle. Correlation analyses were performed using Spearman's correlation, comparisons between groups were done using the Wilcoxon Rank-Sum test and principal coordinate analysis (PCoA) was performed on Bray-Curtis dissimilarity using phyloseq [34], and vegan [35] packages. Code used for analyses is available on Github/vedomics. P-values ≤ 0.05 were considered significant.

All sequencing data is available here: <http://www.ncbi.nlm.nih.gov/bioproject/759575>

Results

We included 28 patients and 14 healthy controls (Supplementary Figure 1). Twenty-five patients (89%) completed four visits, though data from seven visits that did not fit the anticipated schedule were removed from longitudinal analyses. In total, 540 samples were analyzed. Demographic and clinical characteristics can be found in Table 1. Patients in both treatment groups had similar characteristics and baseline SCORAD values.

***S. aureus* dominates the microbiome on lesional sites and correlates with AD severity.**

Consistent with expectations from other AD cohorts, a striking pattern in the relative abundance of *S. aureus* at the baseline visit was observed: patients with AD had significantly higher relative abundances of this pathogen both in actively lesional (36.35%) and non-lesional sites (7.20%) compared to all sites on healthy controls (2.08%; $p < 0.001$). Accordingly, healthy controls had non-significantly higher abundances of the health-like flora *Staphylococcus capitis* ($p = 0.096$) and *Micrococcus sp.* ($p = 0.046$) than all sites on AD patients (Supplementary Table 2, Figure 2a).

The relative abundance of *S. aureus* on likely lesional sites was positively correlated with disease severity as measured by SCORAD ($\rho = 0.545$, $p < 0.001$) (Figure 2b). Shannon diversity, an ecological measure of diversity that is heavily influenced by evenness (relative proportion of species) [36], was inversely associated with SCORAD ($\rho = -0.556$, $p < 0.001$, Supplementary Figure 4b) and with the relative abundance of *S. aureus* ($\rho = -0.307$, $p < 0.01$) consistent with a model in which an increased abundance of *S. aureus* contributes to lower apparent alpha diversity (Figure 2c). In patients with a lower SCORAD, the relative abundance of *S. aureus* across lesional body sites was decreased and that of all other staphylococci showed a trend towards increase (Figure 2d). The summed relative abundance of all non-*S. aureus* staphylococcal species was not found to be significantly correlated with SCORAD, although the beneficial species *S. epidermidis* and *S. hominis* were inversely correlated with SCORAD ($p < 0.05$; Supplementary Figure 3).

Treatment gradually shifts bacterial community composition in patients with AD towards that of healthy controls

In order to better understand longitudinal trends, we analyzed the composition of all sites except the usually unaffected forearm. During the course of the study (from baseline to final visit), the relative abundance of *S. aureus* at these sites decreased significantly over time (31.83% to

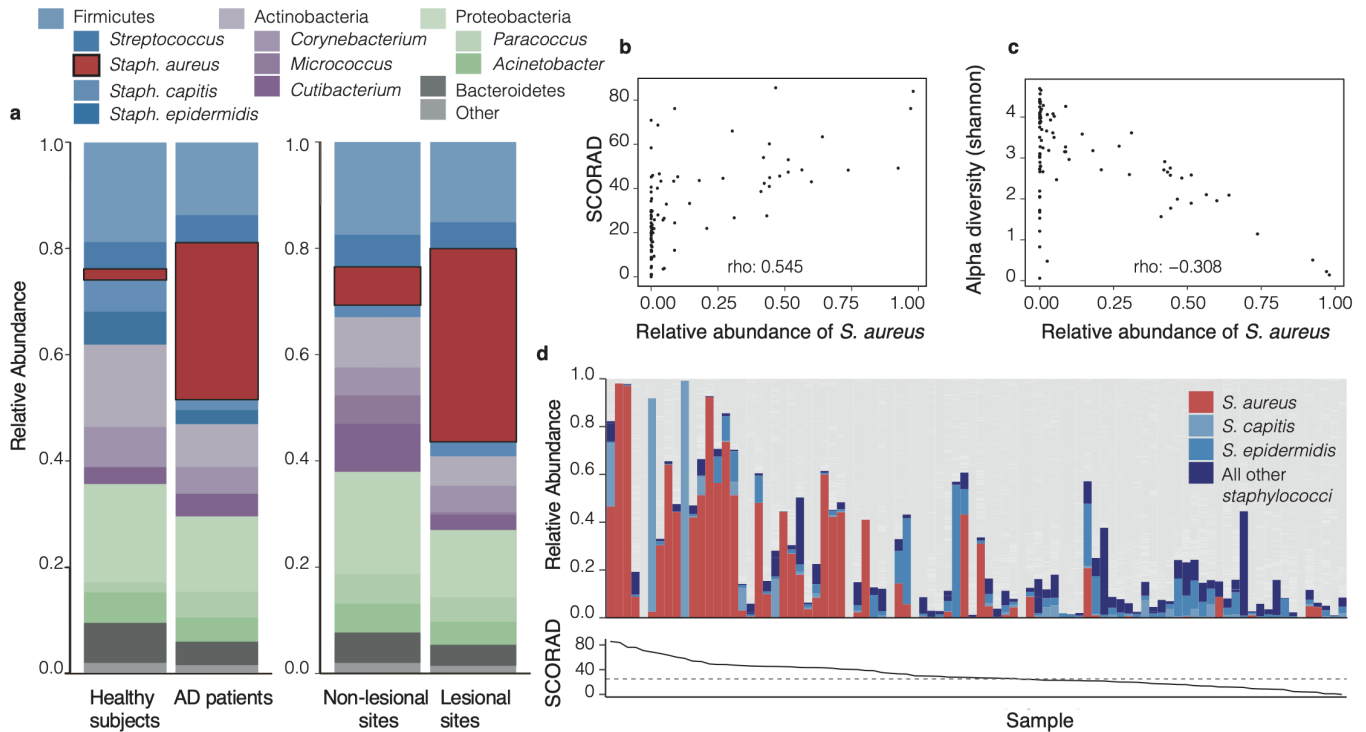


Figure 2: Atopic Dermatitis (AD) sites are dominated by *Staphylococcus aureus*.

(a) At baseline (visit 1), AD patients have a significantly higher relative abundance of *S. aureus* across all sites (29.56%) when compared to all sites on healthy controls (2.08%, $p=1.8 \times 10^{-6}$). Within AD patients, actively lesional sites had a significantly higher relative abundance of *S. aureus* (36.35%) than non-lesional sites (7.20%, $p=0.01$). (b-c) Each datapoint represents an average across all likely lesional and lesional sites from a subject at a given visit (excludes right forearm as a non-lesional site). (b) A higher relative abundance of *S. aureus* correlates with higher SCORAD in AD patients (Spearman's rho = 0.545, $p=2.7 \times 10^{-8}$). (c) *S. aureus* relative abundance inversely correlates with Shannon diversity (rho: -0.307, $p=0.003$). (d) The skin microbiome of patients with high SCORAD often have a correspondingly higher relative abundance of *S. aureus* and smaller amounts of beneficial Staphylococcus species, though this is not always the case. Top: the relative abundances of *S. aureus*, *S. capitis*, *S. epidermidis* and other staphylococci. Bottom: Corresponding SCORAD values for visits. A dashed line at SCORAD = 25 indicates the cutoff above which disease is considered moderate-severe.

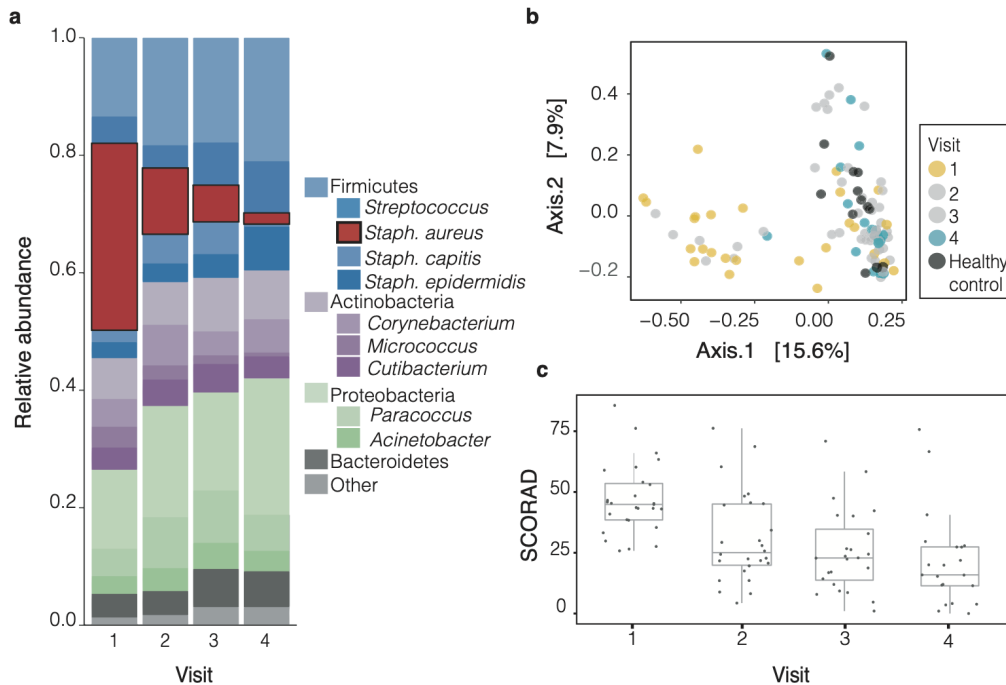


Figure 3: Treatment gradually shifts microbiomes of children with AD towards healthy-like microbiota.

(a) The relative abundance of *S. aureus* decreases significantly ($p=1.4 \times 10^{-5}$) with treatment from visit 1 (31.83%) to visit 4 (1.90%) across likely lesional sites on AD patients. The decrease in relative abundance of *S. aureus* is significant across treatment groups (+DBB, $p < 0.001$, -DBB, $p = 0.014$, Supplementary Figure 1). (b) By visit 4 (cyan), the composition of microbiota of likely lesional sites on AD patients is much more similar to healthy controls (dark grey) than at visit 1 (yellow), although there is variation in the severity of disease at both timepoints (PCoA on Bray-Curtis distance). (c) Severity of disease as measured by SCORAD decreases with treatment across visits.

1.90%, $p < 0.001$) while that of other species including *S. epidermidis* and members of the genus *Corynebacterium* increased, although none significantly (Table 3, Figure 3a). Principal coordinate analysis (PCoA) on Bray-Curtis distances demonstrates that the bacterial community of children with AD shifted toward that of healthy controls gradually over the course of treatment (Figure 3b). Severity of AD as measured by SCORAD decreased over subsequent visits for all subjects (Figure 3c).

Lower relative abundance of *S. aureus* in patients treated with DBB at the final visit

We found that patients treated with DBB in addition to standard treatment had significantly less *S. aureus* averaged across all likely lesional sites at visit 4 than the standard treatment group (0.05% vs 3.99%; $p = 0.01$) (Figure 4a), although both groups showed a decrease in *S. aureus* abundance over time (Supplementary Figure 2). In Figure 4b, we illustrate individual patient trajectories over time by treatment groups. We note that, at baseline, patients treated with DBB had lower, but not significantly lower, relative abundances of *S. aureus* at these sites ($p = 0.25$). The number of

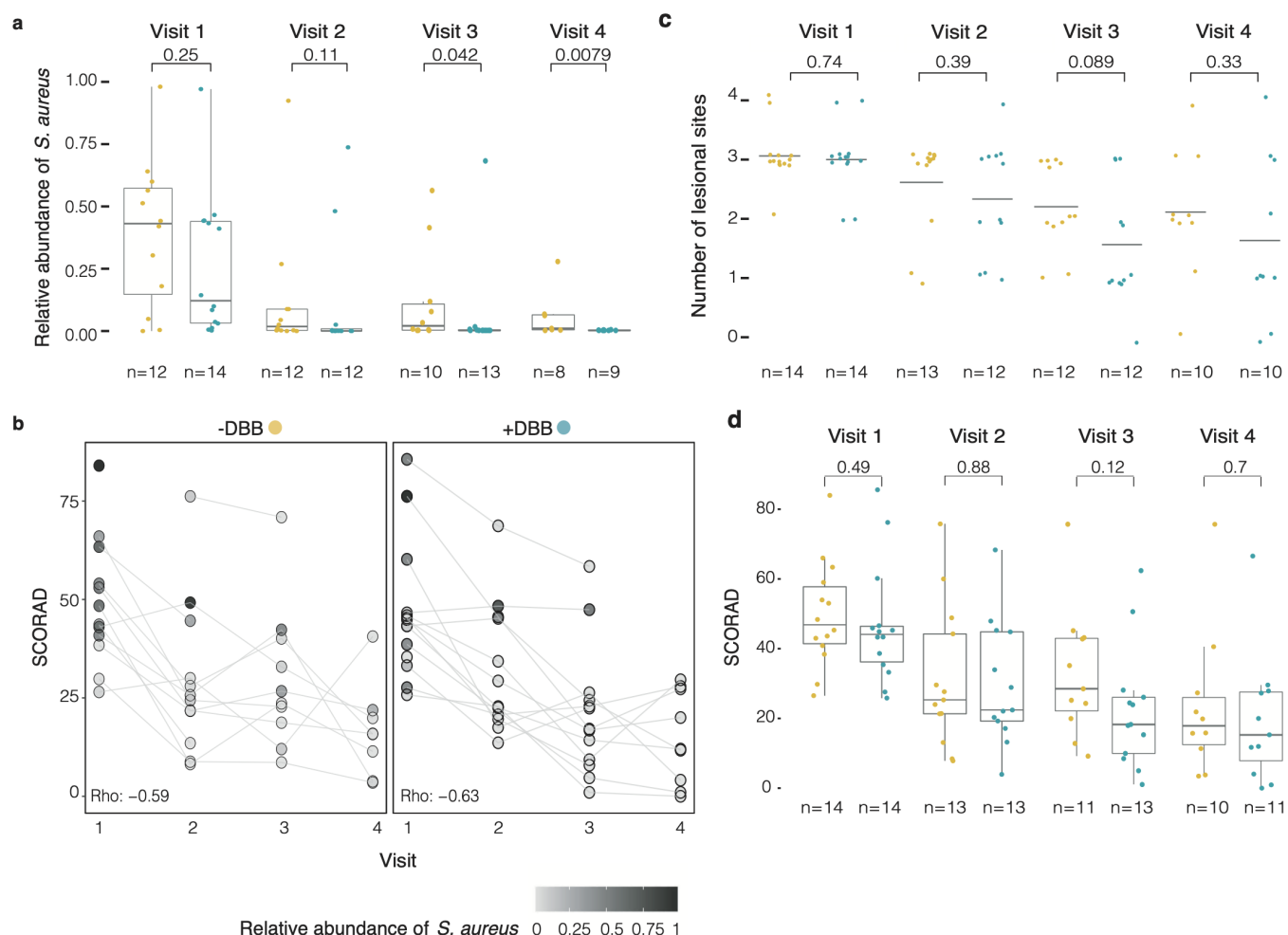


Figure 4: *S. aureus* abundance but not SCORAD is lower in patients after DBB treatment. (a) The relative abundance of *S. aureus* decreased a significantly larger amount for patients treated with standard treatment + DBB (cyan) than those receiving standard treatment alone (yellow) after 3 months from initial visit, visit 4 ($p=0.01$), even though both treatment groups had similar baseline visit relative abundances of *S. aureus* (+DBB 25.6%; -DBB 39.13%, $p=0.25$). (b) Individual patient trajectories (patients are represented by grey circles, lines indicate SCORAD trajectory and gradient indicates *S. aureus* relative abundance) highlight that patients treated with DBB had larger decreases in the relative abundance of *S. aureus* than the standard treatment group, despite having similar values for both SCORAD and *S. aureus* abundance at the initial visit. In both groups, SCORAD exhibited a decrease over time, as evaluated by a correlation of SCORAD and timepoint (+DBB Spearman's rho = -0.63, $p=1.6 \times 10^{-6}$; -DBB Spearman's rho = -0.59, $p=4 \times 10^{-5}$). (c) The number of actively lesional sites per patient decreases across both treatment groups over time. Both treatment groups display a similar number of actively lesional sites at baseline visit ($p=0.74$), and have similarly decreased numbers of lesional sites by visit 4, reflecting improvement in condition as indicated by SCORAD. (d) In both groups, treatment results in improved patient condition, as indicated by SCORAD. At baseline, both treatment groups present with similar SCORAD values (mean +DBB: 46.6; mean -DBB: 49.6; $p=0.49$), which decrease with treatment by visit 4 (mean +DBB: 19.5; mean -DBB: 23.6, $p=0.38$).

sites affected by AD (Figure 4c) and disease severity (Figure 4d) decreased over time similarly in both groups, and there was a trend towards lower SCORAD across visits in patients who received standard treatment plus DBB.

Discussion

To our knowledge, we have performed the most detailed longitudinal study of changes in the skin microbiome during AD treatment. We find that the skin microbiomes of children treated with DBB in addition to standard treatment have a significantly lower abundance of *S. aureus* after 3 months of treatment compared to the standard treatment group (Figure 4). Patients treated with DBB also had lower disease severity as measured by SCORAD, though this was not statistically significant. Adjuvant DBBs have been traditionally used to treat patients with AD and reduce disease severity. However, there are conflicting hypotheses regarding the effects and mechanisms of action of DBB on AD. The concentration most often used in AD treatment is 0.005% (0.002-0.016%), and *in vitro* studies have shown that DBB in concentrations as low as 0.005% are effective in reducing *S. aureus* abundance ([37, 38]. Other studies have suggested that bleach changes the expression of virulence factors in *S. aureus* [39] or that it provides a direct anti-inflammatory action [16, 19, 40]. Regardless of their mechanism of action, our findings support the idea that DBB may be beneficial in patients with AD, thus avoiding the harmful effects antibiotic therapy has of altering other body sites' microbiomes, perturbing the rest of the skin bacterial community (Supplementary Figure 2d), or increasing the risk of bacterial resistance. While other studies have also suggested a benefit of DBB in lowering *S. aureus*, our longitudinal study covered a longer, three-month period, allowing us to capture differences in *S. aureus* abundance and SCORAD across treatment groups at later visits.

Our baseline samples confirm previously noted differences between healthy individuals and patients with AD. In particular, we confirm that the skin of patients with AD is characterized by a higher relative abundance of *S. aureus* than healthy controls [7, 9, 32]. We also confirm that *S. aureus* is more abundant on lesional skin than non-lesional skin, and that a higher abundance of *S. aureus* is correlated with disease severity. In line with these results, previous work has shown that AD patients who are colonized with *S. aureus* have increased Type 2 immune responses and increased disease severity [41]. While this and other observational studies cannot disentangle causation from correlation, and a disrupted or inflamed skin barrier may facilitate colonization with pathogenic bacteria, *S. aureus* colonization has been shown to precede the detection of AD development and flares [7, 42]. Moreover, *S. aureus* is known to potentiate skin barrier defects and inflammation through toxins with superantigen properties, toll-like receptor ligands, proteases, surface proteins [15, 43, 44], and by stimulating the proliferation of T cells [45].

This study shows with unprecedented longitudinal resolution the recovery process of the skin microbiome during treatment for AD and bolsters findings from other studies [7, 9]. As expected, the relative abundance of *S. aureus* decreased gradually in both treatment groups. By the final visit, the relative abundance of *S. aureus* in AD lesional sites had decreased significantly compared to baseline, such that the bacterial microbiome of children with AD became more similar to that of healthy controls after two months of treatment.

We also confirmed previous findings of lower alpha diversity in AD patients relative to controls and an increase of alpha diversity following treatment citekong2012a, gonzalez2016a. However, we recommend caution in interpreting this metric, as much of the apparent reduction in alpha diversity in AD patients can be explained by blooms of *S. aureus* or other taxa (Supplementary Figure 4). By

its nature, 16S amplicon sequencing measures the fraction of sequencing reads that originate from a given species and not their absolute abundance in the sample. Therefore, all conventional alpha diversity metrics, including Shannon diversity, are confounded when a single species rises in absolute abundance [11, 32]. We illustrated this problem by removing *S. aureus* reads from our data and recalculating diversity metrics; this approach shows a diminished relationship between AD severity and diversity (Supplementary Figure 4). We note that even this analysis does not sufficiently assess community differences between samples, as the low number of sequencing reads that remain after removal of *S. aureus* creates imprecision in measurements of remaining taxa.

Our study had several limitations and potential biases. As a relatively small cohort size limited our power to detect differences in clinical outcomes between treatment groups. Emollient and corticosteroid use were not standardized, adding more variation in outcomes between subjects, and we did not characterize host genetics or host disease beyond the use of SCORAD. While subjects were randomized to treatment groups, investigators and patients were not blinded, as subjects self-administered treatment it is possible that those in the DBB group paid more attention to skin care overall. In addition, not every sample was included in our final analysis, due to removal of samples with low sequencing reads after quality control steps (Methods).

In conclusion, this longitudinal study confirmed the association between *S. aureus* and AD severity. We find higher *S. aureus* abundances in patients with AD relative to healthy controls, in lesional sites relative to non-lesional sites, and in patients with higher vs lower SCORAD. Moreover, the abundance of *S. aureus* decreases and the skin microbiomes of patients measurably shifts towards that of healthy controls as patients' disease severity improves with standard treatment. Crucially, we find that the addition of DBB to a standard treatment regimen resulted in significantly lower relative abundances of *S. aureus* and a non-significantly lowered disease severity, generally improving upon standard treatment.

These findings add support to the use of DBB to complement traditional AD therapy. Additional studies, particularly with larger sample sizes, are needed to fully establish the benefit of DBB in treating AD and modifying the skin microbiome.

Acknowledgements

We thank our patients who participated in this study, Adriana Canul-Sánchez and David León-Cortés for technical support, and the funding awarded to complete this project by the Mexican Foundation for Dermatology, the Mexican Government Ministry of Taxes Program E022 Health Research and Technological Development, MIT International Science and Technology Initiatives (MISTI) Global Seed Funds, and Deutsche Forschungsgemeinschaft (DFG) research fellowship (KE 2408/1-1 to F.M.K.).

Table 1. Demographic and clinical characteristics of healthy controls and patients included in the study.

	Healthy controls	Patients with AD			P
		All	Standard treatment	Standard treatment + DBB	
n	14	28*	14*	14*	
Female gender	5 (35.7%)	16 (57.1%)	7 (53.8%)	8 (66.6%)	0.64
Age in years, median (range)	10 (5-16)	11.5 (5-15)	12 (5-15)	11 (6-13)	0.14
Years since AD diagnosis, median (range)		3 (1-14)	3 (0-14)	2 (1-13)	
Baseline SCORAD, median (range)		45.10 (25.8-85.6)	46.85 (26.5-84)	44.1 (25.8-85.6)	0.47
Visit 2 SCORAD, median (range)		25.05 (4.3-76.2) <i>n=26</i>	25.7 (8.2-76.2) <i>n=13</i>	22.8 (4.3-68.7) <i>n=13</i>	0.85
Visit 3 SCORAD, median (range)		22.9 (1-70.9) <i>n=24</i>	26.70 (8.6-70.9) <i>n=11</i>	17.1 (1-58.4) <i>n=13</i>	0.12
Visit 4 SCORAD, median (range)		15.90 (0-75.7) <i>n=21</i>	17.9 (3.5-75.7) <i>n=10</i>	15.3 (0-66.6) <i>n=11</i>	0.7

*Number of patients at the beginning of the study; AD = atopic dermatitis; DBB = dilute bleach baths

References

1. Bylund, S., Kobyletzki, L., Svalstedt, M. & Svensson, A. Prevalence and Incidence of Atopic Dermatitis: A Systematic Review. en. *Acta Derm Venereol* **100** (2020).
2. Bieber, T. Atopic Dermatitis. en. *New England Journal of Medicine* **358**, 1483–94 (2008).
3. Eyerich, K., Eyerich, S. & Biedermann, T. The Multi-Modal Immune Pathogenesis of Atopic Eczema. sn. *Trends Immunol* **36**, 788–801 (2015).
4. Paller, A. *et al.* The microbiome in patients with atopic dermatitis. en. *J Allergy Clin Immunol* **143**, 26–35 (2019).
5. Leung, D. & Guttman-Yassky, E. Deciphering the complexities of atopic dermatitis: shifting paradigms in treatment approaches. en. *J Allergy Clin Immunol* **134**, 769–79 (2014).
6. Brussow, H. Turning the inside out: the microbiology of atopic dermatitis. en. *Environ Microbiol* **18**, 2089–102 (2016).
7. Kong, H. *et al.* Temporal shifts in the skin microbiome associated with disease flares and treatment in children with atopic dermatitis. en. *Genome Res* **22**, 850–9 (2012).
8. Bjerre, R., Bandier, J., Skov, L., Engstrand, L. & Johansen, J. The role of the skin microbiome in atopic dermatitis: a systematic review. en. *Br J Dermatol* **177**, 1272–8 (2017).
9. Gonzalez, M. *et al.* Cutaneous microbiome effects of fluticasone propionate cream and adjunctive bleach baths in childhood atopic dermatitis. en. *J Am Acad Dermatol* **75**, 481–93 (2016).
10. Totte, J. *et al.* Prevalence and odds of Staphylococcus aureus carriage in atopic dermatitis: a systematic review and meta-analysis. en. *Br J Dermatol* **175**, 687–95 (2016).
11. Gloor, G., Macklaim, J., Pawlowsky-Glahn, V. & Egozcue, J. Microbiome Datasets Are Compositional: And This Is Not Optional. en. *Front Microbiol* **8** (2017).
12. Park, B., Iwase, T. & Liu, G. Intranasal application of *S. epidermidis* prevents colonization by methicillin-resistant Staphylococcus aureus in mice. es. *PLoS One* **6** (2011).
13. Lai, Y. *et al.* Activation of TLR2 by a small molecule produced by Staphylococcus epidermidis increases antimicrobial defense against bacterial skin infections. en. *J Invest Dermatol* **130**, 2211–21 (2010).
14. Iwase, T. *et al.* Staphylococcus epidermidis Esp inhibits Staphylococcus aureus biofilm formation and nasal colonization. la. *Nature* **465**, 346–9 (2010).
15. Kobayashi, T. *et al.* Dysbiosis and Staphylococcus aureus Colonization Drives Inflammation in Atopic Dermatitis. en. *Immunity* **42**, 756–66 (2015).
16. Huang, J., Abrams, M., Tloughan, B., Rademaker, A. & Paller, A. Treatment of Staphylococcus aureus colonization in atopic dermatitis decreases disease severity. la. *Pediatrics* **123** (2009).
17. Harkins, C. *et al.* The widespread use of topical antimicrobials enriches for resistance in Staphylococcus aureus isolated from patients with atopic dermatitis. en. *Br J Dermatol* **179**, 951–8 (2018).
18. Barnes, T. & Greive, K. Use of bleach baths for the treatment of infected atopic eczema. en. *Australas J Dermatol* **54**, 251–8 (2013).
19. Wong, S., Ng, T. & Baba, R. Efficacy and safety of sodium hypochlorite (bleach) baths in patients with moderate to severe atopic dermatitis in Malaysia. en. *J Dermatol* **40**, 874–80 (2013).
20. Ryan, C., Shaw, R., Cockerell, C., Hand, S. & Ghali, F. Novel sodium hypochlorite cleanser shows clinical response and excellent acceptability in the treatment of atopic dermatitis. en. *Pediatr Dermatol* **30**, 308–15 (2013).
21. Chopra, R., Vakharia, P., Sacotte, R. & Silverberg, J. Efficacy of bleach baths in reducing severity of atopic dermatitis: A systematic review and meta-analysis. en. *Ann Allergy Asthma Immunol* **119**, 435–40 (2017).
22. Fritz, S., Camins, B. & Einsenstein, K. Effectiveness of measures to eradicate Staphylococcus aureus carriage in patients with community-associated skin and soft-tissue infections: a randomized trial. en. *Control Hosp Epidemiol* **32** (2011).
23. Metry, D., Browning, J. & Aea, R. Sodium hypochlorite (bleach) baths: a potential measure to reduce the incidence of recurrent, cutaneous Staphylococcus aureus superinfection among susceptible populations. en. *Society for Pediatric Dermatology annual meeting; Chicago* (2007).
24. Hanifin, J. & Rajka, G. Diagnostic features of atopic dermatitis. la. *Acta Dermatovener* **92**, 44–7 (1980).

25. Key, F. *et al.* On-person adaptive evolution of *Staphylococcus aureus* during atopic dermatitis increases disease severity. en. bioRxiv. 2021.
26. Rohland, N. & Reich, D. Cost-effective, high-throughput DNA sequencing libraries for multiplexed target capture. en. *Genome Res* **22**, 939–46 (2012).
27. Baym, M. *et al.* Inexpensive multiplexed library preparation for megabase-sized genomes. en. *PLoS One* **10** (2015).
28. Bolyen, E. *et al.* Reproducible, interactive, scalable and extensible microbiome data science using QIIME 2. en. *Nat Biotechnol* **37**, 852–7 (2019).
29. Amir, A. *et al.* Deblur Rapidly Resolves Single-Nucleotide Community Sequence Patterns. en. *mSystems* **2** (2017).
30. Quast, C. *et al.* The SILVA ribosomal RNA gene database project: improved data processing and web-based tools. en. *Nucleic Acids Res* **41** (2013).
31. Kozlov, A., Zhang, J., Yilmaz, P., Glockner, F. & Stamatakis, A. Phylogeny-aware identification and correction of taxonomically mislabeled sequences. en. *Nucleic Acids Res* **44**, 5022–33 (2016).
32. Byrd, A. L. *et al.* And Strain Diversity Underlying Pediatric Atopic Dermatitis. en. *Science Translational Medicine* **9**. <https://doi.org/10.1126/scitranslmed.aal4651>. (2017).
33. Salter, S. *et al.* Reagent and laboratory contamination can critically impact sequence-based microbiome analyses. en. *BMC Biology* **12** (2014).
34. McMurdie, P. Holmes S. phyloseq: an R package for reproducible interactive analysis and graphics of microbiome census data. en. *PLoS One* **8** (2013).
35. Oksanen, J. *et al.* vegan. en. *Community Ecology Package*. Available from: <https://cran.r-project.org> (2017).
36. Strong, W. Biased richness and evenness relationships within Shannon–Wiener index values. en. *Ecological Indicators* **67**, 703–13 (2016).
37. McKenna, P., Lehr, G. & Leist, P. Antiseptic effectiveness with fibroblast preservation. de. *Ann Plast Surg* **27**, 265–8 (1991).
38. Rutala, W., Cole, E. & Thomann, C. Stability and bactericidal activity of chlorine solutions. en. *Infect Control Hosp Epidemiol* **19**, 323–7 (1998).
39. Sawada, Y. *et al.* Dilute bleach baths used for treatment of atopic dermatitis are not antimicrobial in vitro. en. *J Allergy Clin Immunol* **143**, 1946–8 (2019).
40. Leung, T. *et al.* Topical hypochlorite ameliorates NF-kappaB-mediated skin diseases in mice. en. *J Clin Invest* **123**, 5361–70 (2013).
41. Simpson, E. *et al.* Patients with Atopic Dermatitis Colonized with *Staphylococcus aureus* Have a Distinct Phenotype and Endotype. en. *J Invest Dermatol* **138**, 2224–33 (2018).
42. Meylan, P. *et al.* Skin Colonization by *Staphylococcus aureus* Precedes the Clinical Diagnosis of Atopic Dermatitis in Infancy. en. *J Invest Dermatol* **137**, 2497–504 (2017).
43. Nakamura, Y. *et al.* *Staphylococcus* δ -Toxin Induces Allergic Skin Disease by Activating Mast Cells. en. *Nature* **503**, 397–401 (2013).
44. Cau, L. *et al.* *Staphylococcus epidermidis* protease EcpA can be a deleterious component of the skin microbiome in atopic dermatitis. en. *J Allergy Clin Immunol* (2020).
45. Iwamoto, K. *et al.* *Staphylococcus aureus* from atopic dermatitis skin alters cytokine production triggered by monocyte-derived Langerhans cell. en. *J Dermatol Sci* **88**, 271–9 (2017).

Supplementary Tables

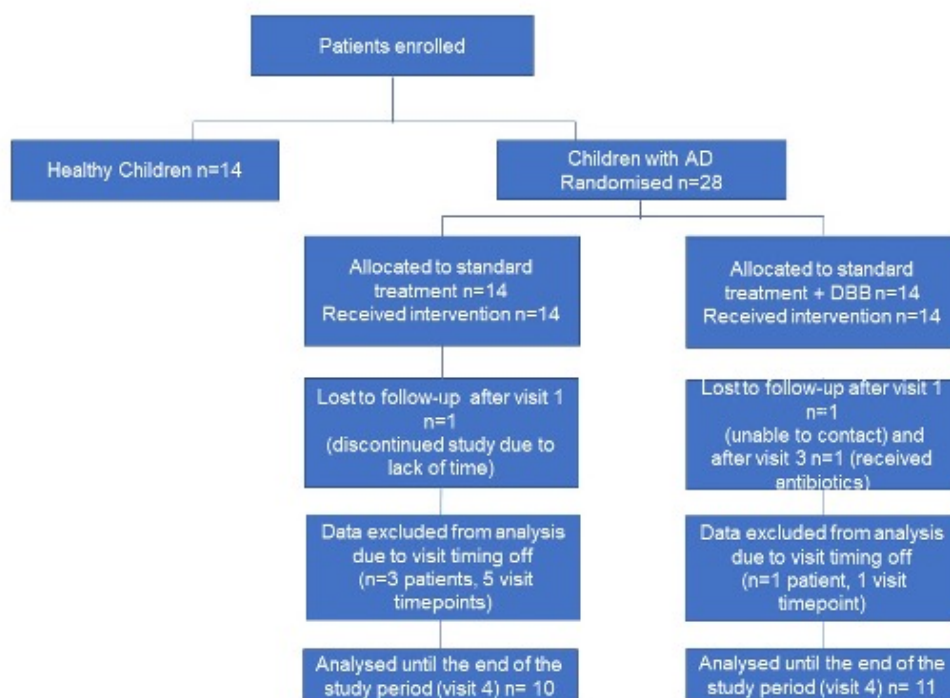
For complete supplemental tables, please visit <https://doi.org/10.3389/fcimb.2021.720674>

Supplementary Table 1: Patient overview, AD severity, and treatments.

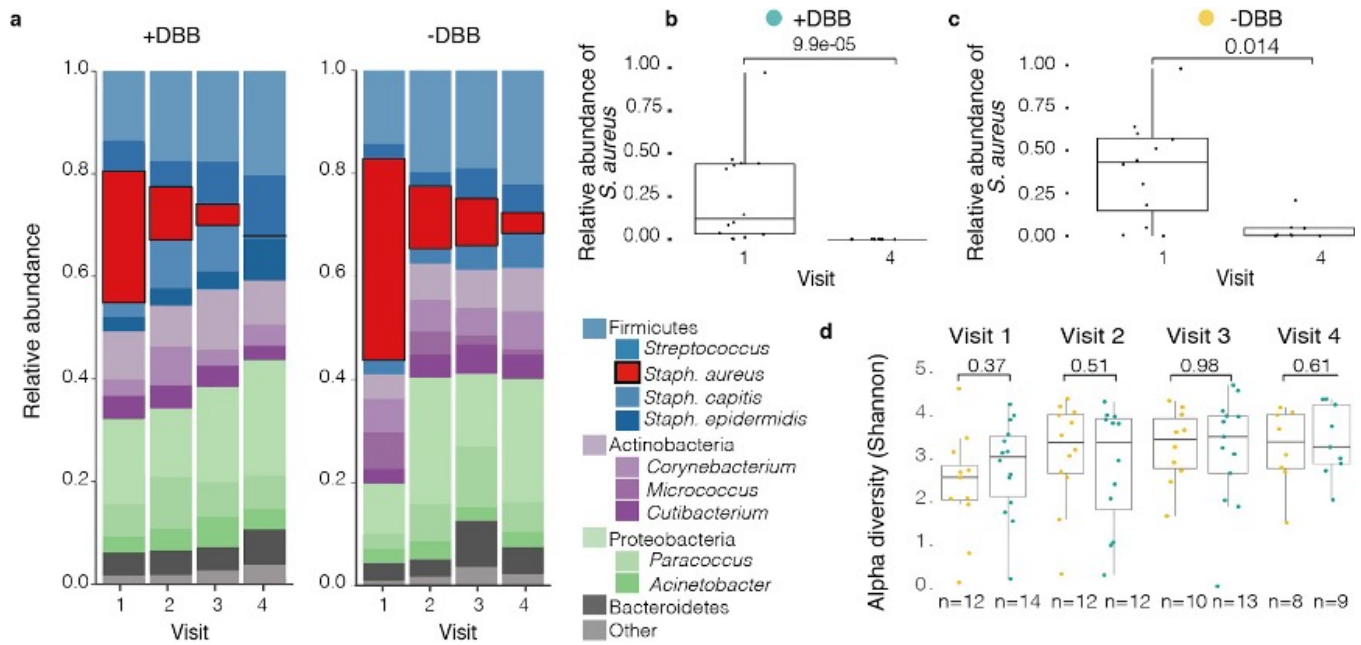
Supplementary Table 2: Comparison of relative abundances of taxa of interest in healthy controls and AD patients and within AD patients at visit 1.

Supplementary Table 3: Change in relative abundance of taxa of interest from visit 1 to visits 3 and 4 in all likely lesional sites of AD patients.

Supplementary Figures

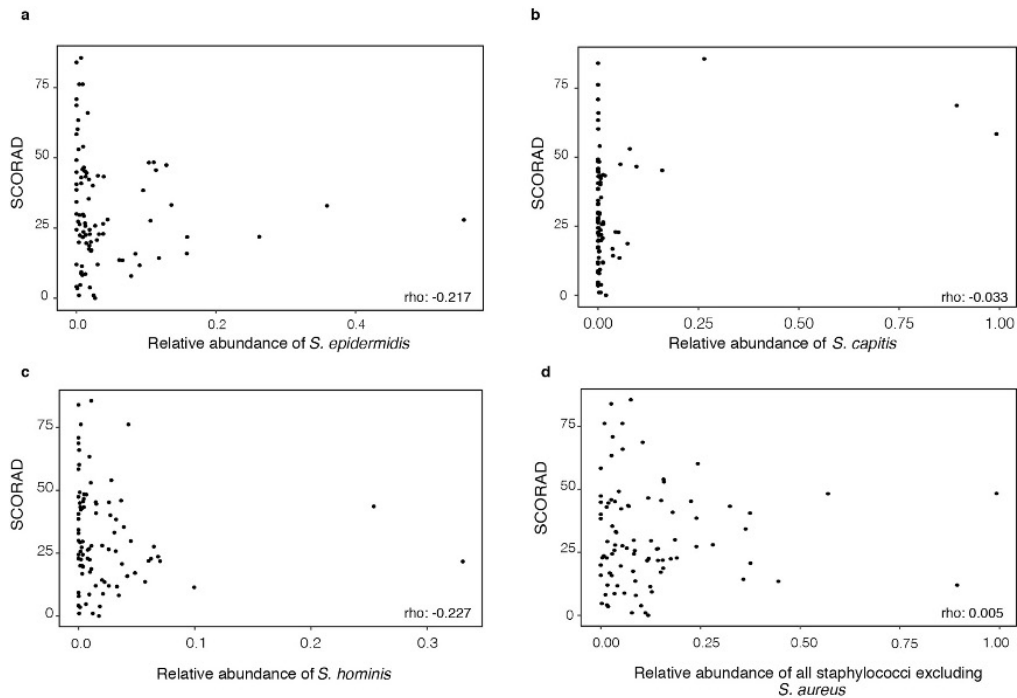


Supplementary Figure 1: Flowchart of patient enrollment and clinical data analysis.

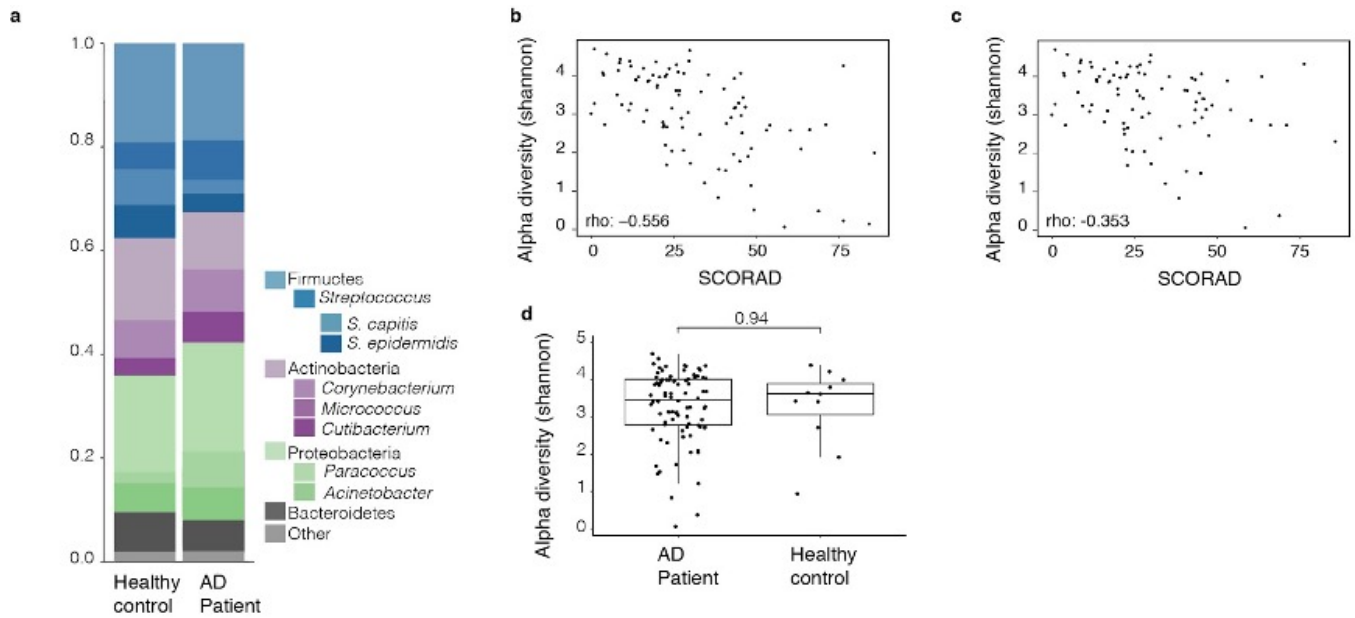


Supplementary Figure 2: Differences in composition and diversity between treatment groups.

(a) Patients treated with DBB contain little to no taxa of the genus *Micrococcus*, whereas patients that did not receive treatment with DBB had little to no *S. capitis* in their microbiomes, in addition to differences in the relative abundance of *S. aureus* between the two groups. (b,c) Both treatment groups displayed a significant decrease in the relative abundance of *S. aureus* by visit 4 (3 months after initial visit). (d) There were no significant differences in alpha diversity (Shannon) between the two treatment groups, though the group that received DBB tended to have a slightly greater alpha diversity by later visits.



Supplementary Figure 3: Health-like staphylococci are inversely correlated with disease severity. (a) *S. epidermidis*, a bacterium thought to be associated with a “healthy” or “health-like” microbiota, is mildly correlated with SCORAD, largely driven by the presence of outliers, Spearman’s rho: -0.217, $p=0.04$ (b) *S. capitis* is not significantly correlated with SCORAD, Spearman’s rho: -0.033, $p=0.758$. (c) *S. hominis* is mildly correlated with SCORAD Spearman’s rho: -0.227, $p=0.031$. (d) The relative abundance of all staphylococcal species, excluding *S. aureus*, is not significantly correlated with SCORAD Spearman’s rho: 0.005, $p=0.964$



Supplementary Figure 4: Community composition underlying *S. aureus* dominance is similarly diverse in patients and controls. (a) Community composition of skin microbiome of healthy controls and AD patients with *S. aureus* removed. Taxa present at high abundance (> 5%) are similar between the two groups. Baseline samples with an average of 300 reads or less following *S. aureus* removal (n=2) were discounted and samples were merged into subject-level groupings. (b) Shannon diversity (alpha) is inversely correlated with disease severity ($p < 0.001$) in AD patients when *S. aureus* dominates the community at likely lesional sites (c) Shannon diversity (alpha) remains correlated with disease severity in AD patients when *S. aureus* is removed from community structure, although much less so ($p < 0.001$). (d) Distribution of alpha diversity between healthy controls and AD patients is not significantly different once *S. aureus* is removed.

THIS PAGE INTENTIONALLY LEFT BLANK

3. Commensal skin bacteria exacerbate inflammation and delay skin barrier repair

This work was published as Khadka, Veda D. & Markey, Laura, et al. "Commensal skin bacteria exacerbate inflammation and delay skin barrier repair" *Journal of Investigative Dermatology* (2024). V. D. K. and L.M. contributed equally to this work.

Abstract

The skin microbiome can both trigger beneficial immune stimulation and pose a potential infection threat. Previous studies have shown that colonization of mouse skin with the model human skin commensal *Staphylococcus epidermidis* is protective against subsequent excisional wound or pathogen challenge. However, less is known about concurrent skin damage and exposure to commensal microbes, despite growing interest in interventional probiotic therapy. Here, we address this open question by applying commensal skin bacteria at a high dose to abraded skin. While depletion of the skin microbiome via antibiotics delayed repair from damage, probiotic-like application of commensals— including the mouse commensal *Staphylococcus xylosum*, three distinct isolates of *S. epidermidis*, and all other tested human skin commensals— also significantly delayed barrier repair. Increased inflammation was observed within four hours of *S. epidermidis* exposure and persisted through day four, at which point the skin displayed a chronic wound-like inflammatory state with increased neutrophil infiltration, increased fibroblast activity, and decreased monocyte differentiation. Transcriptomic analysis suggested that the prolonged upregulation of early canonical proliferative pathways inhibited the progression of barrier repair. These results highlight the nuanced role of members of the skin microbiome in modulating barrier integrity and indicate the need for caution in their development as probiotics.

Introduction

In daily life, the gut, oral cavity, and skin are both a physical barrier to pathogens and a site of frequent immune crosstalk with resident microbes. These sites are subject to a daily barrage of superficial damage that allows for microbial entry across the physical barrier. Whether and how the host distinguishes friend from foe and how this impacts barrier health are foundational questions in understanding the host-microbe relationship. This work seeks to address how the host responds to commensal microbes when skin barrier integrity is compromised.

We focus on the skin because, among all barrier tissues, the skin provides a uniquely accessible and tractable system for the study of microbe-host interactions. Intact skin is composed of two layers: the outer epidermis, composed of proliferating keratinocytes and melanocytes protected by an outermost layer of cornified dead cells; and the inner dermis, composed of hair follicles, blood vessels, nerves and immune cells. The human skin microbiome is thought to colonize both the epidermal skin surface and hair follicles within the dermis [1, 2].

In adulthood, the healthy human skin microbiome is dominated by *Cutibacterium acnes*, *Staphylococcus epidermidis* and *Corynebacterium* species [3]. These commensal microbes are thought to protect the host against opportunistic pathogens by competing for resources [4], engaging in microbial warfare via the secretion of antimicrobial peptides [4, 5], and interfering with pathogen quorum sensing [6–9]. When the integrity of the skin barrier is compromised, as occurs in atopic dermatitis patients during disease flares, opportunistic pathogens such as *Staphylococcus aureus* can exploit the damaged barrier, dominate the skin microbial community, and secrete cytotoxic factors that trap the host in a chronic inflammatory loop [10–12]. The inability of these opportunistic pathogens to cause damage when the barrier is intact highlights the role of host barrier integrity in determining the response to pathogen exposure.

Comparatively little is known about how the host responds to commensal microbes when barrier integrity is compromised. Previous work in this area has primarily used full-thickness excisional wound models (in which all layers of the skin are removed or damaged) or commensal colonization followed by pathogen infection challenge. In these models, colonization is beneficial: germ-free mice mount impaired immune responses [13–15], and conventional mice colonized with *S. epidermidis* prior to excisional wounding display improved healing outcomes [13–15]. A few studies using simultaneous damage and *S. epidermidis* exposure have observed contradictory responses. Following mild epidermal abrasion, Zheng et. al found that application of high doses of *S. epidermidis* promoted skin repair [16]. However, in the presence of atopic dermatitis-like inflammation [17] or after abrasive damage in combination with *S. aureus* co-infection [18], *S. epidermidis* has been shown to be detrimental to skin health.

Here, we use moderate tape-stripping to disrupt the upper layers of the epidermis and apply a range of commensal skin bacteria to the damaged skin. In contrast to the excisional wound models, which penetrate both epidermis and dermis, the abrasive damage of tape-stripping mimics superficial damage common to daily life [19]. We apply a high microbial load throughout the period of study to model topical probiotic treatment of damaged skin and test the effects of a range of bacterial species, from pathogens to well-characterized probiotics. We find that application of all tested opportunistic pathogens and commensal skin bacteria, including three isolates of the model commensal *S. epidermidis*, delayed healing from epidermal abrasion. Delayed healing in response to *S. epidermidis* was mediated by amplification of the innate immune response to damage, expression

of the cytokine IL-17A, and aberrantly prolonged epithelial proliferation. Our results suggest that application of most skin commensal bacteria to a damaged skin barrier is detrimental to the host and may be unsuitable for development into therapeutic applications.

Results

Perturbation of the skin microbiome affects recovery from barrier repair

To investigate how native skin commensals affect barrier repair from epidermal abrasion, we first disrupted the skin barrier by tape-stripping (Fig. 1a). Hair was removed from the back of each mouse and Tegaderm (3M) was repeatedly applied and removed in order to abrade much of the epidermis (Fig. 1a and Fig. S1g). Histopathological analysis showed that tape-stripping resulted in erosion of the top layers of the epidermis and rarely extended to the dermis, indicating that abrasion by tape-stripping is distinct from full-thickness wounding (Fig. S1). Each day, 100 μ L of washed bacterial cells or phosphate-buffered saline vehicle (PBS) was pipetted onto damaged skin and gently spread across the skin surface using a sterile cotton swab. Application occurred immediately after tape-stripping and then daily until experimental endpoint. Barrier recovery was assessed daily by transepidermal water loss (TEWL) and a severity score that semi-quantitatively assessed erythema (redness), crust, and thickness (Fig. S1c-d). To quantify healing over time and enable comparison between cohorts, the TEWL and severity score trajectories for each animal were summarized using area under the curve (AUC) and normalized to the average values for the control group from that cohort (Fig. S2a-b).

To determine the role of the native skin microbiome in repair from abrasion, we depleted the microbiome of Specific Pathogen Free (SPF) mice, using an antibiotic cocktail designed to target the skin flora [13]. We confirmed that this treatment depleted recoverable bacteria on the skin 10,000-fold (Fig. 1b-c, $P=0.001$), while only minimally impacting the gut microbiome (Fig. S2g-i).

Antibiotic-treated mice had higher TEWL and severity scores compared to control mice for the entirety of the exposure period (Fig. 1d, Fig. S2a-b, $P<0.003$), suggesting that depletion of the skin microbiome delayed healing. Control mice (which healed faster) had a less diverse skin microbiome when compared to antibiotic-treated mice at the end of the exposure period (Fig. S2c-f, $P=0.016$). This result was surprising given many examples of low diversity communities being associated with disease severity [10, 20, 21]. *Staphylococcus xylosum*, a species commonly recovered from mouse skin during health [22], dominated the skin microbiomes of these control mice (Fig. 1c and Fig. S2c-d). In line with a beneficial role for *S. xylosum* after tape-stripping, the endpoint relative abundance of *S. xylosum* was negatively correlated with skin damage as assessed by severity score AUC (Fig. 1d, $R=-0.76$, $P=0.017$) or TEWL AUC (Fig. S2a, $R=-0.53$, $P=0.14$) across both control and antibiotic-treated mice. Microbiome-wide correlation analyses revealed no other significant associations with severity score (Methods, Fig. S2j). These results suggest that a decreased abundance of native *S. xylosum* could delay barrier recovery.

We therefore hypothesized that supplementation of the skin microbiome with exogenous *S. xylosum* might improve healing in mice with a complete microbiome. To test this hypothesis, we cultured commensal *S. xylosum* from SPF mice and applied either PBS (vehicle control) or 10^9 CFUs immediately following tape-stripping damage and daily until experimental endpoint. Contrary to our hypothesis and in line with previous reports of *S. xylosum*-exacerbated disease in compromised

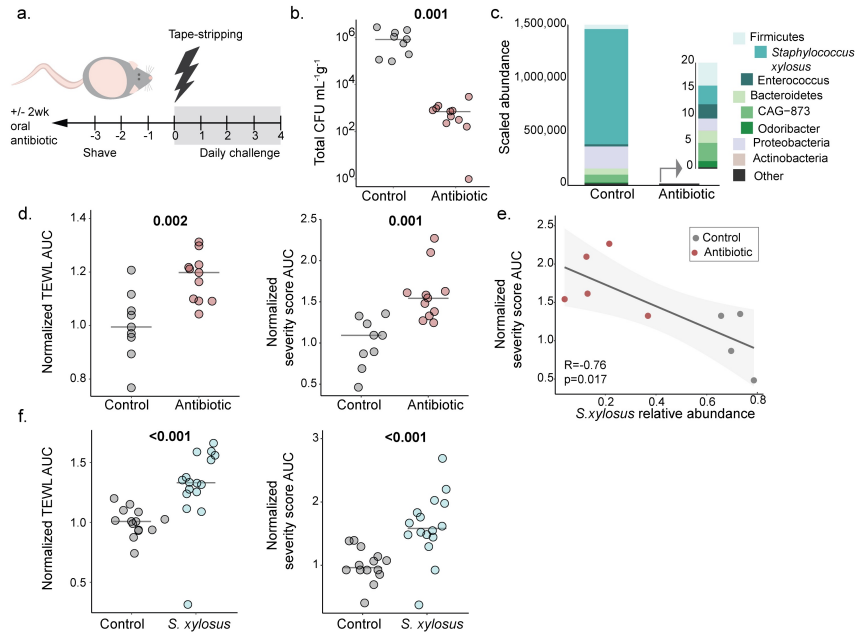


Figure 1: Perturbation of the native skin microbiome by depletion or supplementation delays healing.

a) Two-week antibiotic treatment prior to depilation and tapestripping followed by daily application of either PBS (control) or bacteria. b) Endpoint bacteria from skin homogenate plated on mannitol salt agar (control N=9, antibiotics N=11). c) 16s sequencing of endpoint skin swabs (control N=4, antibiotics N=5). Scaled abundance=average CFUs*average taxon abundance. d) Skin barrier integrity assessed by TEWL and severity score which were summarized by area under the curve (AUC) and normalized to cohort control average (control N=9, antibiotics N=11). e) Correlation between *S. xylosus* relative abundance and severity score AUC (f) TEWL and severity score summarized by normalized AUC (control N=10, *S. xylosus* N=10). For strip-plots, symbols represent mice and bars indicate medians.

skin [23–25], mice exposed to *S. xylosus* displayed delayed healing by both elevated TEWL and severity score compared to control mice (Fig. 1f, $P < 0.001$). Thus, either depletion or addition of the native mouse commensal *S. xylosus* after barrier damage delays healing.

Additional commensal skin bacteria do not improve skin healing following mechanical damage

We next tested if the delayed recovery from barrier damage was specific to supplementation with *S. xylosus* or generalizable across diverse skin commensals. To test this, we selected a variety of members of the healthy human skin microbiome previously shown to improve barrier immunity [5, 16, 26]: *S. epidermidis*, *Staphylococcus hominis*, and *Corynebacterium accolens*, as well as a community-associated, methicillin-resistant isolate of *S. aureus* (USA300). For all species, exponential phase bacterial cultures were washed in PBS twice and $10^8 - 10^9$ CFUs were applied to damaged skin on a daily basis throughout the experiment.

Surprisingly, all tested human skin commensal microbes significantly delayed healing relative to controls, by both TEWL and severity score (Fig. 2a, $P < 0.03$). Application of the opportunistic

pathogen *S. aureus* also significantly delayed healing by both measures (Fig. 2a, $P < 0.001$). Mice exposed to *S. aureus* were substantially more damaged than those exposed to commensals, displaying the highest severity score possible (Fig. S4a-c), in line with an expected difference in virulence between various organisms.

We next tested if delayed skin healing was a universal response to microbial exposure during damage. Laboratory isolates of *Escherichia coli* (MG1655) and the soil bacterium *Bacillus subtilis*, as well as a human isolate of the putative gut probiotic *Limosilactobacillus reuteri* (ATCC 23272) were applied to damaged skin immediately after tape-stripping and daily thereafter. *L. reuteri* was applied at a lower dose than that used for other bacteria due to growth limitations (10^8 CFU; similar low doses of *S. epidermidis* also delay healing, Fig. S3a). Neither *E. coli* nor *L. reuteri* delayed healing over controls when applied to tape-stripped skin (Fig. 2a, $P > 0.1$ and $P > 0.3$). Mice challenged with *B. subtilis* during damage displayed significantly elevated TEWL and severity scores (Fig. 2a, $P < 0.03$). *B. subtilis* has been found in infected burn wounds [27] and is sometimes considered an opportunistic pathogen, thus its deleterious effect on skin healing is not completely unexpected. These results show that the detrimental effect of microbial exposure on murine barrier repair is not common to all bacteria applied to damaged skin and appears to be limited to human and mouse skin commensals and opportunistic pathogens.

Multiple isolates of *S. epidermidis* delay healing when applied during damage

Given prior work on the beneficial properties of *S. epidermidis* in mouse models, we next asked whether the observed delay in healing was unique to the tested isolate (Sepi-TDL44, isolated from a healthy volunteer) or a generalized feature of *S. epidermidis*. We tested a *S. epidermidis* isolate previously characterized as beneficial in wound healing, Sepi-NIHLM087 [28], as well as a second commensal isolate of *S. epidermidis* from a healthy volunteer (Sepi-TDL105). Both Sepi-NIHLM087 and Sepi-TDL105 delayed healing significantly over controls (Fig. 2b, $P \leq 0.008$), and there was no significant difference between isolates (Fig. S3f). Moreover, all three isolates of *S. epidermidis* could be recovered from mouse skin at the experimental endpoint (24h after last application) at an equivalent microbial load (Fig. S3d). These data suggest that delayed skin healing is a generalized host response to *S. epidermidis* and not a strain-dependent effect.

Moreover, milder treatment with Sepi-TDL44 (hereafter referred to as *S. epidermidis*) also delayed healing from tape-stripping. When lower doses (10^7 and 10^8 CFUs) were applied daily after tape-stripping, we observed delayed skin healing by TEWL and severity score relative to vehicle controls, similar to that observed upon addition of 10^9 CFUs (Fig. S3a). Additionally, a single application of *S. epidermidis* immediately following tape-stripping resulted in an intermediate phenotype, with *S. epidermidis*-exposed animals having elevated severity score but not TEWL (Fig. S3b, $P = 0.013$). This single application resulted in a similar microbial load at the experimental endpoint as animals dosed with daily application, consistent with a model in which *S. epidermidis* is able to colonize damaged skin. These results highlight that even exposure to lower levels of *S. epidermidis* delays skin barrier repair.

In contrast to the delayed healing observed when *S. epidermidis* was applied to damaged skin, daily application to depilated healthy skin did not induce any morphological changes or impact skin health as measured by TEWL or severity score (Fig. S5a-b). Moreover, *S. epidermidis* exposure during health did not change the response to subsequent barrier damage (Fig S5c-d). This neutral response to *S. epidermidis* applied to healthy skin demonstrates a clear difference in the host response

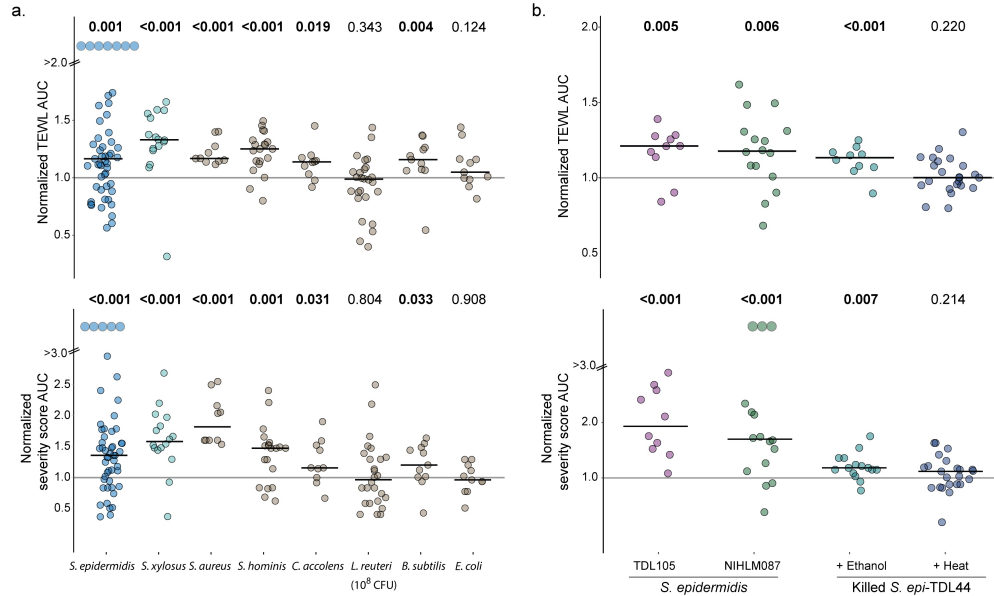


Figure 2: Human skin commensals including *S. epidermidis* delay barrier repair.

a) Bacteria were applied to skin after tapestripping and then daily until endpoint (10^9 CFU, except *L. reuteri* 10^8 CFU). TEWL (top) and severity score (bottom) for each animal summarized using area under the curve (AUC). b) TEWL (top) and severity score (bottom) AUCs after application of two additional isolates of *S. epidermidis* (left) or heat-killed or ethanol-killed Sepi-TDL44 (right). Throughout, symbols indicate individual mice normalized to cohort control average ($y = 1$) and bars represent medians. Sepi-TDL44 N=51, *S. xyloso* N=16, *S. aureus* N=10, *S. hominis* N=20, *C. accolens* N=10, *L. reuteri* N=27, *B. subtilis* N=11, *E. coli* N=11, Sepi-TDL105 N=10, Sepi-NIHLM087 N=16, ethanol-killed Sepi-TDL44 N=10, heat-killed Sepi-TDL44 N=20. 2-3 cohorts per experimental condition.

to *S. epidermidis* depending on skin barrier health during exposure.

To test whether live bacterial activity was required for delayed healing, mice were exposed to either heat-killed or ethanol-killed *S. epidermidis*. Application of heat-killed bacteria (boiled lysates of washed cells at equivalent cell density) did not delay skin healing (Fig. 2b, $P=0.63$). In contrast, when bacteria were exposed to 80% ethanol (which kills bacteria through coagulation and disruption of their cell membranes [29]), washed, and applied to damaged skin, healing was significantly delayed over controls (Fig. 2b, $P<0.007$). These results indicate that cell-bound components of *S. epidermidis* are sufficient to delay skin healing in our model and agree with a previous report that *S. epidermidis* cell wall components are highly immunogenic [30], though secreted products may also play a role [17].

Application of *S. epidermidis* after damage induces an inflammatory innate response

To better understand how *S. epidermidis* changes the host response to damage, we conducted histopathological analysis at multiple timepoints after tape-stripping. By pathology score (Methods), tape-stripped skin exposed to *S. epidermidis* was less healed four days after tape-stripping damage (Fig. 3a and Fig. S1e), in line with TEWL and severity score measurements. *S. epidermidis*-exposed mice displayed marked epidermal ulceration with serocellular crust, as well as inflammatory

infiltrates consisting primarily of neutrophils, fibroblasts, and some mast cells (Fig. 3a and further magnification in Fig. S1g). In contrast, controls displayed lesions that were much more healed, characterized by epidermal hyperplasia, hyperkeratosis, and increased dermal fibroblasts.

Next, we wanted to define immune pathways contributing to the delayed healing observed in response to *S. epidermidis*. Previous reports have shown the adaptive immune response to application of Sepi-NIHLM087 on healthy skin (induction of IL-17A producing CD8+ T-cells 14 days after bacterial application) is protective against pathogen challenge and excisional wounding [26]. On day seven post-damage and *S. epidermidis* exposure, we measured an increase in both bulk T-cells and $\gamma\delta$ -T cells specifically (Fig. S6c, $P=0.004$ and $P=0.0087$ respectively) in response to *S. epidermidis*; however, skin barrier repair remained delayed relative to controls (Fig. S6a-b). This finding suggests that the T cell response to *S. epidermidis* does not promote healing from tape-stripping.

To identify additional immune pathways involved in the delayed healing response to *S. epidermidis*, we used a multiplex ELISA to characterize the cytokines (Fig. S7a) produced in the skin three days post-damage. We measured a significant increase only in IL-17A in mice exposed to *S. epidermidis* (Fig. 3d, $P<0.001$; p-value threshold corrected for multiple hypotheses). Previous work has shown that skin IL-17A can have many sources including CD8+ [26] and CD4+ T cells [31], $\gamma\delta$ -T cells [32], and innate immune cells including neutrophils and mast cells [33]. Given the rapidity of the inflammatory response observed after *S. epidermidis* exposure, we next used flow cytometry to quantify innate immune cell populations in the skin.

We performed flow cytometric analysis four days after concurrent damage and *S. epidermidis* exposure to capture innate immune cell populations present. We observed an increase in neutrophils in mice exposed to *S. epidermidis* compared to controls, but a decrease in monocytes, macrophages, and dendritic cells (Fig. 3b). Supporting a pathological role for excess neutrophil recruitment, mouse skin severity scores were strongly and significantly correlated with the number of neutrophils (Fig. 3c, $R=0.78$, $P=0.007$). Altogether, our flow cytometry results indicate that *S. epidermidis* induces both innate and adaptive immune cell populations, which could interfere with the precise succession of immune cells and cytokines required for successful initiation and resolution of the first, inflammatory, phase of skin wound healing [34].

Transcriptomic analysis of the damaged flank skin from three acute timepoints after damage (4h, 24h and 4 days) confirmed strong induction of the innate immune response in mice exposed to *S. epidermidis*. Significantly upregulated genes were enriched in gene annotations related to the immune system in *S. epidermidis*-exposed mice at 4h and 24h after damage (Fig. 3e, $P<0.001$). More specifically, the IL-1 response pathway was upregulated in *S. epidermidis*-exposed mice at all timepoints, in agreement with multiple literature reports of IL-1 activation after *Staphylococcus* sp. exposure on the skin [15, 35]. Additionally, immune cell chemotaxis pathways were enriched among upregulated genes at all timepoints (Fig. 3f), including pathways for neutrophil migration (consistent with histopathology and flow cytometry, Fig. 3a-b), leukocyte migration, and general chemotaxis.

Many of the immune pathways upregulated by *S. epidermidis* are part of the normal inflammatory phase of wound healing, which typically lasts 0-3 days [36]. Critically, expression of genes in immune pathways decreased over time in controls but remained higher in *S. epidermidis*-exposed mice (Fig. 4c, Fig. S7b-d). This led to their relative upregulation compared to controls at later timepoints. Thus, *S. epidermidis* stimulation exacerbated normal inflammation and extended it beyond its expected duration of normal wound healing.

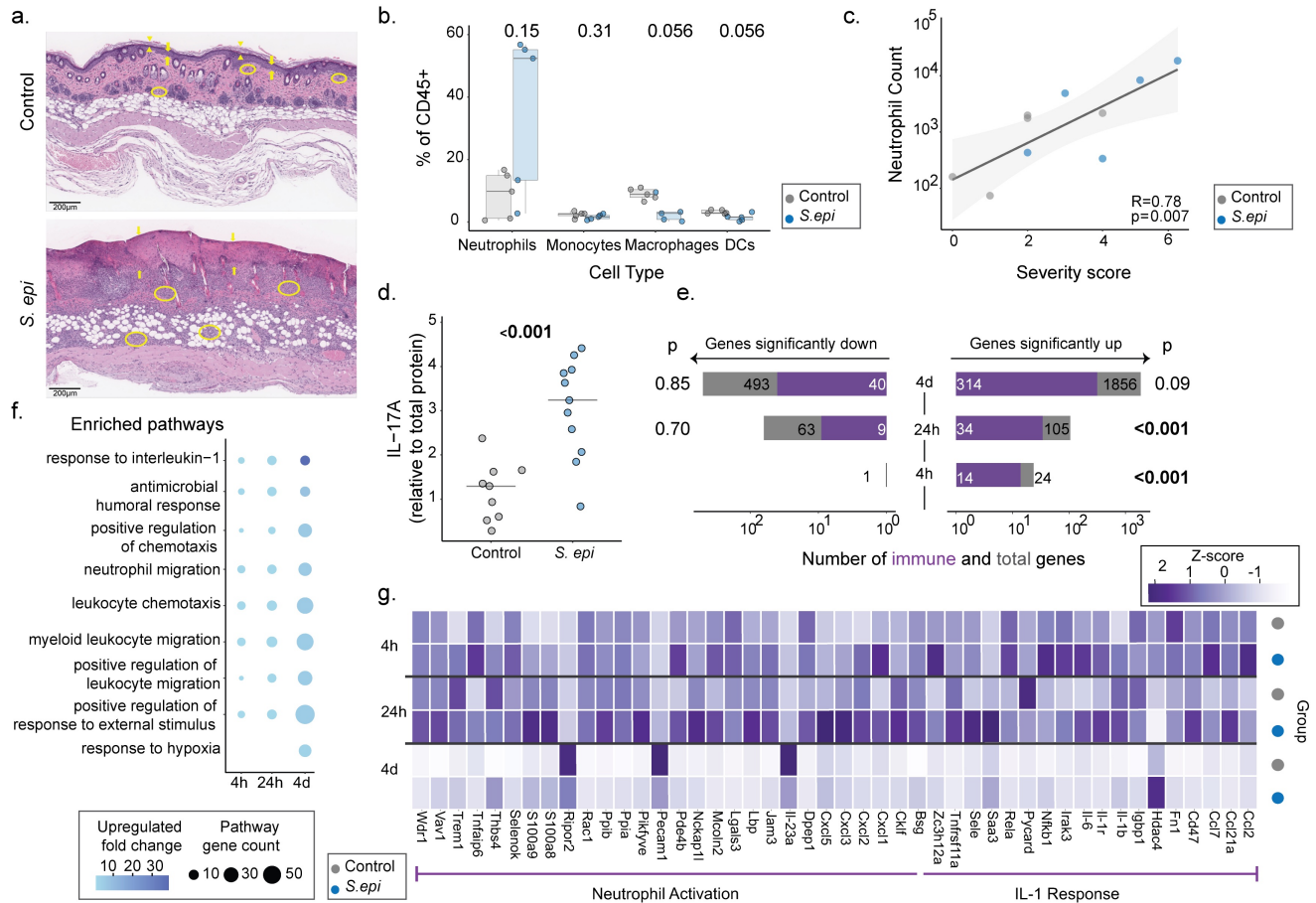


Figure 3: Application of *S. epidermidis* following barrier damage induces an innate inflammatory immune response.

PBS (control) or *S. epidermidis* was applied to skin daily after tapestripping. a) H&E-stained flank skin four days post-damage. Top: hyperplasia (large arrow) and hyperkeratosis (arrowheads) with fibroblasts (circles); bottom: serocellular crust (arrows) and inflammatory infiltrate (circles). b) Flow cytometry four days post-damage (control N=5, *S. epidermidis* N=5). c) Correlation between neutrophils and day 4 raw severity score. d) IL-17A in skin lysate (control N=9, *S. epidermidis* N=11). e) Bulk skin RNAseq differential expression analysis (likelihood ratio test). Total height of gray bar indicates all significantly differential genes; immune genes subset in purple (4h control N=5, *S. epidermidis* N=5; 24h control N=4, *S. epidermidis* N=5; 4 days control N=6, *S. epidermidis* N=9). f) Pathway enrichment analysis of *S. epidermidis*-upregulated immune genes. g) Average normalized immune gene expression (TPM).

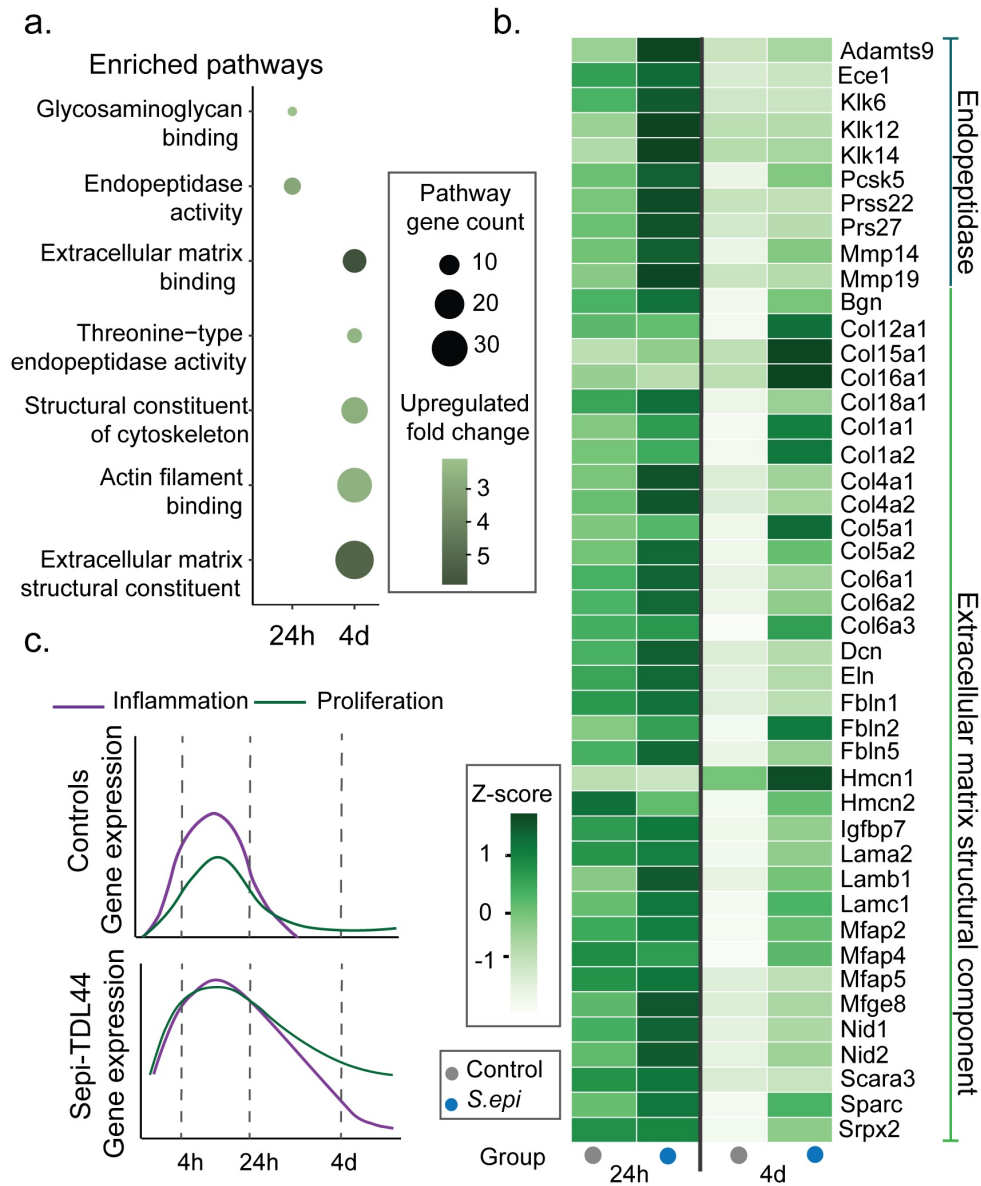


Figure 4: *S. epidermidis* application after barrier damage increases and prolongs expression of epithelial cell proliferation pathways.

PBS (control) or *S. epidermidis* was applied to skin after tapestripping and then daily until endpoint. a) Pathway enrichment analysis of non-immune genes upregulated in *S. epidermidis*-exposed mice relative to controls. b) Average normalized gene expression (TPM) of selected GO processes shown in c (4h control N=5, *S. epidermidis* N=5; 24h control N=4, *S. epidermidis* N=5; 4 days control N=6, *S. epidermidis* N=9). c) Graphic illustrating that mice exposed to *S. epidermidis* after damage show an increased and prolonged expression of inflammation and proliferation genes compared to controls. For all RNAseq analysis, gene-level statistical significance comparing *S. epidermidis*-exposed mice to controls was calculated using the likelihood ratio test with Benjamini-Hochberg correction for multiple comparisons.

***S. epidermidis* prolongs expression of epithelial proliferation pathways**

In healing skin, immune cell recruitment is followed by re-epithelization through cell migration and proliferation. Inflammatory cytokines such as IL-1 stimulate epithelial cell proliferation, and products of proliferation such as extracellular matrix (ECM) fragments further stimulate inflammation [37]. This creates a positive feedback loop that promotes re-epithelization and is normally terminated upon production of anti-inflammatory factors with healing progression [38]. In addition to amplifying the innate immune response, *S. epidermidis* exposure also upregulated pathways involved in these downstream proliferative phases of healing. *S. epidermidis*-exposed mice showed prolonged expression of genes involved in ECM and epithelial proliferation, with significantly increased expression at day 4, indicating aberrant elongation of this phase of healing (Fig. 4).

Among re-epithelization pathways upregulated by *S. epidermidis*, host-produced protease expression was particularly noteworthy. Multiple classes of ECM-targeting endopeptidases were upregulated 24h after damage, including kallikrein, matrix metalloprotease, ADAM metalloproteinase and threonine-type protease gene families (Fig. 4a-b). While protease activity is required to debride the damaged skin and provide access for migrating cells [38, 39], persistent protease activity produces proinflammatory ECM fragments [37] and degrades factors required for skin closure [40]. Excessive protease expression has been shown to directly delay healing in elderly patients [40]. *S. epidermidis*-exposure also upregulated skin and ECM structural proteins (Fig. 4a-b), including glycosaminoglycan binding proteins, collagen, and other ECM/cytoskeleton structural constituents. This upregulation suggests increased influx and activity of fibroblasts [41]. Consistent with this result, histopathology showed increased fibroblasts within the dermis of *S. epidermidis*-exposed mice at sites of delayed healing (Fig. 3a). Together these results indicate that delayed healing in the skin of *S. epidermidis*-exposed mice is driven by an excess of innate inflammation and prolonged cellular proliferation (Fig. 4c).

Discussion

In health, the skin microbiome can play a protective role by promoting barrier integrity and providing colonization resistance against opportunistic pathogens [4]. Our results show that, despite their beneficial role during health, the application of native human and mouse skin commensals to damaged skin delays healing by exacerbating inflammation and prolonging proliferation. Our results also highlight the importance of host barrier context in influencing the response to commensal microbes: both depletion and supplementation of the native skin microbiome during damage are harmful for barrier repair, though others have shown responses may be beneficial during health.

Interestingly, our results indicate that IL-17A induction by *S. epidermidis* in the context of barrier damage correlates with delayed healing, while induction of the same cytokine by *S. epidermidis* applied to healthy skin has been shown to boost beneficial T-cell responses, which defend against infection and promote wound closure [14, 26, 28]. This differential response to IL-17A suggests that early skin healing in response to full-thickness excisional wounding is distinct from skin healing after epidermal abrasion. The increased IL-17A expression in *S. epidermidis*-exposed mice with delayed barrier repair is reminiscent of diabetic and infected wounds, where IL-17A expression has been implicated in delayed healing [42, 43]. Similarly, the innate cell imbalance observed in *S. epidermidis*-exposed mice, created by a prolonged influx of neutrophils and absence of macrophages, is also present in chronic wounds [44].

Supporting our interpretation that *S. epidermidis*-induced neutrophil influx and expression of IL-17A contribute to delayed skin healing, other researchers have shown that these immune factors are induced by tapestripping and that their depletion improves skin barrier repair [45, 46]. Our results add to this body of work demonstrating a pathological role for excessive innate inflammation in skin healing and emphasize that host barrier context plays a critical role in determining the consequence of commensal-induced cytokine expression.

Our results suggest that commensal bacteria could amplify inflammation and other disease pathology in people with a weakened or inflamed skin barrier, such as patients with atopic dermatitis. Shifts in microbiome composition are common among atopic dermatitis patients, and Staphylococci (largely *S. aureus* but occasionally *S. epidermidis* and other coagulase-negative Staphylococci) generally dominate the inflamed skin microbiome [47–50]. Our results suggest that one way in which Staphylococci-dominated microbiomes could contribute to disease pathology is through microbe-induced upregulation of host protease production, as increased endogenous protease expression also associated with pathology in atopic dermatitis patients [51–53].

While recent work has promoted the use of commensals to benefit the host by directly inhibiting the overgrowth of pathogenic *S. aureus* in intranasal and skin infection disease models [5, 54, 55], the co-application of *S. epidermidis* and *S. aureus* to abraded skin significantly increased *S. aureus* burden in the skin [18]. These contrasting results highlight the role of host barrier integrity in modulating the outcome of probiotic therapy. We thus caution researchers to assess the ability of their chosen microbe to induce inflammation or support pathogenic overgrowth during host barrier damage when developing probiotic therapies.

Further studies are needed to determine the mechanism underlying delayed healing in response to commensal skin microbes other than *S. epidermidis*, which may or may not proceed through similar host signaling. While future work will be needed to understand the clinical implications of our results given the structural and regenerative differences between mouse and human skin [56], our results nonetheless highlight several pathways via which *S. epidermidis*, and potentially other commensal skin bacteria, can exacerbate skin pathology in the context of a weakened skin barrier.

As studies accumulate showing the key role of the native skin microbiome in local immune development and homeostasis, there is a temptation to conclude commensal microbes represent suitable candidates for interventional probiotic therapy. Although we and others [13, 15] find that depletion of the skin microbiome significantly decreases the ability of the skin to recover from damage, we also observe that supplementation of the native microbiome with additional bioburden of commensals is decidedly detrimental. In developing probiotic therapies, it is thus critical to consider the context of microbial exposure and the range of immune responses that may result therein.

Methods

Animals

Eight-week-old C57BL/6 male and female mice were purchased from Taconic Biosciences (New York) and housed in individually ventilated cages in a specific pathogen free facility under the Division of Comparative Medicine (DCM) at MIT. Female mice were housed in groups of 3-5 animals per cage and male mice were housed singly to avoid any fighting behaviors that could compromise the skin barrier. Mice were maintained on a 12h light-dark cycle at ambient humidity in sterilized

cages and given sterile food and water to limit exposure to facility bacteria. Cages were changed at the beginning of each experiment or every week. All mouse experiments were conducted under protocols approved by MIT DCM IACUC (protocol number 213-0000-585).

Animal experiments study design

Both male and female mice were used in experiments to establish the tape-stripping model. We did not observe a significant difference in the delayed healing response to commensal bacteria as a result of sex (Fig. 2a and Fig. S1 include both male and female mice across experimental groups). The effect size of increased TEWL and severity score AUC observed as a consequence of *S. epidermidis*-exposure in a pilot experiment (total N=17) was used for power calculations which determined the total sample size per group required for statistical significance (N=12); this number was split between 2-3 cohorts of animals (N=4-5 per cohort) to ensure reproducibility across experimental repeats. Unless noted in text, experimental groups (bacterial exposure or antibiotic treatment) were compared to a control group which undergoes hair removal and tape-stripping damage and has PBS vehicle applied to skin daily after damage. Animals were randomly assigned to experimental conditions.

Animals were excluded from analysis if hair regrowth occurred during the three day interval between hair removal and tape-stripping. Comparable tape-stripping damage was not possible or if hair regrew significantly by 24h post-tape-stripping.

Statistical analysis

Throughout the text, when comparing an experimental group to the control a two-sided Wilcoxon rank-sum test was used to compare the medians of the two groups. Only PBS control animals from cohorts that included the experimental group of interest were used for comparison. When multiple groups were being compared to the control this was followed by the Benjamini Hochberg correction for multiple hypothesis testing. Pearson's correlation coefficient was calculated to quantify correlation. Likelihood ratio test followed by Benjamini Hochberg correction was used for differential expression analysis of transcriptomic data. Fisher's exact test was used to calculate enrichment. Statistical analysis was performed in R 4.1.3 or python (SciPy).

Tape-stripping Barrier Damage Model

Mice were shaved and depilated (Nair) 72 hours prior to barrier damage. Depilation itself did not induce inflammation or damage to the skin barrier by histopathological assessment (Fig. S1). Tape-stripping was performed by applying and removing a Tegaderm bandage (3M) to the depilated dorsal flank skin 10 times, resulting in significant disruption of the epidermis observed as skin reddening and glistening. Mice were allowed to recover from damage and anesthesia in a heated recovery cage and then placed back in their home cage.

To assess barrier damage, transepidermal water loss (TEWL) was measured using a noninvasive probe (Tewameter, C+K). Continuous TEWL measurements for each animal were taken for up to 20s, or until the standard deviation between readings fell below 0.5 g/m²/h. TEWL values immediately following tape-stripping were between 60–80 g/m²/h. TEWL was measured once daily following damage and severity score was assessed beginning 48h after damage (prior to 48h no

morphological changes in skin were apparent). For consistency, the same experimenter performed all tape-stripping and TEWL measurements. Disease severity score assessed gross morphological changes during healing and included skin thickness (0-3), scale (0-3), and erythema (0-3). To limit duration of daily anesthesia required for both bacterial application and TEWL and score assessment, all manipulations were performed by the same experimenter and thus experimenters could not perform blinded scoring. Mice were euthanized at the end of the experiment by 5% CO₂ inhalation.

Application of bacteria or vehicle control

100 μ L of phosphate-buffered saline vehicle (PBS, ThermoFisher) or washed bacterial cultures (10⁹ CFUs) was pipetted onto damaged flank skin and then gently rolled across the skin surface using a sterile swab (Puritan Medical Products). In developing our model, we tested three therapeutic doses of *S. epidermidis*, as widely reported in the literature [5, 6, 26, 35]: 10⁷ CFU, 10⁸ CFU and 10⁹ CFU. We found that *S. epidermidis* similarly delayed healing across all three doses, and chose to focus on the most commonly used therapeutic dose of 10⁹ CFU (Fig. S2).

Bacterial growth and preparation

Bacteria were subcultured (1:100) from overnight cultures and grown to exponential phase at 37 °C with shaking. Bacterial cells were then washed twice with PBS and resuspended at a concentration of 10¹⁰ CFU/ml except *L. reuteri* which was resuspended at a concentration of 10⁹ CFU/ml. *S. epidermidis* (TDL44 and TDL105) and *S. hominis* strains were isolated from healthy volunteers and are part of the lab strain collection. *S. epidermidis* NIHLM087 was a generous gift from Dr. Chris Voigt. *S. xylosus* was isolated from mouse skin from animals housed in the MIT animal facilities. *S. aureus* USA300 LAC [57] was used and was a generous gift from Dr. Isaac Chiu. *C. accolens* (ATCC 49725) and *L. reuteri* (ATCC 23272) were obtained from the ATCC.

Bacterial inactivation

Exponential phase cultures of *S. epidermidis*(TDL44) were washed and resuspended in PBS to a density of 10¹⁰ CFU/mL. Cells were heat-killed by exposure to 95°C for 1 hour. Ethanol inactivation was achieved by resuspending cells in 80% ethanol (freshly prepared) for 2 hours on ice, with periodic mixing. The ethanol inactivated cells were pelleted and washed with ice-cold PBS twice and resuspended at the original concentration. For both methods, killing was confirmed by plating the inactivated cells on tryptic soy agar.

Bacterial gene expression analysis

RNA was extracted from exponential phase cultures of *S. epidermidis* as follows: cells were collected from 1ml of culture by centrifugation and supernatant discarded. Cells were subjected to enzymatic lysis (100 μ L of 40 μ g/ml lysostaphin, Sigma Aldrich) for 20 minutes followed by chemical lysis (500 μ L of 10% SDS, Sigma Aldrich) and mechanical lysis with phenol/chloroform extraction with addition of 500 μ L QIAzol (Qiagen) and transfer to ZR BeadBashing lysis tubes (Zymogen, 0.1mm and 0.5mm beads) followed by homogenization in the TissueLyserII (Qiagen) for 5 minutes at 30hz. Supernatant was mixed with 200 μ L chloroform (Sigma Aldrich) and then centrifuged for 10 minutes at 10,000xg at 4°C. Aqueous phase was mixed with 70% ethanol, loaded

onto columns and purified further using Ambion PureLink Mini Kit (Thermo Fisher Scientific) as per kit instructions, including on-column DNase treatment. 100ng of RNA was used as template for reverse transcriptase reaction using Invitrogen SuperScriptIV First Strand Synthesis System (Thermo Fisher Scientific) as per manufacturer's instructions. mRNA expression was measured using quantitative PCR and LightCycler480 (Roche) using SYBR Green qPCR mastermix (Thermo Fisher Scientific) and the following primers: *ecpA*-F 5'-TGTGCTTAAAACGCCACGTA-3' and *ecpA*-R 5'-GTATAGCCGGCACACCAACT-3' [58]; *gyrB*-F 5'-AAGGCGGCTGAGCAATATAA-3', *gyrB*-R 5'-CAGGTGAAGATACACGAGAAGG-3' [17]. All samples were run on the same plate and standard curve method used to compare gene expression across samples. All three strains express the protease *ecpA* (Fig. S3e), a secreted enzyme characterized previously as a virulence factor in an epicutaneous *S. epidermidis* skin infection model [17], which may play a role in the delayed healing observed here.

Bacterial enumeration from murine skin

Animals were euthanized via CO₂ inhalation, and a roughly 1cm² area of flank skin was collected in PBS kept on ice. Skin sections were weighed before being minced and homogenized using a TissueLyserII (Qiagen). Dilutions of skin homogenate were plated on Mannitol Salt Agar (Oxoid) and colonies enumerated.

Antibiotic treatment

Antibiotic depletion was performed as per [13]. Briefly, metronidazole (1g/L, Sigma), sulfamethoxazole (0.8g/L, Sigma), trimethoprim (0.16g/L, Sigma), cephalexin (4g/L, Sigma) and Baytril (0.025g/L, Sigma) were dissolved in drinking water containing Splenda (1 packet/250ml) as a sweetener and was provided to mice for two weeks prior to tape-stripping barrier damage and throughout the barrier damage protocol to the endpoint of the experiment. Cages were changed 3 times/week to ensure decreased microbial burden in antibiotic treated mice. Control cages were given drinking water containing Splenda and cages were changed once per week to ensure microbial diversity.

Tissue dissociation and flow cytometry

Flank skin was harvested from euthanized animals and placed in RPMI 1640 with L-glutamine and HEPES (Gibco), containing 10% serum (Gibco). Tissue was minced and digested in RPMI with 1% serum, 0.1mg/mL DNase 0.25mg/mL TL liberase (Roche) overnight at 37°C with 5% CO₂. The digestion reaction was quenched using 10mL of RPMI 1640 with 10% serum and 1mM EDTA. Digested cells were filtered through a 70µm filter before being washed twice with PBS. After antibody blocking (CD16/32, ebioscience), cells were stained with an amine reactive live/dead dye (efluor506, Thermo Scientific) and an antibody panel (Ly6G-PE, F4/80-BrilliantViolet600, CD11c-BV711, MHCII-Alexa700, CD11b-PECy5, Ly-gC-Alexa488, CD45-efluor450, CD3-APC, CD8-Alexa488, CD4-SuperBright600, Thermofisher) and fixed using CytoFix (BD) for 30m at 4°C in the dark. Fixative was washed, and stained cells were captured on a BD 5L LSR Fortessa.

DNA extraction and 16S sequencing

The dorsal flank skin of mice was sampled using a swab pre-wetted in a TES solution containing 1.2% Triton X-100 (Sigma) vigorously rubbed on the skin surface. The swab was stored in DNA/RNA Shield (Zymo) in a Zymo Bead Bashing Lysis tube (Zymo) and frozen. Fecal pellets were also collected and frozen dry. DNA was extracted from both skin and fecal samples using the ZymoBIOMICS 96 DNA kit (Zymo), following manufacturer’s protocol. The 16S region of the bacterial rRNA gene was amplified using V1-V3 primers (27F - 543R). Libraries were prepared for sequencing following the Hackflex protocol (Gaio et al. 2022). Nextera-compatible primers (IDT) were used for index PCR and amplicons were purified using DNA-binding beads (Cytiva) for size selection.

Microbiome analysis

Sequencing was performed at the MIT BioMicro Center on an Illumina Miseq using 300bp paired-ends reads to an average depth of 300,000 reads per sample. All data processing was done using QIIME2 (v2021.2) [59]. Only forward reads were used, as reverse read quality was too low to overlap pairs. Adapters were trimmed using the cutadapt plugin for QIIME2, and data were denoised using DADA2 [60] to generate the amplicon sequence variant (ASV) table. As described previously [61], a custom classifier based on the SILVA database (v132) [62] was used for taxonomic assignment. Exported taxa abundance from QIIME2 were analyzed using R version 4.1.3 and phyloseq version 1.38 [63]. ASVs unassigned at the phylum level and below, as well as ASVs assigned to eukaryotes, were removed. ASVs with fewer than 250 reads across all samples were removed and analyses performed on the remaining subset. For correlation analyses, ASVs were aggregated to the species level. For species above 1% relative abundance in at least one sample, the Pearson correlation coefficient was calculated for species relative abundance and severity score and multiple-hypothesis correction performed on resulting p-values (Fig. S2j).

RNA isolation and cDNA library synthesis

A small (roughly 1cm^2) piece of skin from the area subjected to damage (when applicable) was dissected immediately after euthanasia and either placed in RNAlater (Invitrogen) or snap-frozen in liquid nitrogen. Samples placed in RNAlater were placed on ice for 1-4 hours and then frozen at -80°C . Snap-frozen samples were placed on dry ice and then transferred to -80°C . To extract RNA, samples were placed in a 2ml tube with 1ml of QIAzol (Qiagen) containing a sterile 4.5mm ball bearing and homogenized with 2 rounds of bead-beating (2m30s, 30 beats/s) in a TissueLyserII (Qiagen). The lysate was then transferred to a new tube and 1/5 volume of chloroform (Avantor) added and lysate shaken by hand for 15 seconds. This tube was centrifuged for 15 minutes at 4°C at 12,000xg and the aqueous layer transferred to a new tube and 1 volume of 70% ethanol added. RNA was then purified using a PureLink RNA kit with on-column DNase treatment (Invitrogen) as per manufacturer’s guidelines. RNA was quantified using a Nanodrop and 500ng was used for cDNA synthesis as per the Smart-seq2 protocol [64]. cDNA libraries were fragmented and prepared for sequencing following the Hackflex protocol [65]) modified as follows: bead-linked transposase was diluted 1:5 in buffer and used for tagmentation as per protocol. Nextera-compatible unique dual index primers (IDT) were used for index PCR and fragments were purified using DNA-binding beads (Cytiva) for double-sided size selection.

RNA sequencing and differential expression analysis

Libraries were sequenced using a Novaseq S4 flow cell (50 basepair single-end reads) at an average sequencing depth of 25 million reads per sample. Reads were pseudoaligned to the mouse transcriptome using kallisto ([66], default parameters) and differential expression analysis performed using sleuth ([67], default parameters). Differential expression analysis included animals from multiple cohorts sacrificed at multiple timepoints after damage. Experimental cohort was included as a variable such that genes shown are differentially expressed between experimental conditions at the timepoint shown regardless of cohort effects.

Statistically significant genes (likelihood ratio test, p-value <0.05, Benjamini-Hochberg correction for multiple comparisons) from each timepoint were used as input for pathway enrichment analysis using clusterProfiler [68] and the GO database (release date 2023-01-01, version 10.5281/zenodo.7504797, [69, 70]). Pathway enrichment analysis was performed on the entire set of differentially expressed genes as well as exclusively on the subset of genes annotated as part of the immune response in the Mouse Genome Database [71]. Enrichment was calculated based on over-representation analysis and a one-sided Fisher's exact test, with Benjamini-Hochberg correction for multiple comparisons. Pathways were then filtered to include those with at least 5 differentially expressed genes and curated for processes of interest. Uncurated clusterProfiler output for immune genes and non-immune genes is available on Github: https://github.com/vedomics/commensal_staph.

Histology / pathology

A representative strip of skin taken from the most damaged section of the tapestripped area was fixed in 10% neutral buffered formalin, embedded in paraffin, sectioned at 5 μ m thickness and stained with hematoxylin and eosin. Sections were scored by a board-certified veterinary pathologist. Skin was assessed for the presence of serocellular crust as follows: 0=none, 1=little/occasionally observed, 2=severe crust formation. The following criteria were used for scoring dermal and subcutaneous neutrophil infiltrates: 0=none, 1=minimal, 2=moderate and 3=marked. The total score per animal is shown (Fig. S1). Slides were imaged using a digital slide scanner (Aperio) at 20x magnification.

The thickness of the top layer of skin (epidermis and/or serocellular crust depending on degree of epidermal ulceration) was quantified using ImageJ and a custom python script as follows: two representative sections per animal were annotated in ImageJ such that x-y coordinates of the top and bottom of the epidermis were saved as a text file. The distance between the top and bottom of that area was then calculated using euclidean distance in python and averaged across both sections per animal.

Immunoassay for skin cytokine protein quantification

Skin samples were snap-frozen in liquid nitrogen immediately after sacrifice and stored at -80°C. To prepare whole skin lysate, frozen samples were diced using a scalpel then 500 μ L of lysis buffer (RIPA with 1mM PMSF) was added per 100mg of sample and two sterile 4.5mm ball-bearing were added to the tube prior to mechanical dissociation using the TissueLyserII (Qiagen): 25 beats/s for 3 minutes, repeated up to 3 times until homogenized. Lysate was centrifuged at 4°C for 10 minutes at 16,000xg to remove unhomogenized debris and then supernatant was aliquoted and frozen at -80°C. Total protein was measured using a Bradford Assay (BioRad). Skin lysates were diluted

1:10 in ProcartaPlex Universal Assay Buffer prior to use in custom Procartaplex Immunoassay (ThermoFisher) analyzed using the FlexMap3D (Luminex). Skin lysates were subjected to acid-ethanol extraction [72] lyophilized and resuspended in Procartaplex Universal Assay Buffer and stored at -80°C prior to measurement of TGF- β using Procartaplex Single-plex assay (ThermoFisher).

Protein quantification was performed on samples collected three days post-tape-stripping. This earlier timepoint was chosen as pilot studies showed a decrease in skin cytokine IL-17A over time and that ELISA from skin homogenates was less sensitive than other assays (flow cytometry, histology) and thus it was more difficult to recover inflammatory cytokines from later timepoints.

Data and materials availability

Sequencing data are available as BioProject PRJNA1047182. Other data and code used for analysis and visualization are available on Github: https://github.com/vedomics/commensal_staph.

Acknowledgements

We would like to thank Yiyin Erin Chen for helpful conversations and manuscript review, the Ragon Institute Flow Core (director Michael Waring) for training and assistance in flow cytometry and multiplex ELISA analysis, the MIT Division of Comparative Medicine (DCM) veterinary and husbandry staff, MIT DCM comparative pathology staff member Caroline Atkinson for helpful discussions and sample processing, the Koch Institute Genomics Core and MIT BioMicro Center (director Stuart Levine) for sequencing, and members of the Lieberman lab for useful discussions and comments on the manuscript.

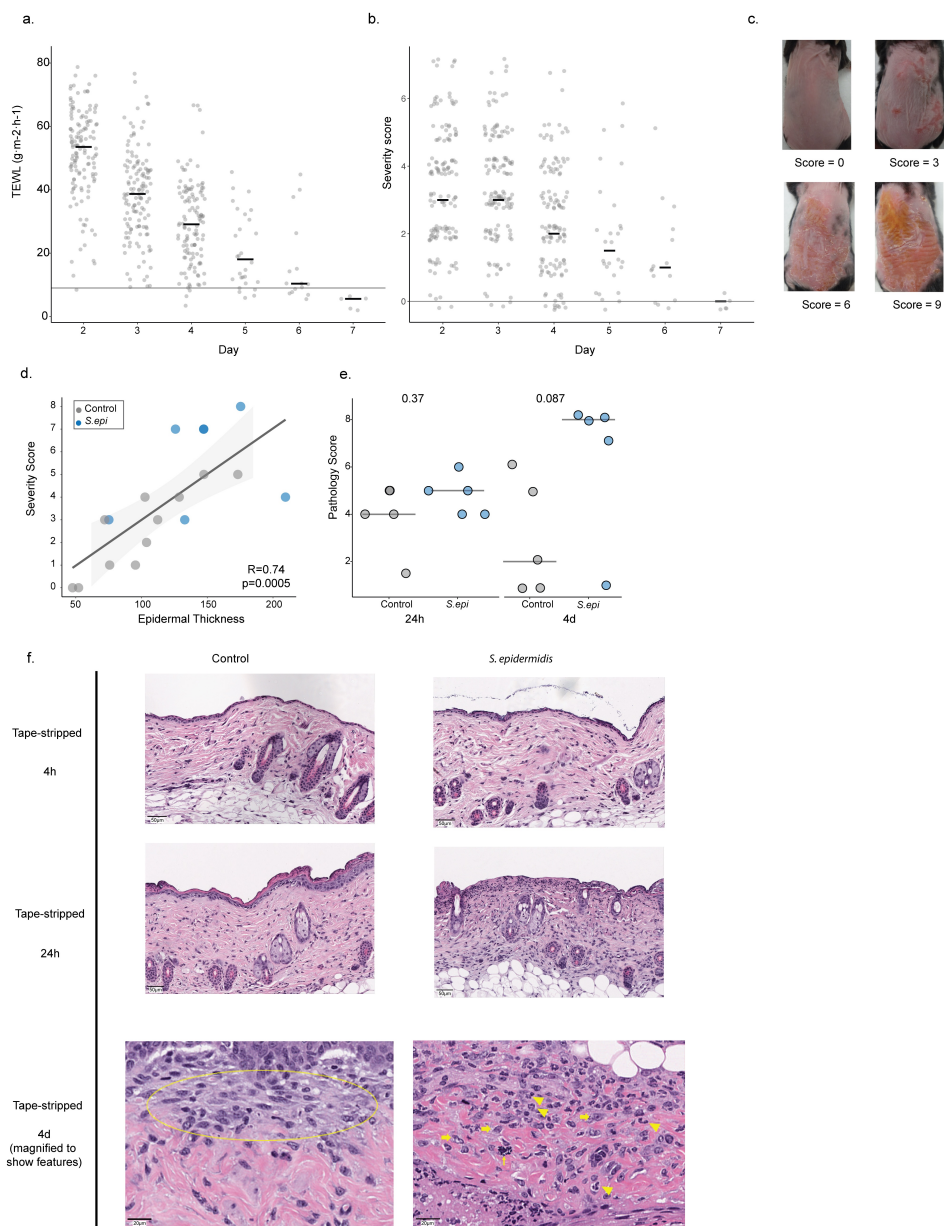
References

1. Conwill, A. *et al.* Anatomy Promotes Neutral Coexistence of Strains in the Human Skin Microbiome. en. *Cell Host & Microbe* **30**, 171–82 7 (2022).
2. Acosta, E. M. *et al.* Bacterial DNA on the Skin Surface Overrepresents the Viable Skin Microbiome en. eLife 12 (June). 2023. <https://doi.org/10.7554/eLife.87192>.
3. Grice, E. A. *et al.* Topographical and Temporal Diversity of the Human Skin Microbiome. en. *Science* **324**, 1190–92 (2009).
4. Wei, M. *et al.* Harnessing diversity and antagonism within the pig skin microbiota to identify novel mediators of colonization resistance to methicillin-resistant *Staphylococcus aureus* en. mSphere. 2023 Aug 24;8(4):e0017723.
5. Nakatsuji, T. *et al.* Antimicrobials from Human Skin Commensal Bacteria Protect against *Staphylococcus Aureus* and Are Deficient in Atopic Dermatitis. en. *Science Translational Medicine* **9**. <https://doi.org/10.1126/scitranslmed.aah4680>. (2017).
6. Williams, M. R. *et al.* Quorum Sensing between Bacterial Species on the Skin Protects against Epidermal Injury in Atopic Dermatitis. af. *et al* **5**. <https://doi.org/10.1126/scitranslmed.aat8329>. (2019).
7. Canovas, J. *et al.* Cross-Talk between *Staphylococcus Aureus* and Other Staphylococcal Species via the Agr Quorum Sensing System. en. *Frontiers in Microbiology* **7**, 223156 (2016).
8. Ramsey, M., Freire, M., Gabriliska, R., Rumbaugh, K. & Lemon, K. *Staphylococcus aureus* Shifts toward Commensalism in Response to *Corynebacterium* Species en. Front Microbiol [Internet]. 2016 [cited 2021 Jan 13];7. Available from: <https://www.frontiersin.org/articles/10.3389/fmicb.2016.01230/full>.
9. Paharik, A. E. *et al.* Coagulase-Negative Staphylococcal Strain Prevents *Staphylococcus Aureus* Colonization and Skin Infection by Blocking Quorum Sensing. en. *Cell Host & Microbe* **22**, 746–56 5 (2017).
10. Kong, H. *et al.* Temporal shifts in the skin microbiome associated with disease flares and treatment in children with atopic dermatitis. en. *Genome Res* **22**, 850–9 (2012).
11. Wanke, I. *et al.* *Staphylococcus aureus* skin colonization is promoted by barrier disruption and leads to local inflammation. en. *Exp Dermatol* **22**, 153–5 (2013).
12. Nakagawa, S. *et al.* *Staphylococcus Aureus* Virulent PSM α Peptides Induce Keratinocyte Alarmin Release to Orchestrate IL-17-Dependent Skin Inflammation. en. *Cell Host & Microbe* **22**, 667–77 5 (2017).
13. Uberoi, A. *et al.* Commensal microbiota regulates skin barrier function and repair via signaling through the aryl hydrocarbon receptor. en. *Cell Host Microbe* **29**, 1235–48 (2021).
14. Naik, S. *et al.* Compartmentalized Control of Skin Immunity by Resident Commensals. en. *Science* **337**, 1115–19 (2012).
15. Wang, G. *et al.* Bacteria induce skin regeneration via IL-1 β signaling. en. *Cell Host Microbe* **91** (May 2021).
16. Zheng, Y. *et al.* Commensal *Staphylococcus Epidermidis* Contributes to Skin Barrier Homeostasis by Generating Protective Ceramides. en. *Cell Host & Microbe* **30**, 301–13 9 (2022).
17. Cau, L. *et al.* *Staphylococcus Epidermidis* Protease EcpA Can Be a Deleterious Component of the Skin Microbiome in Atopic Dermatitis. en. *The Journal of Allergy and Clinical Immunology* **147**, 955–66 16 (2021).
18. Burian, M., Bitschar, K., Dylus, B., Peschel, A. & Schitteck, B. The Protective Effect of Microbiota on *S. Aureus* Skin Colonization Depends on the Integrity of the Epithelial Barrier. en. *The Journal of Investigative Dermatology* **137**, 976–79 (2017).
19. Leung, D., Berdyshev, E. & Goleva, E. Cutaneous barrier dysfunction in allergic diseases. ga. *J Allergy Clin Immunol* (June 6, 2020).
20. Gevers, D. *et al.* The treatment-naïve microbiome in new-onset Crohn’s disease. en. *Cell Host Microbe* **12;15(3):382–92** (Mar. 2014).
21. Clausen, M. *et al.* Association of Disease Severity With Skin Microbiome and Filaggrin Gene Mutations in Adult Atopic Dermatitis. en. *JAMA Dermatol* **1;154(3):293–300** (Mar. 2018).
22. Belheouane, M. *et al.* Assessing similarities and disparities in the skin microbiota between wild and laboratory populations of house mice. en. *ISME J* **Oct;14(10):2367–80** (2020).
23. Gimblet, C. *et al.* Cutaneous Leishmaniasis Induces a Transmissible Dysbiotic Skin Microbiota that Promotes Skin Inflammation. en. *Cell Host Microbe* **22**, 13–24 (2017).
24. Won, Y. *et al.* Identification of *Staphylococcus xylosum* isolated from C57BL/6J-Nos2(tm1Lau) mice with dermatitis. en. *Microbiol Immunol* **46**, 629–32 (2002).

25. Reshamwala, K. *et al.* Identification and characterization of the pathogenic potential of phenol-soluble modulin toxins in the mouse commensal *Staphylococcus xylosus*. en. *Front Immunol* **13** (2022).
26. Naik, S. *et al.* Commensal-Dendritic-Cell Interaction Specifies a Unique Protective Skin Immune Signature. en. *Nature* **520**, 104–8 (2015).
27. Saleh, F., Kheirandish, F., Azizi, H., Azizi, M. & Departement, D. Molecular diagnosis and characterization of *Bacillus subtilis* isolated from burn wound in Iran. en. *Res Mol Med* **1;2(2):40–4** (May 2014).
28. Linehan, J. L. *et al.* Non-Classical Immunity Controls Microbiota Impact on Skin Immunity and Tissue Repair. en. *Cell* **172**, 784–96 18 (2018).
29. Taddese, R. *et al.* Production of inactivated gram-positive and gram-negative species with preserved cellular morphology and integrity. en. *J Microbiol Methods* (May 1, 2021).
30. Y, E. C. *et al.* *Decoding commensal-host communication through genetic engineering of Staphylococcus epidermidis [Internet]. bioRxiv* en. p. 664656. Available from: Jan. 25, 2019. <https://www.biorxiv.org/content/10.1101/664656v1.abstract>.
31. Asarch, A., Barak, O., Loo, D. & Gottlieb, A. Th17 cells: a new paradigm for cutaneous inflammation. en. *J Dermatolog Treat* **19**, 259–66 (2008).
32. Cai, Y. *et al.* Pivotal role of dermal IL-17-producing $\gamma\delta$ T cells in skin inflammation. en. *Immunity* **28;35(4):596–610** (Oct. 2011).
33. Lin, A. *et al.* Mast cells and neutrophils release IL-17 through extracellular trap formation in psoriasis. en. *J Immunol* **1;187(1):490–500** (July 2011).
34. Landén, N., Li, D. & Ståhle, M. Transition from inflammation to proliferation: a critical step during wound healing. en. *Cell Mol Life Sci* **1;73(20):3861–85** (Oct. 2016).
35. Leech, J. *et al.* Toxin-Triggered Interleukin-1 Receptor Signaling Enables Early-Life Discrimination of Pathogenic versus Commensal Skin Bacteria. en. *Cell Host Microbe* **809** (Dec. 2019).
36. Singh, S., Young, A. & McNaught, C. The physiology of wound healing. en. *Surgery* **1;35(9):473–7** (Sept. 2017).
37. Adair-Kirk, T. & Senior, R. Fragments of extracellular matrix as mediators of inflammation. mt. *Int J Biochem Cell Biol* **40**, 1101–10 (2008).
38. Michopoulou, A. & Rousselle, P. How do epidermal matrix metalloproteinases support re-epithelialization during skin healing? jv. *Eur J Dermatol* **1**, 33–42 (Apr. 25, 2015).
39. Hattori, N. *et al.* MMP-13 plays a role in keratinocyte migration, angiogenesis, and contraction in mouse skin wound healing. en. *Am J Pathol* **Aug;175(2):533–46** (2009).
40. Herrick, S. *et al.* Up-regulation of elastase in acute wounds of healthy aged humans and chronic venous leg ulcers are associated with matrix degradation. en. *Lab Invest* **Sep;77(3):281–8** (1997).
41. Bergmeier, V. *et al.* Identification of a myofibroblast-specific expression signature in skin wounds. en. *Matrix Biol* (Jan. 2018).
42. Lee, J. *et al.* Interleukin-23 regulates interleukin-17 expression in wounds, and its inhibition accelerates diabetic wound healing through the alteration of macrophage polarization. en. *FASEB J* **Apr;32(4):2086–94** (2018).
43. Lecron, J. *et al.* IL-17 and IL-22 are pivotal cytokines to delay wound healing of infected skin. en. *Front Immunol* (Oct. 7, 2022).
44. Joshi, N. *et al.* Comprehensive characterization of myeloid cells during wound healing in healthy and healing-impaired diabetic mice. en. *Eur J Immunol* **50**, 1335–49 (2020).
45. Takagi, N. *et al.* IL-17A promotes neutrophilic inflammation and disturbs acute wound healing in skin. *Experimental dermatology* **26**, 137–144 (2017).
46. Strakosha, M. *et al.* Basophils Play a Protective Role in the Recovery of Skin Barrier Function from Mechanical Injury in Mice. *Journal of Investigative Dermatology* (2024).
47. Byrd, A. L. *et al.* And Strain Diversity Underlying Pediatric Atopic Dermatitis. en. *Science Translational Medicine* **9**. <https://doi.org/10.1126/scitranslmed.aal4651>. (2017).
48. Chang, H. *et al.* Alteration of the cutaneous microbiome in psoriasis and potential role in Th17 polarization. en. *Microbiome* **5;6(1):154** (Sept. 2018).
49. Williams, M. *et al.* Interplay of Staphylococcal and Host Proteases Promotes Skin Barrier Disruption in Netherton Syndrome. en. *Cell Rep* **33** (Mar. 2020).

50. Khadka, V. *et al.* The Skin Microbiome of Patients With Atopic Dermatitis Normalizes Gradually During Treatment. en. *Front Cell Infect Microbiol* (Sept. 24, 2021).
51. Komatsu, N. *et al.* Human tissue kallikrein expression in the stratum corneum and serum of atopic dermatitis patients. de. *Exp Dermatol* (June 16, 2007).
52. Voegeli, R. *et al.* Increased stratum corneum serine protease activity in acute eczematous atopic skin. it. *Br J Dermatol* (July 1, 2009).
53. Nomura, H. *et al.* Multifaceted Analyses of Epidermal Serine Protease Activity in Patients with Atopic Dermatitis. en. *Int J Mol Sci [Internet]*. Available from: <http://dx.doi.org/10.3390/ijms21030913> (Jan. 30, 2020).
54. Park, B., Iwase, T. & Liu, G. Intranasal application of *S. epidermidis* prevents colonization by methicillin-resistant *Staphylococcus aureus* in mice. es. *PLoS One* **6** (2011).
55. Liu, Y. *et al.* Skin microbiota analysis-inspired development of novel anti-infectives. en. *Microbiome* **5;8(1):85** (June 2020).
56. Zomer, H. & Trentin, A. Skin wound healing in humans and mice: Challenges in translational research. en. *J Dermatol Sci* **1;90(1):3–12** (2018).
57. Diep, B. *et al.* Complete genome sequence of USA300, an epidemic clone of community-acquired methicillin-resistant *Staphylococcus aureus*. en. *Lancet* **4;367(9512):731–9** (Mar. 2006).
58. Olson, M. *et al.* *Staphylococcus epidermidis* agr quorum-sensing system: signal identification, cross talk, and importance in colonization. en. *J Bacteriol* **Oct;196(19):3482–93** (2014).
59. Bolyen, E. *et al.* Reproducible, interactive, scalable and extensible microbiome data science using QIIME 2. en. *Nat Biotechnol* **37**, 852–7 (2019).
60. Callahan, B. *et al.* DADA2: High-resolution sample inference from Illumina amplicon data. en. *Nat Methods* (July 13, 2016).
61. Gupta, S. *et al.* Cutaneous Surgical Wounds Have Distinct Microbiomes from Intact Skin. en. *Microbiol Spectr* **14;11(1):e0330022** (Feb. 2023).
62. Quast, C. *et al.* The SILVA ribosomal RNA gene database project: improved data processing and web-based tools. en. *Nucleic Acids Res* **41** (2013).
63. McMurdie, P. Holmes S. phyloseq: an R package for reproducible interactive analysis and graphics of microbiome census data. en. *PLoS One* **8** (2013).
64. Picelli, S. *et al.* Full-length RNA-seq from single cells using Smart-seq2. no. *Nat Protoc* (Jan. 9, 2014).
65. Gaio, D. *et al.* Hackflex: low-cost, high-throughput, Illumina Nextera Flex library construction. zh. *Microb Genom* (Jan. 8, 2022).
66. Bray, N., Pimentel, H., Melsted, P. & Pachter, L. Near-optimal probabilistic RNA-seq quantification. bg-Latn. *Nat Biotechnol* (May 5, 2016).
67. Pimentel, H., Bray, N., Puente, S., Melsted, P. & Pachter, L. Differential analysis of RNA-seq incorporating quantification uncertainty. en. *Nat Methods* (July 14, 2017).
68. Wu, T. *et al.* *clusterProfiler 4.0: A universal enrichment tool for interpreting omics data* en. *Innovation (Camb)*. 2021 Aug 28;2(3):100141.
69. Ashburner, M. *et al.* Gene ontology: tool for the unification of biology. en. *The Gene Ontology Consortium. Nat Genet* (May 25, 2000).
70. Consortium, G. O. *et al.* The Gene Ontology knowledgebase in 2023. en. *Genetics [Internet]*. Available from: <http://dx.doi.org/10.1093/genetics/iyad031> (May 4, 2023).
71. Blake, J. *et al.* Mouse Genome Database (MGD): Knowledgebase for mouse-human comparative biology. en. *Nucleic Acids Res* **8;49(D1):D981–7** (Jan. 2021).
72. Flanders, K. *et al.* Quantitation of TGF- β proteins in mouse tissues shows reciprocal changes in TGF- β 1 and TGF- β 3 in normal vs neoplastic mammary epithelium. en. *Oncotarget* **21;7(25):38164–79** (June 2016).

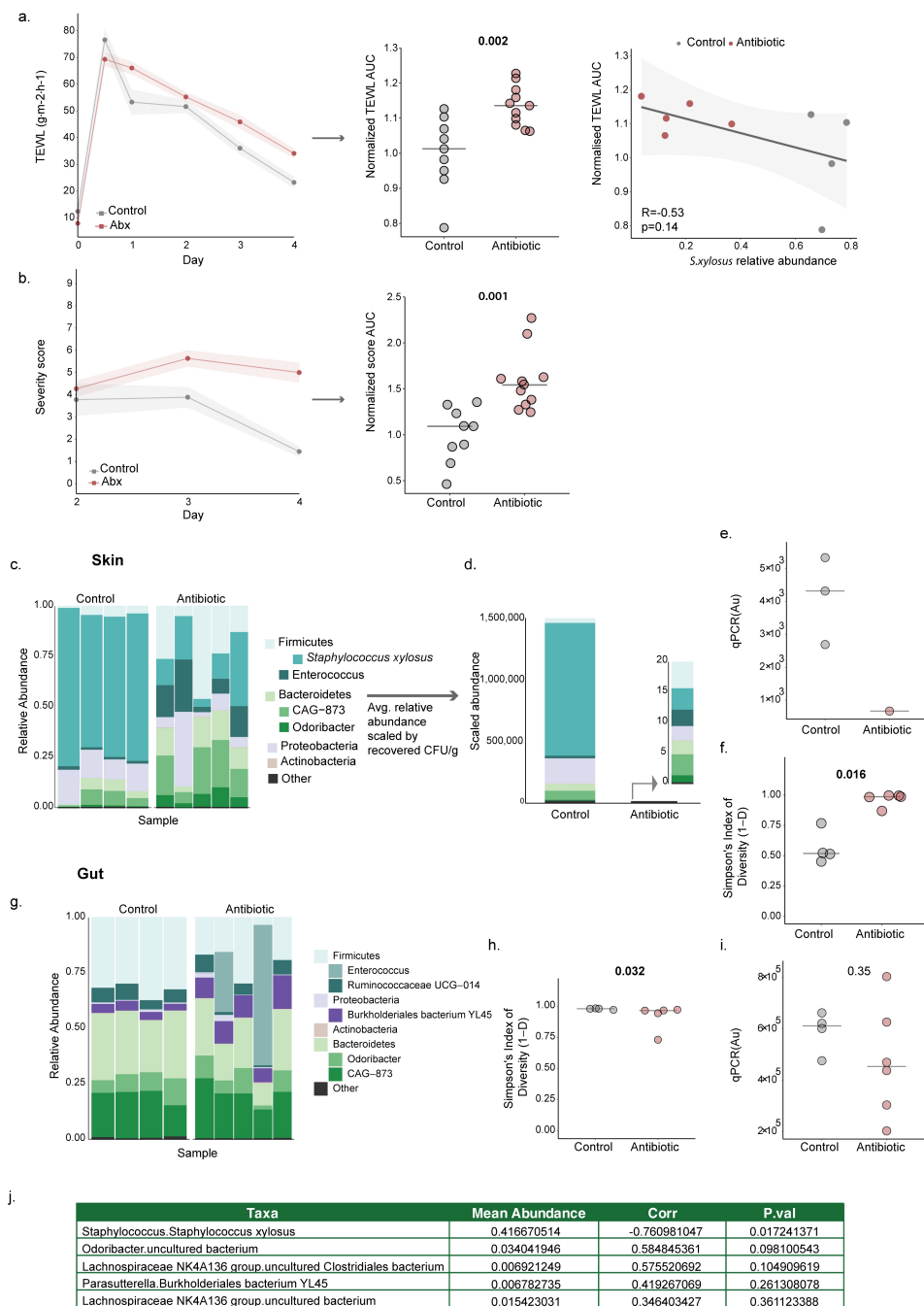
Supplementary Figures



Supplementary Figure 1: *S. epidermidis* induced inflammation and delayed barrier repair at multiple timepoints
(Continued on the following page.)

Supplementary Figure 1: *S. epidermidis* induced inflammation and delayed barrier repair at multiple timepoints

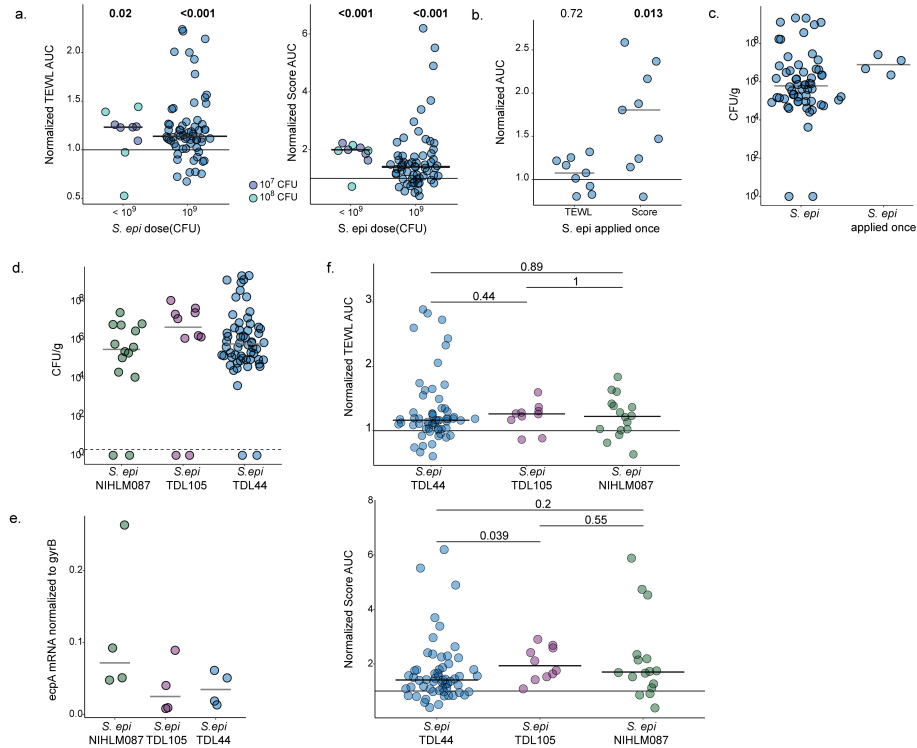
Adult mice had hair removed three days prior to tape-stripping damage (day 0). a and b) Immediately following damage and daily until the endpoint, PBS was applied to skin and TEWL was measured and severity score assessed for up to 7 days. a) TEWL was elevated 2 days after damage and returned to baseline level measured on intact skin (shown as horizontal line) by 7 days after damage. b) Mouse skin thickness (forceps measurement), scale (area) and erythema (redness) were scored for each mouse from 0-3. Cumulative severity score is shown for days 2 through 7 after damage. Skin was comparable to healthy skin (score of 0) by 7 days after damage. Values have been jittered to better represent overlapping data points. c) Representative images of mice with skin severity scores as indicated beneath each picture. d-g) PBS or *S. epidermidis* was applied to skin immediately after tape-stripping and then daily until experimental endpoint. d) Raw skin severity score correlates significantly with epidermal thickness measured from histology sections (H&E-stained sections of a subset of animals were imaged and average epidermal thickness calculated using ImageJ). Pearson's correlation coefficient $R=0.74$, $P=0.0005$ (control $N=11$, *S. epidermidis* $N=6$). e) H&E-stained sections were examined by a veterinary pathologist and scored for crust and neutrophil infiltrates of dermis and subcutaneous fat. Cumulative pathology scores are shown and were increased in *S. epidermidis*-exposed mice 4 days after tape-stripping damage ($P=0.087$, control $N=5$, *S. epidermidis* $N=5$ per timepoint). f) Representative H&E-stained sections from animals sacrificed 4h (top), 24h (middle), and 4 days (bottom) after tape-stripping damage and application of either vehicle or *S. epidermidis*. By 24h, there was clear regeneration of the epidermis in control mice, absent from *S. epidermidis* mice. 4 days after damage, *S. epidermidis*-exposed mice had significantly increased dermal inflammation and epidermal ulceration compared to controls as described in main text and Fig. 3a. Images are shown here at 30x magnification to highlight the epidermal fibroblasts present in vehicle controls (yellow circle) and the specific inflammatory infiltrates present in *S. epidermidis*-exposed mice: neutrophils (arrowheads), fibroblasts (large arrow) and infrequent mast cells (small arrow). Throughout, symbols indicate individual mice. Bars in a, b and e indicate median. Rank sum test was used to compare groups.



Supplementary Figure 2: Oral antibiotic treatment depleted the skin microbiome with minimal impact on gut microbiome
Continued on the following page.)

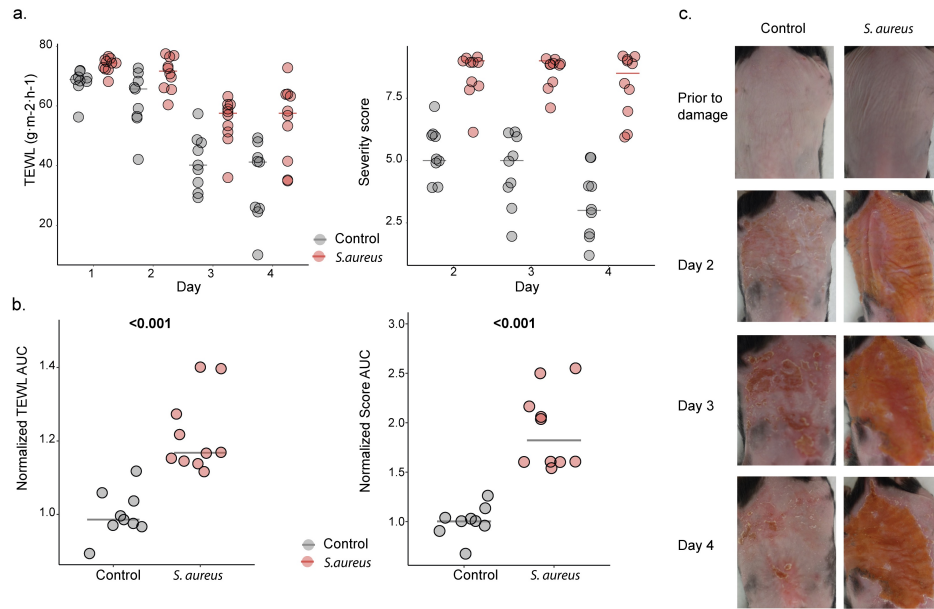
Supplementary Figure 2: Oral antibiotic treatment depleted the skin microbiome with minimal impact on gut microbiome

Mice were given an oral antibiotic cocktail designed to target the skin microbiome for two weeks prior to tape-stripping barrier damage. a) Daily TEWL values (left) were summarized per animal using AUC and normalized to cohort control (no antibiotic) average (middle) and correlated with relative abundance of *S. xyloso* as measured by 16s sequencing (right). b) Daily severity score measurements (left) were summarized per animal using AUC and normalized to cohort control (right). c-i) Animals were sacrificed 4 days after barrier damage and skin was swabbed to collect skin microbiome samples; colon samples were collected for gut microbiome analysis (control N=4 and antibiotics N=5). DNA was extracted and 16s amplicon sequencing performed to define the microbiome. c-f) Analysis of the skin microbiome. There was a dramatic change in skin microbiome composition as a result of antibiotic treatment. c) Relative abundance of bacterial taxa at multiple phylogenetic levels is shown. Bars indicate individual mice. *S. xyloso* dominates control mouse skin microbiome while many taxa comprise skin microbiome of antibiotic-treated mice. d) To demonstrate the depletion of the skin microbiota in antibiotic-treated mice, scaled abundance was calculated and is shown here. Scaled abundance reflects the average relative abundance of each taxa (per experimental group) as measured by sequencing multiplied by the average CFU/g recovered from endpoint skin homogenate CFU (plated on mannitol salt agar). e) qPCR using universal 16s rRNA primers was used to quantify total bacterial load present on skin. Many skin swab samples from antibiotic-treated mice were comparable to water control and thus are not shown; one sample with detectable DNA was significantly lower than skin swab samples collected from control animals consistent with CFU plating (Fig. 1b). f) Simpson's diversity was higher in antibiotic-treated mice compared to controls (P=0.016). g-i) Analysis of the colon microbiome. In most mice analyzed, there were no significant changes in gut microbiome composition as a result of antibiotic administration. g) Relative abundance of bacterial taxa at multiple phylogenetic levels is shown. Bars indicate individual mice. h) Simpson's diversity was significantly decreased (P=0.016) in antibiotic-treated mice, due to one mouse with a dramatic decrease in overall microbiome diversity. i) qPCR with universal 16s primers was used to quantify the total amount of bacterial DNA present in sequenced samples. There was no significant difference in total bacterial DNA detected in control versus antibiotic treated colon samples (P=0.35). For strip-plots, symbols represent mice and bars indicate medians. For line-plots, symbols indicate mean and shading indicates SEM. Rank sum test was used to compare medians.



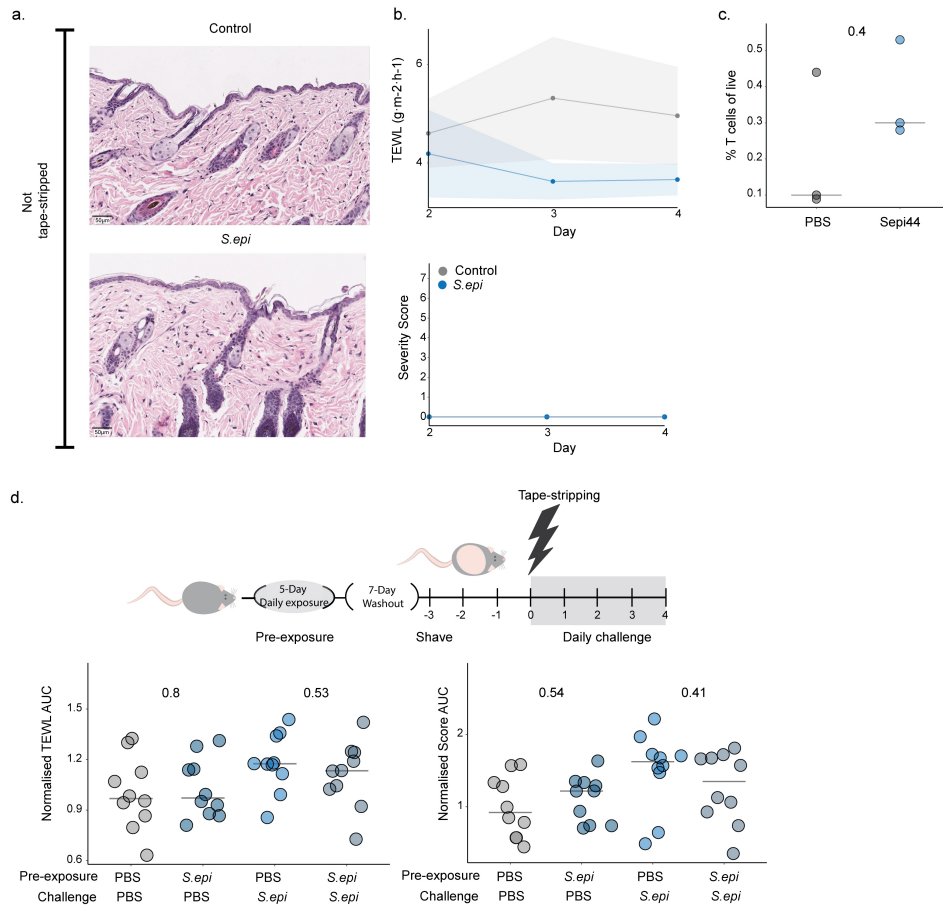
Supplementary Figure 3: Multiple strains of *S. epidermidis* colonize tape-stripped skin, express *ecpA* and delay healing

Multiple doses and strains of *S. epidermidis* were recovered from skin at experimental endpoint and are shown to express the bacterial protease *ecpA*. a) Adult mice had hair removed three days prior to tape-stripping damage (day 0). PBS or *S. epidermidis* was applied to skin immediately after tape-stripping and then daily until experimental endpoint. TEWL (left) and severity score (right) were significantly elevated when either a lower dose (107 or 108 as indicated by color) or 109 CFUs of *S. epidermidis* were applied daily (107 N=5, 108 N=4, 109 N=64). Numbers shown are p-values from rank-sum test comparing *S. epidermidis*-exposed group of specified dose to vehicle control. b) 109 CFUs of *S. epidermidis* was applied only immediately after tapestripping (*S. epi* applied once). *S. epidermidis* applied once did not significantly increase TEWL (P=0.72) but did significantly increase skin severity score (P=0.013) compared to cohort vehicle controls demonstrating an intermediate phenotype with decreased incidence of *S. epidermidis* exposure (PBS N=10, *S. epidermidis* N=9). c) We recovered a comparable amount of viable *S. epidermidis* after daily application (24h after last application, *S. epi*) and four days after application (*S. epi* applied once) suggesting that *S. epidermidis* is able to persistently colonize damaged skin in our model. d) The three strains of *S. epidermidis* used in Fig. 2b were recovered from skin homogenate (24h after last application) at a similar microbial load, demonstrating comparable colonization of skin across strains (Sepi-NIHLM087 N=14, Sepi-TDL105 N=10, Sepi-TDL44 N=58). e) RNA was isolated from three strains of *S. epidermidis* used in Fig. 2b after growth as 1:100 subcultures from overnight cultures. qPCR was used to quantify expression of the known virulence factor protease *ecpA* (normalized to housekeeping gene *gyrB*) and was comparable across strains (N=4 biological replicates of overnight and subculture per strain). f) Pairwise rank-sum comparisons of TEWL (top) and severity score (bottom) were not significantly different between mice exposed to different strains of *S. epidermidis* after correction for multiple hypotheses (Bonferroni correction).



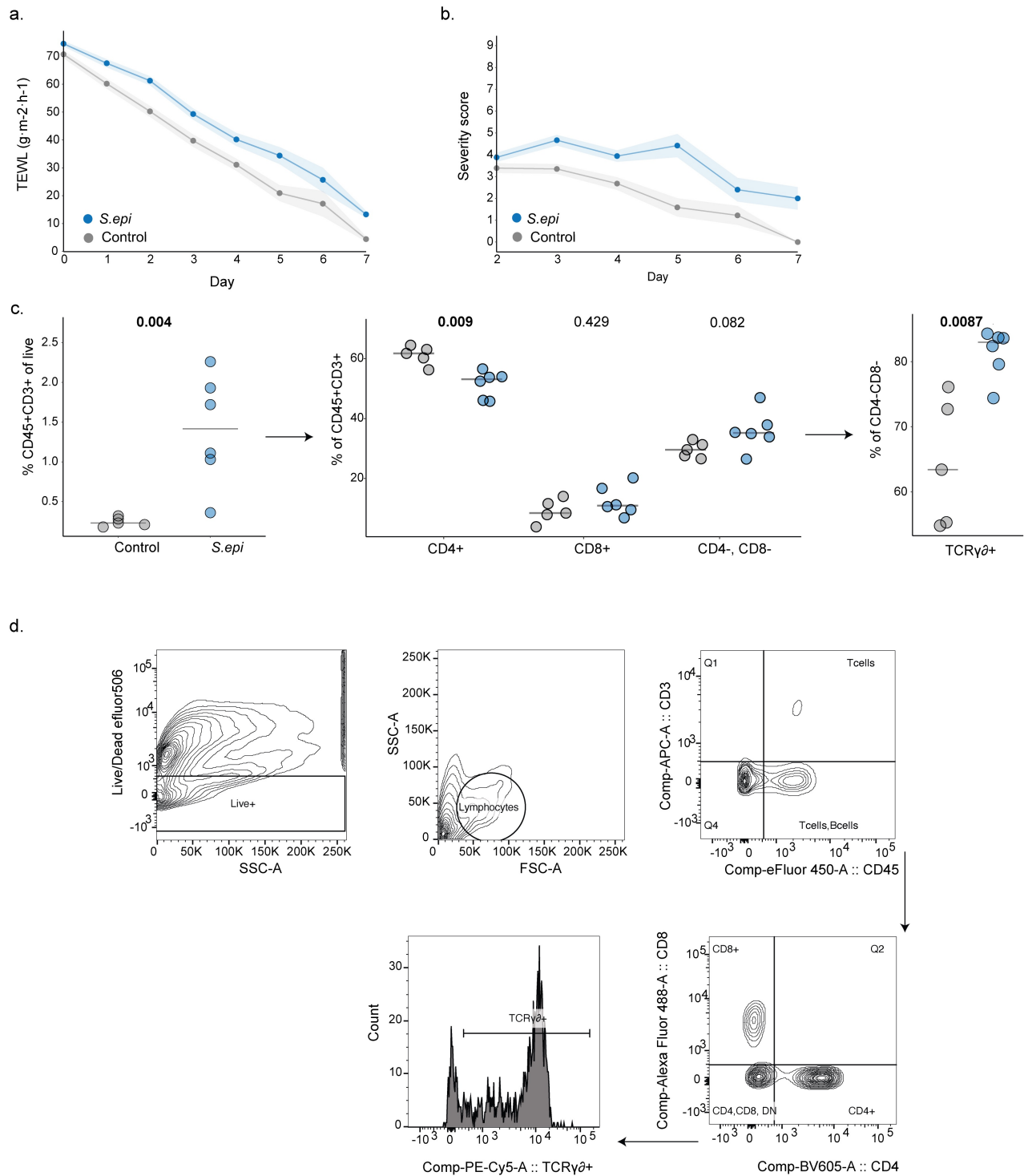
Supplementary Figure 4: Mice exposed to *S. aureus* after tape-stripping do not heal 4 days post-damage

PBS or *S. aureus* USA300 was applied to skin immediately after tape-stripping and then daily until experimental endpoint (control N=9 and *S. aureus* N=10). a) Raw TEWL and severity score values were elevated in *S. aureus*-exposed mice for the duration of the experiment. Raw score is shown to demonstrate the number of *S. aureus*-exposed animals with maximal severity score. b) Normalized TEWL and severity score AUC are significantly higher in *S. aureus*-exposed mice compared to controls, rank sum test, P=0.00002 and P=0.00002. c) Representative images of control (left) and *S. aureus*-exposed (right) skin prior to damage (top) and throughout the post-damage exposure period. Mice were equivalent prior to tape-stripping and exposure. A thick, red crust covered the majority of the tape-stripped skin of *S. aureus*-exposed mice from day two onward compared to the minimal crust and redness observed in PBS control mice.



Supplementary figure 5: Application of *S. epidermidis* to intact skin had no effect on skin barrier function or subsequent response to tape-stripping damage

a-c) Three days after hair removal, either PBS or *S. epidermidis* was applied to intact skin of mice for four days. a) Representative H&E stained sections after four days of PBS or *S. epidermidis* application (no tape-stripping damage). Histopathological analysis indicated no change in skin pathology or morphology as a result of *S. epidermidis* application. b) TEWL (top) and severity score (bottom) were assessed daily during the exposure period. TEWL values remained in the undamaged baseline range (2-10 g/m²/h) and no changes in gross morphology (thickness, erythema or scale) were noted so all mice had a score of 0 throughout the exposure period. c) We observed a trend towards an increase in bulk T-cells in mice exposed to *S. epidermidis* after seven days of bacterial application on intact skin. d) pre-damage exposure model (top): PBS or 10⁹ CFUs of *S. epidermidis* were gently pipetted and then spread across intact skin (no hair removal) daily for five days followed by a seven-day washout period. Hair was then removed and three days later mice were subjected to one round of tape-stripping damage. Either PBS or *S. epidermidis* was applied to skin immediately following tape-stripping and then daily until endpoint. TEWL AUC (bottom left) and severity score AUC (bottom right) normalized to the cohort control (PBS::PBS) was elevated in mice exposed to *S. epidermidis* during damage compared to mice exposed to PBS during damage regardless of prior exposure. There was no effect of pre-exposure to *S. epidermidis* when comparing groups exposed to PBS after damage, suggesting that exposure during health to *S. epidermidis* does not improve healing from tape-stripping barrier damage. (Pre-exposure::challenge exposure: PBS::PBS N=11, PBS::Sepi N=10, Sepi::PBS N=11, Sepi::Sepi-TDL44 N=11). Symbols indicate individual mice and lines indicate median.

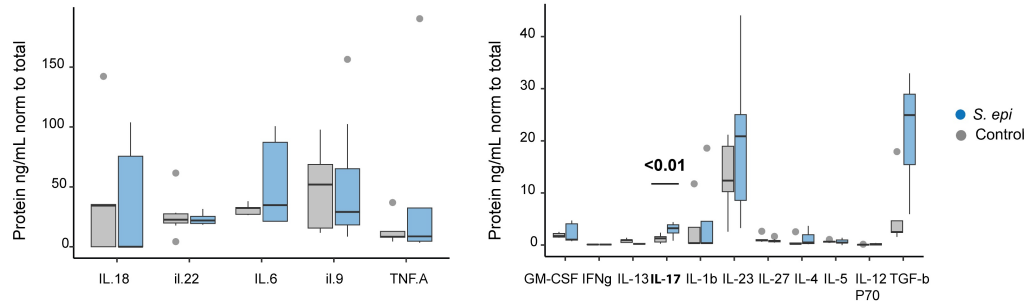


Supplementary Figure 6: *S. epidermidis* applied after damage induces T cell response.
(Continued on the following page.)

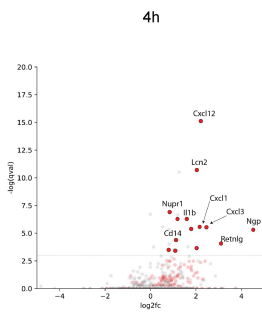
Supplementary Figure 6: *S. epidermidis* applied after damage induces T cell response.

Mice had hair removed three days prior to tapestripping damage. PBS or *S. epidermidis* was applied to skin immediately after tape-stripping and then daily until experimental endpoint (control N=4, *S. epidermidis* N=6). TEWL was measured daily while severity score was measured starting 2 days after damage (prior to 48h skin is unchanged in gross morphology). a) TEWL and b) severity score were elevated in *S. epidermidis*-exposed mice compared to controls for 7 days after damage. Controls were indistinguishable from un-tape-stripped mice on day seven (score =0) while *S. epidermidis*-exposed mice had non-zero scores on day seven. Symbols indicate mean and shading indicates SEM. c) Flow cytometry was used to measure T cell populations in the skin 7 days after barrier damage. Mice exposed to *S. epidermidis* showed a significant increase in total T-cell abundance (left, P=0.004), with a decrease in CD4+ T cells (middle, P=0.009) and an increase in $\gamma\delta$ T cells (right, P=0.0087). Despite this increase in T cells, mice exposed to *S. epidermidis* remained more damaged than controls on day seven indicating that T cell induction did not improve barrier function. Symbols indicate individual mice and lines indicate median. d) Gating strategy used to identify T cell subsets. Antibodies used as follows: blocking antibody CD16/32, amine reactive live/dead effluor 506, CD4 SuperBright600, CD8 Alexa488, CD45-PE, CD3-APC, TCRg/d-PeCy5 (Thermofisher).

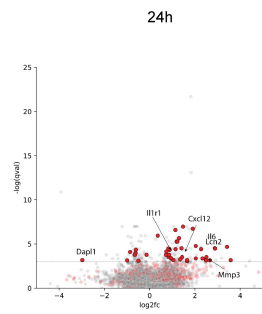
a.



b.



c.

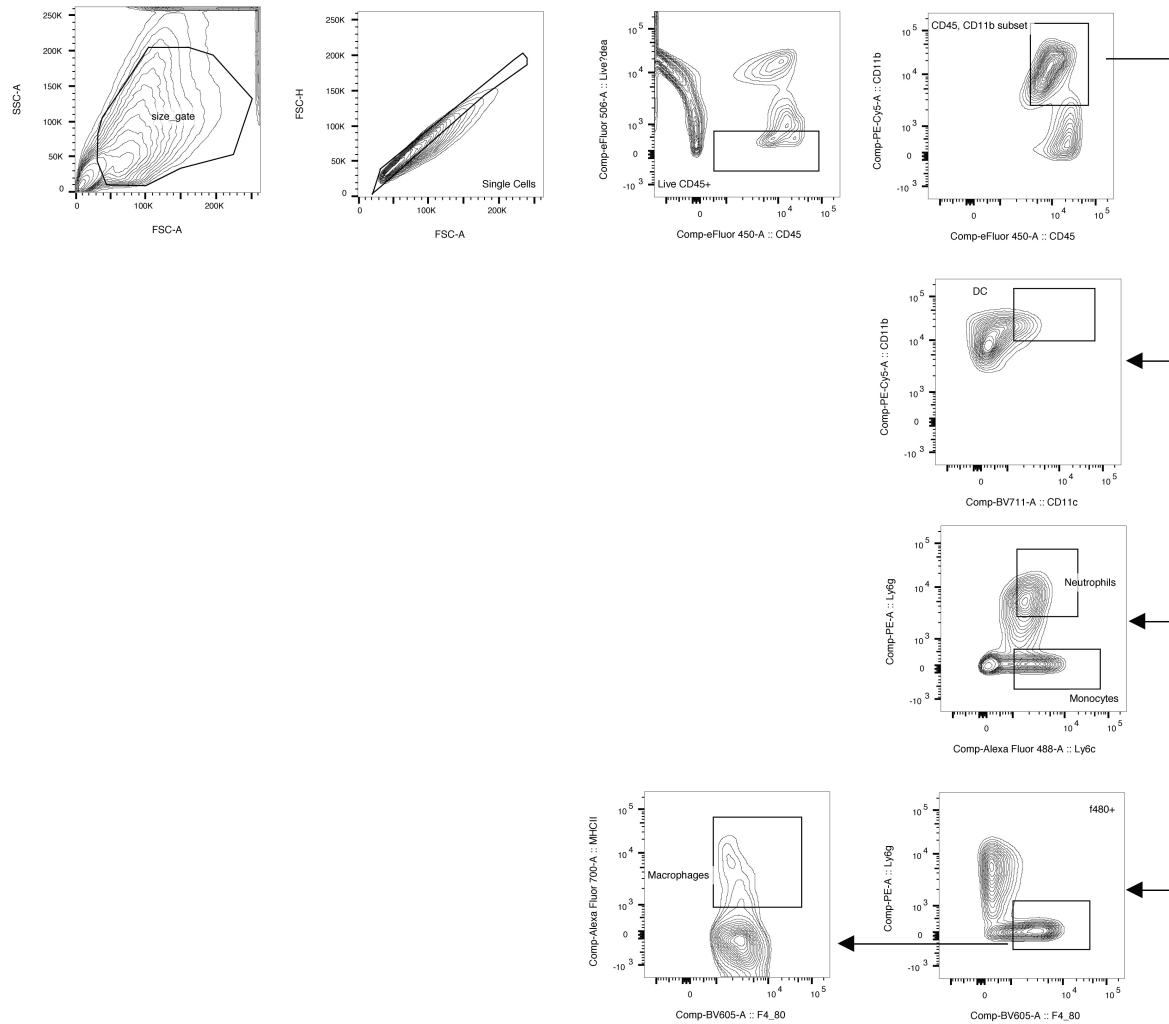


d.



Supplementary Figure 7: *S. epidermidis* increased IL-17A protein and broadly upregulated innate immune response in the skin

PBS or *S. epidermidis* was applied to skin immediately after tape-stripping and then daily until experimental endpoint. a) Mice were sacrificed on day 3 after damage. Protein was extracted from skin lysates. Total protein was measured by Bradford assay and cytokine proteins were measured using multiplex ELISA. *S. epidermidis*-exposed mice had significantly increased IL-17 protein (rank sum test, $P=0.0008$). Other increased cytokine protein levels in *S. epidermidis*-exposed mice were not significant after Benjamini Hochberg correction for multiple comparisons (control $N=9$, *S. epidermidis* $N=11$). b-d) Animals were sacrificed 4h (b), 24h (c) and 4 days (d) after damage and exposure to PBS or *S. epidermidis* and skin samples were used for RNAseq analysis. Transcripts were aligned to the mouse transcriptome and differential expression analysis was performed at the gene-level. Genes annotated as part of the immune response in the Mouse Genome Database are shown in red; all other genes are shown in gray. Dashed line indicates statistical significance of $P=0.05$. Genes of interest are highlighted with text and arrows (4h control $N=5$, *S. epidermidis* $N=5$; 24h control $N=4$, *S. epidermidis* $N=5$; 4 days control $N=6$, *S. epidermidis* $N=9$).



Supplementary Figure 8: Flow cytometry gating strategy for innate immune cell populations in skin

Flow cytometry gating strategy to identify innate immune cell subpopulations (neutrophils, macrophages, and conventional dendritic cells) from digested flank skin. Antibodies used were as follows: Ly6G-PE, F4/80-BrilliantViolet600, CD11c-BV711, MHCII-Alexa700, CD11b-PECy5, Ly-gC-Alexa488, CD45-efluor450, CD3-APC.

4. Conclusions and Future Perspectives

The host and its microbiome are entangled in an intricate web of interactions between and among themselves. The ramifications of these interactions impact the holistic health of the host, with consequences for education of the immune system [1], social behaviors [2], and the exacerbation of, if not direct contribution to, host disorders like cancer [3–5], diabetes [6], and assorted inflammatory diseases [7–9]. This work uses the ecological niche of the skin and its microbes to probe the impact of microbial colonization on host health.

Healthy human skin can be subcategorized into sebaceous (oily), moist and dry sites, each of which support their own unique set of microbes which generally feature members of the *Cutibacterium*, *Staphylococcus*, and *Corynebacterium* genera [10]. The composition of the skin microbiome has been extensively studied by both culture-dependent [11] and independent (sequencing) techniques [10, 12]. It is well understood that inflammatory skin disease is characterized by rapid decreases in microbiome diversity [13] and a rise in abundance of *Staphylococcus* species, particularly the well-known pathogen *Staphylococcus aureus*.

I recapitulated this result in the second chapter, where I analyzed the skin microbiome of a cohort of 28 children with Atopic Dermatitis (AD) via amplicon sequencing over the course of treatment. This study was the largest and longest (three months) survey of the skin microbiome during treatment for AD. This study showed that both conventional treatment and treatment with dilute bleach baths helped to reduce the amount of *S. aureus* on the skin, allowing the skin microbiome to slowly normalize. In the future, datasets like these could be used to develop a better understanding of *Staphylococcus* species involved in the exacerbation of AD: some studies have shown that common skin resident *Staphylococcus epidermidis* can similarly underlie AD [14, 15], but other *Staphylococcus* species may similarly be at play.

These broad surveys of microbial presence on the skin are insufficient for developing an understanding of functional consequences, however. As sequencing technologies advance in sophistication and decline in cost, studies of the skin microbiome now aim to better characterize strain-level, rather than genus-level dynamics as a means to explore the functional consequences of microbial colonization [16].

Previous work in the Lieberman lab leveraged data from individual *S. aureus* genomes to detect significantly more genomes with truncations in genes encoding their external polysaccharide capsules on patients with AD [17], but failed to uncover a motivating functional mechanism. Such sequencing-based studies are limited to serving as a post-hoc census of microbial residents that cannot reliably address questions of function. Similarly, work done to elucidate key mutational drivers of colonization in *S. aureus* genomes functionally verified very few of the many predicted mutations [18], further highlighting the many processes that lie between DNA and function: transcriptional or post-transcriptional regulation, community interactions, etc. Forward-looking studies must thus not rely solely on genomic data, but directly assess the functional contributions of individual microbiome

residents through the generation of testable hypotheses.

In my third chapter, I more directly probed the consequences of colonization of skin colonization by using an animal model to approximate skin barrier damage, and measured the effect on healing by applying several different skin resident microbes, mimicking topical probiotic treatment. The model of mechanical skin barrier damage used, tape-stripping, damages only the topmost layer of skin (the epidermis), leaving the dermis intact. This form of barrier damage is perhaps most reflective of the more mild, everyday damage skin experiences, and can be thought of as akin to damage induced by scratching in AD [19].

I found that the application of skin resident microbes to this damaged skin barrier was comprehensively damaging to the host: mice exposed to any skin resident bacteria experienced delayed healing compared to their control counterparts. This delayed healing effect was mediated by the innate immune system, contrary to reports of protective effects seen after adaptive immune system engagement with microbes on healthy skin [20–22], suggesting the importance of host barrier context in microbial exposure and the resulting immune responses. Specifically, I show that the generation of cytokines such as IL-17 in response to the model commensal *S. epidermidis*, shown to have important implications for anti-parasitic immune response and wound healing during health, was associated with damaging inflammation in our model and is associated with delayed healing in chronic wounds [23, 24]).

Interestingly, while supplementation of the skin microbiome with native skin commensals was detrimental to the host, the overall presence of the native skin microbiome was important for improved healing responses, as depletion of the skin microbiota delayed healing. While my work was focused on understanding the role of individual microbes on barrier repair, this result suggests that the application of a microbial consortia to a damaged barrier may be beneficial to the host, either through synergistic effects between microbes, or microbe-microbe interactions that downregulate key virulence factors such as those between *B. subtilis*, *S. hominis* and *S. aureus* [25, 26]. It remains a possibility that while the supplementation of the skin microbiome is detrimental to the host, the presence of native commensals at various microbiota sites throughout the body (not just the skin) is critical for the generation of overall healing responses in the skin. Further characterisation of the gut and skin microbiota, as well as broader systemic immune responses, of mice treated with *S. epidermidis* or other native commensals could help to disentangle the effects of various microbiota on overall health.

Further studies could also be performed to understand the importance of host factors on the response to commensal microbes across a damaged barrier. It is well-understood that immune responses to commensal microbes vary throughout life: early life and weaning represent an important window for the education of the immune system [27] and the development of commensal tolerance [22], adults and neonates respond to commensals differently [22], and individuals later in life are susceptible to an “inflammaging” phenomenon characterized by chronic inflammation and decreased immune response [28]. Though my work focused on adult mice in order to best capture responses to microbes during adulthood, understanding whether microbial exposure during weaning could result in heightened tolerance and whether microbial exposure during aging could result in more severe disease is critical to developing a broader understanding of host-microbe dialogue throughout life. Additionally, while my work was focused on understanding the immune effects of barrier damage in C57BL/6 mice, the use of different strains of mice, which are known to exhibit well-characterized differences in immune profile (for example, Balb/c mice exhibit a Th2 immune response bias [29]) could present a straightforward path to disentangling the contributions of various arms of the immune

system to the observed delayed healing response to skin commensals.

In related work (Appendix I), I found that application of a common probiotic species, *Limosilac-tobacillus reuteri* [30], showed a strong trend toward improving skin barrier healing when applied in a similar manner to tapestripped skin. Although there has been active interest in developing a topical probiotic for inflammatory skin diseases like AD, many of these studies have not met much success [26, 31]. Furthermore, due to variation in treatment regimen, dosing, patient demographics, and compound formulation, there has been no strong consensus on the efficacy of topical probiotics for AD [32]. The skin abrasion model presented in this work could thus be used to standardize the development of topical probiotic or therapeutic microbial formulations: it offers a platform across which many species and strains could be tested across homogeneous conditions. Under this paradigm, it would be pragmatic to start with several candidate *Lactobacillus* species, which have shown some efficacy in AD, such as *Lactobacillus rhamnosus* [33], *Lactobacillus salivarius* [34], *Lactobacillus paracasei* [35] and *Lactobacillus plantarum* [36].

The human body is estimated to be home to 38 trillion bacteria [37], and yet we understand very little of our interactions with these microscopic residents. It is important to not only understand which microbes are present, but the consequences of their colonization for the host. In this work, I present both a landscape of microbial residents during inflammatory skin disease and dynamics in their population during treatment, as well as a more direct interrogation of the functional consequences of colonization on damaged skin. Developing a better understanding of skin microbiome dynamics and their consequences for the host is integral to not just a better understanding of health, but for the production of efficacious probiotic therapies.

References

1. Graham, D. B. & Xavier, R. J. Conditioning of the Immune System by the Microbiome. en. *Trends in Immunology* **44**, 499–511 (2023).
2. Archie, E. A. & Tung, J. Social behavior and the microbiome. *Current opinion in behavioral sciences* **6**, 28–34 (2015).
3. Christl, S., Gibson, G. & Cummings, J. Role of Dietary Sulphate in the Regulation of Methanogenesis in the Human Large Intestine. en. *Gut* **33**, 1234–38 (1992).
4. Scanlan, P. D. *et al.* Culture-Independent Analysis of the Gut Microbiota in Colorectal Cancer and Polyposis. en. *Environmental Microbiology* **10**, 789–98 (2008).
5. Cullin, N., Antunes, C. A., Straussman, R., Stein-Thoeringer, C. K. & Elinav, E. Microbiome and Cancer. en. *Cancer Cell* **39**, 1317–41 (2021).
6. Wen, L. *et al.* Innate Immunity and Intestinal Microbiota in the Development of Type 1 Diabetes. en. *Nature* **455**, 1109–13 (2008).
7. Ley, R. E., Turnbaugh, P. J., Klein, S. & Gordon, J. I. Microbial Ecology: Human Gut Microbes Associated with Obesity. en. *Nature* **444**, 1022–23 (2006).
8. Frank, D. N. *et al.* Molecular-Phylogenetic Characterization of Microbial Community Imbalances in Human Inflammatory Bowel Diseases. en. *Proceedings of the National Academy of Sciences of the United States of America* **104**, 13780–85 (2007).
9. Schommer, N. N. & Gallo, R. L. Structure and Function of the Human Skin Microbiome. en. *Trends in Microbiology* **21**, 660–68 (2013).
10. Costello, E. K. *et al.* Bacterial Community Variation in Human Body Habitats across Space and Time. en. *Science* **326**, 1694–97 (2009).
11. Timm, C. M. *et al.* Isolation and Characterization of Diverse Microbial Representatives from the Human Skin Microbiome. en. *Microbiome* **8**, 58 (2020).
12. Grice, E. A. *et al.* Topographical and Temporal Diversity of the Human Skin Microbiome. en. *Science* **324**, 1190–92 (2009).
13. Kong, H. *et al.* Temporal shifts in the skin microbiome associated with disease flares and treatment in children with atopic dermatitis. en. *Genome Res* **22**, 850–9 (2012).
14. Byrd, A. L. *et al.* And Strain Diversity Underlying Pediatric Atopic Dermatitis. en. *Science Translational Medicine* **9**. <https://doi.org/10.1126/scitranslmed.aa14651>. (2017).
15. Cau, L. *et al.* Staphylococcus Epidermidis Protease EcpA Can Be a Deleterious Component of the Skin Microbiome in Atopic Dermatitis. en. *The Journal of Allergy and Clinical Immunology* **147**, 955–66 16 (2021).
16. Byrd, A. L., Belkaid, Y. & Segre, J. A. The Human Skin Microbiome. en. *Nature Reviews. Microbiology* **16**, 143–55 (2018).
17. Key, F. M. *et al.* On-Person Adaptive Evolution of Staphylococcus Aureus during Treatment for Atopic Dermatitis. en. *Cell Host & Microbe* **31**, 593–603 7 (2023).
18. Coll, F. *et al.* *The Mutational Landscape of Staphylococcus Aureus during Colonisation* fr. bioRxiv. 2023. <https://doi.org/10.1101/2023.12.08.570284>..
19. Leung, D., Berdyshev, E. & Goleva, E. Cutaneous barrier dysfunction in allergic diseases. ga. *J Allergy Clin Immunol* (June 6, 2020).
20. Naik, S. *et al.* Commensal-Dendritic-Cell Interaction Specifies a Unique Protective Skin Immune Signature. en. *Nature* **520**, 104–8 (2015).
21. Naik, S. *et al.* Compartmentalized Control of Skin Immunity by Resident Commensals. en. *Science* **337**, 1115–19 (2012).
22. Scharschmidt, T. C. *et al.* A Wave of Regulatory T Cells into Neonatal Skin Mediates Tolerance to Commensal Microbes. en. *Immunity* **43**, 1011–21 (2015).
23. Lecron, J. *et al.* IL-17 and IL-22 are pivotal cytokines to delay wound healing of infected skin. en. *Front Immunol* (Oct. 7, 2022).
24. Lee, J. *et al.* Interleukin-23 regulates interleukin-17 expression in wounds, and its inhibition accelerates diabetic wound healing through the alteration of macrophage polarization. en. *FASEB J* **Apr;32(4):2086–94** (2018).

25. Piewngam, P. Probiotic for pathogen-specific *Staphylococcus aureus* decolonisation in Thailand: a phase 2, double-blind, randomised, placebo-controlled trial. en. *The Lancet Microbe* **4**, 75–83 (2023).
26. Severn, M. M. *et al.* The Ubiquitous Human Skin Commensal *Staphylococcus Hominis* Protects against Opportunistic Pathogens. en. *mBio* **13**, 0093022 (2022).
27. Nabhani, A. & Ziad. A weaning reaction to microbiota is required for resistance to immunopathologies in the adult. en. *Immunity* **50**, 1276–1288 (2019).
28. Frasca, D. & Blomberg, B. B. Inflammaging decreases adaptive and innate immune responses in mice and humans. id. *Biogerontology* **17**, 7–19 (2016).
29. Fukushima, A. Genetic background determines susceptibility to experimental immune-mediated blepharoconjunctivitis: comparison of Balb/c and C57BL/6 mice. en. *Experimental eye research* **82**, 210–218 (2006).
30. Mu, Q., Tavella, V. J. & Luo, X. M. *Role of Lactobacillus Reuteri in Human Health and Diseases* en. *Frontiers in Microbiology* 9 (April): 315828. 2018.
31. Myles, I. A. *et al.* First-in-Human Topical Microbiome Transplantation with *Roseomonas Mucosa* for Atopic Dermatitis. en. *JCI Insight* **3**. <https://doi.org/10.1172/jci.insight.120608>. (2018).
32. Lunjani, N., Ahearn-Ford, S., Dube, F. S., Hlela, C. & O'Mahony, L. Mechanisms of Microbe-Immune System Dialogue within the Skin. en. *Genes and Immunity* **22**, 276–88 (2021).
33. Wickens, K. *et al.* A Protective Effect of *Lactobacillus Rhamnosus* HN001 against Eczema in the First 2 Years of Life Persists to Age 4 Years. en. *Clinical and Experimental Allergy: Journal of the British Society for Allergy and Clinical Immunology* **42**, 1071–79 (2012).
34. Drago, L., Toscano, M., Vecchi, E., Piconi, S. & Iemoli, E. Changing of Fecal Flora and Clinical Effect of *L. Salivarius* LS01 in Adults with Atopic Dermatitis. en. *Journal of Clinical Gastroenterology* **46 Suppl (October)**, 56–63 (2012).
35. Gueniche, A. *et al.* *Lactobacillus Paracasei* CNCM I-2116 (ST11) Inhibits Substance P-Induced Skin Inflammation and Accelerates Skin Barrier Function Recovery in Vitro. en. *European Journal of Dermatology: EJD* **20**, 731–37 (2010).
36. Han, Y. *et al.* A Randomized Trial of *Lactobacillus Plantarum* CJLP133 for the Treatment of Atopic Dermatitis. en. *Pediatric Allergy and Immunology: Official Publication of the European Society of Pediatric Allergy and Immunology* **23**, 667–73 (2012).
37. Sender, R., Fuchs, S. & Milo, R. Revised Estimates for the Number of Human and Bacteria Cells in the Body. en. *PLoS Biology* **14**, 1002533 (2016).

THIS PAGE INTENTIONALLY LEFT BLANK

Appendix I: Conventional probiotics and pre-exposure to *S. epidermidis* do not improve healing outcomes

Abstract

The second chapter in this work ("Commensal Skin Bacteria Exacerbate Inflammation and Delay Skin Barrier Repair") describes how commensal skin bacteria delay healing from tapestripping barrier damage and focuses on the host response to model commensal *S. epidermidis*. This appendix extends that work by including additional experimental systems used to investigate how prior exposure, timing, and mode of administration might change the host response to microbial exposure during tapestripping barrier damage. Additionally, I include preliminary data on the use of the conventional gut probiotic, *Limosilactobacillus reuteri* to improve skin barrier repair following tape-stripping damage.

A conventional gut probiotic does not significantly improve healing from barrier damage

L. reuteri is an exceptionally well-studied probiotic bacterium that is naturally found in human and animal gastrointestinal tracts [1]. Its ability to easily colonize the digestive tract of a range of hosts, survive low pH environments [2], be safely tolerated at dosages as high as 2.9×10^9 CFU [3] and produce antimicrobial molecules [4], has made it an attractive candidate as a probiotic treatment that broadly promotes health in the host [5]. On ex vivo skin, *L. reuteri* has been shown to reduce the production of pro-inflammatory cytokines IL-6 and IL-8, and displayed an antimicrobial effect against pathogenic Staphylococci on the skin [6].

To test whether the numerous immunomodulatory and antimicrobial effects of *L. reuteri* could improve skin healing, we applied 10^8 CFU of *L. reuteri* immediately following barrier damage and on a daily basis throughout the experiment. Mice exposed to *L. reuteri* did not display significantly improved healing over control animals (Fig. 1a-c, $p > 0.05$), although both Transepidermal Water Loss (TEWL) and severity score values suggested an improving trend. This trend was driven by improved healing within two days of barrier damage, at which point both TEWL and severity score values were more improved than controls (Fig. 1b-d, $p > 0.05$). The protective effect exerted by *L. reuteri* was thus minimal and confined to an early phase of healing.

Mice exposed to the skin commensal *Staphylococcus epidermidis* displayed delayed skin barrier repair and increased expression of the proinflammatory cytokine IL-17 relative to controls. We sought to determine whether the trend toward early improvement in healing seen in mice exposed to *L. reuteri* could be similarly mediated by decreased expression of IL-17 in the skin. However, we found that IL-17 expression in mice exposed to *L. reuteri* was not significantly decreased relative to controls (Fig. 1e), indicating that the response to *L. reuteri* was likely being mediated through other immune pathways.

Topical or oral pre-exposure to *L. reuteri* does not improve barrier repair

Previous work suggests that *L. reuteri* may improve host health via the upregulation of regulatory T-cells, a critical anti-inflammatory component of the adaptive immune system [7–10]. To stimulate the generation of microbe-specific adaptive T-cell responses, we altered our model to include a topical pre-exposure period, during which mice were exposed to 10^9 CFU of *L. reuteri* (Fig. 2a). Two weeks after the induction of the pre-exposure period, mice were depilated, their dorsal skin abraded by tape-stripping, and challenged with *L. reuteri*. Unlike the single challenge model, topical pre-exposure to *L. reuteri* did not improve skin barrier healing relative to controls by any metric (Fig. 2, b-e, $p > 0.2$).

As *L. reuteri* is not commonly considered a member of the natural skin flora but rather thought to colonize the digestive tract, it is most efficacious when ingested, even for the amelioration of skin disorders [7, 11]. To test whether oral pre-exposure to *L. reuteri* could improve healing in our barrier damage model, we fed mice 10^9 CFU of *L. reuteri* five days prior to tape-stripping (Fig. 2f). Mice were then subjected to barrier damage by tape-stripping and challenged with either PBS or *L. reuteri*. Oral pre-exposure to *L. reuteri* did not significantly improve skin barrier repair by any metric (Fig. 2g-j, $p > 0.08$), although mice that were exposed to *L. reuteri* twice (during pre-exposure and challenge) displayed a trend towards improvement by severity score. These data,

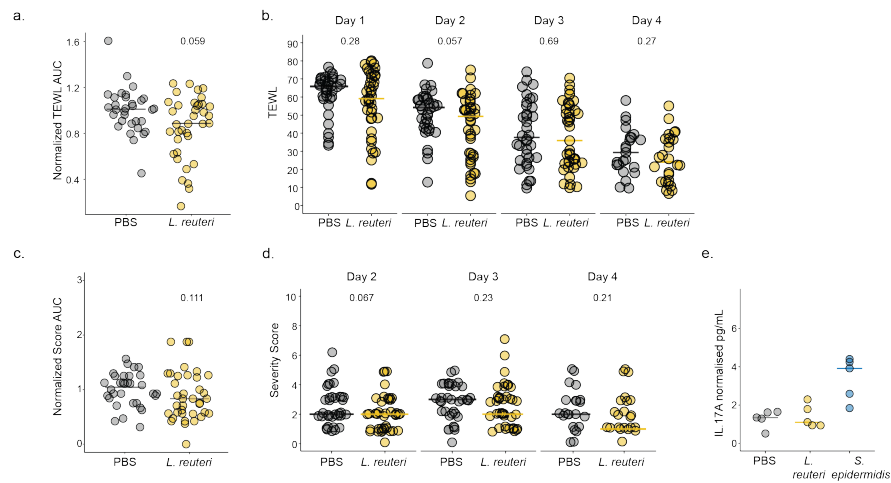


Figure 1: Exposure to conventional probiotic *L. reuteri* during barrier abrasion does not improve skin healing.

L. reuteri was applied to skin immediately following damage and daily thereafter. Healing was measured via TEWL and severity score, which are cumulatively reported as their areas under the curve (AUC) and normalized to control values. Throughout, points represent individual mice and lines represent median values. (a) Normalised TEWL AUC (PBS n=32, *L. reuteri* n = 37), showing slight improvement in mice exposed to *L. reuteri*. (b) Daily raw TEWL values that were used in the calculation of (a). (c) Normalized severity score AUC (PBS n=32, *L. reuteri* n = 37). (d) Daily raw severity score values that were used in the calculation of (c). (e) IL-17A expression in skin lysate.

in conjunction with data from our single-challenge model, suggest that further studies to validate and optimise the barrier recovery potential of Lactobacillus species are necessary.

***Staphylococcus epidermidis* delays barrier repair in a Staphylococcus-naive mouse model**

Staphylococci are common constituents of the skin microbiome where they reside as pathobionts. Although mouse and human skin are physiologically different [12], they both can support the colonization of pathobiont staphylococci - in humans, these include coagulase-negative staphylococci like *S. epidermidis* and *Staphylococcus capitis* [13], and in mice these include *Staphylococcus xylosum* [14]. This presence of Staphylococci in the skin microbiome during weaning has been shown to result in microbe-specific adaptive T-cell responses later in life [15].

The use of specific-pathogen free (SPF) mice colonized by *S. xylosum* in our barrier damage model lead us to hypothesize that the delay in barrier repair following exposure to *S. epidermidis* could be the result of early-life generated adaptive responses to Staphylococci. To avoid inciting such adaptive immune responses in our barrier damage model, we tested whether the exposure of staphylococci-naive mice to *S. epidermidis* would similarly result in delayed barrier repair. We used mice colonized with a defined gut microbiota (Altered Schaedler's Flora, ASF) comprised of eight strains of Lactobacillus, Bacteroides, and Clostridia [16]. Notably, these mice lack any Staphylococci in their microbiota, ensuring that experimental application of *S. epidermidis* would constitute primary exposure. Additionally, we sought to test whether adaptive responses to a novel commensal generated during secondary exposure could potentially ameliorate the observed delayed healing response.

ASF mice were shaved, depilated and exposed to either PBS or *S. epidermidis* in the absence of damage. Upon completion of a hair growth cycle (3-4 weeks), mice were once again shaved and depilated. The skin barrier was damaged by tape-stripping, and mice were exposed to either PBS (control) or *S. epidermidis* (Fig. 3a). Mice pre-exposed to PBS and challenged with *S. epidermidis* mimic "primary exposure", and mice both pre-exposed to and challenged with *S. epidermidis* mimic "secondary exposure". Both primary and secondary exposure groups demonstrated delayed healing over controls, and there were no significant differences in healing between groups (Fig. 3b-e, $p > 0.7$). These data confirm that the delayed healing seen in response to *S. epidermidis* in SPF mice was not a result of early-life adaptive responses generated against staphylococci.

Consistent with previous reports, primary exposure to *S. epidermidis* led to an expansion of CD8+ T-cells (Fig. 3f) [17]. While *S. epidermidis*-generated CD8+ T-cells are thought to be involved in the promotion of skin homeostasis and barrier repair in the context of full-thickness wounds [18, 19], here they appear to be a result of exposure to *S. epidermidis* during barrier damage. Interestingly, both primary and secondary exposure groups demonstrated a significant increase in the amount of $\gamma\delta$ -T cells in the skin. The expansion in $\gamma\delta$ -T cells in the secondary exposure group suggests that this arm of the adaptive immune response is involved in the generation of inflammatory memory to *S. epidermidis*. Together, these results suggest that the involvement of adaptive immune cells in response to *S. epidermidis* may hinder skin barrier repair, rather than promote it.

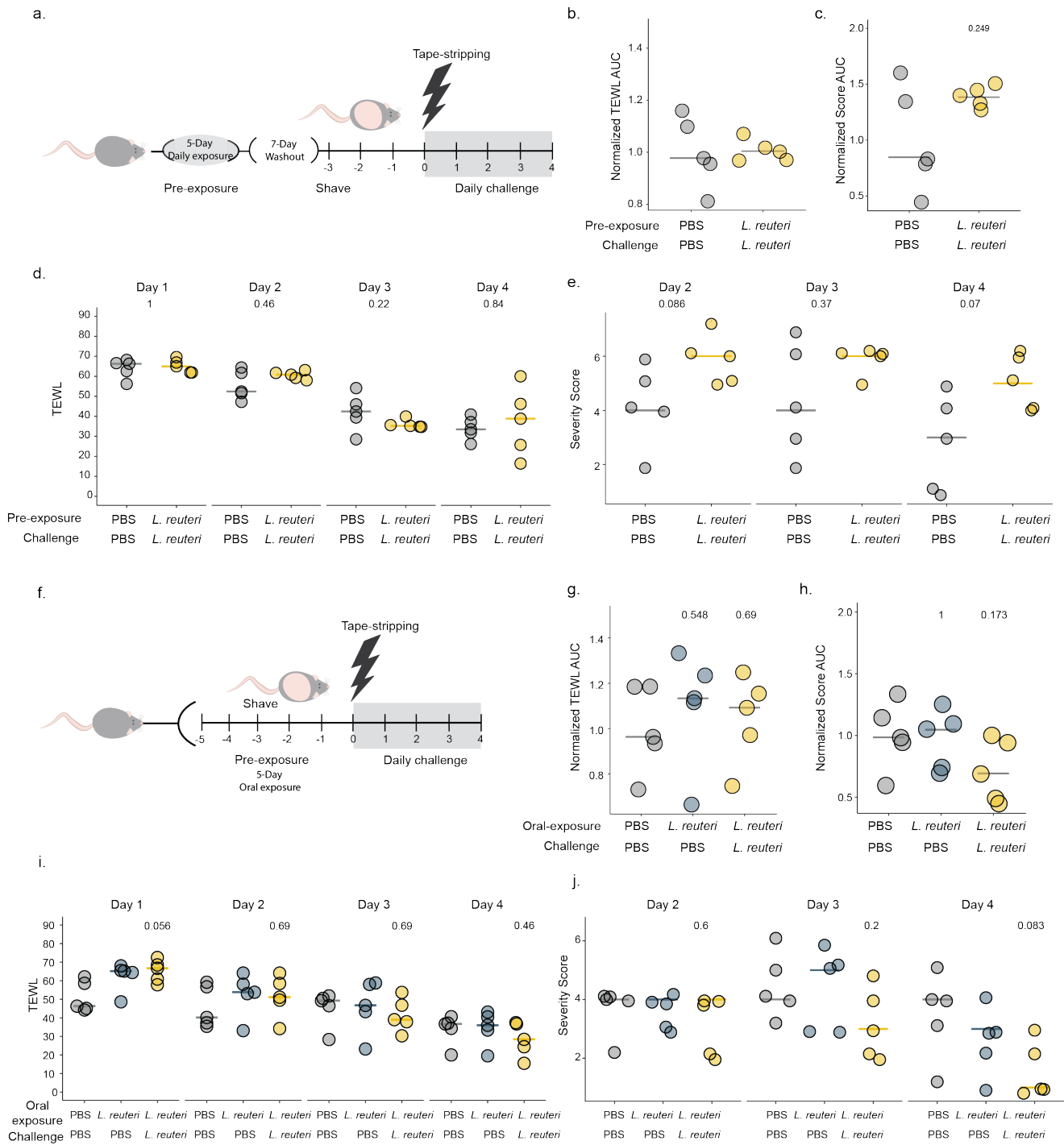


Figure 2: Pre-exposure to conventional probiotic *L. reuteri* does improve healing.
 (Continued on the following page.)

Figure 2: Pre-exposure to conventional probiotic *L. reuteri* does improve healing.

(a) Pre-exposure model diagram. Mice were exposed to 10^9 CFU of *L. reuteri* 12-14 days before skin barrier damage. Following a washout period, mice were tape-stripped and challenged with 10^8 CFU *L. reuteri* immediately following damage and daily thereafter. Healing was measured via TEWL and severity score, which are cumulatively reported as their areas under the curve (AUC) and normalised to control values. Throughout, points represent individual mice and lines represent median values. (b) Normalised TEWL AUC (n =5 for both groups) (c) Normalized Score AUC (n = 5 for both groups). (d-e) Daily raw TEWL and severity score values for mice pre-exposed to *L. reuteri* and controls (PBS). (f) Oral colonisation model diagram: mice were fed 10^8 CFU of *L. reuteri* every other day five times prior to barrier damage by tape-stripping. Mice were then depilated, tape-stripped and challenged with daily application of *L. reuteri* or PBS. Healing was measured via TEWL and severity score, which are cumulatively reported as their areas under the curve (AUC) and normalised to control values. (g-h) Normalised TEWL (n =5 for both groups) and severity score (n=5 for both groups) AUC for controls, mice fed *L. reuteri* and challenged with either *L. reuteri* or PBS. (i-j) Daily raw TEWL and severity score values for controls, mice fed *L. reuteri* and challenged with either *L. reuteri* or PBS.

Methods

ASF mice

7-9 week old C57Bl/6 male ASF mice were purchased from Taconic Biosciences (New York) and housed individually in ventilated cages in a specific pathogen free facility under the Division of Comparative Medicine at MIT. Mice were housed individually to limit any fighting behaviors that could affect the skin barrier. Mice were maintained on a 12h light-dark cycle at ambient humidity and given sterile food and water to limit exposure to external bacteria. All mouse experiments were conducted under protocols approved by MIT IACUC (protocol number: number 213-0000-585)

Bacterial cultures

L. reuteri was subcultured (1:100) from overnight cultures and grown to exponential phase in MRS media with 5% CO₂. Bacterial cells were pelleted and washed twice in PBS before being resuspended to a concentration of 10^9 CFU/mL. For oral and topical pre-exposure experiments, washed and resuspended overnight cultures were used to yield a higher cell density.

Topical pre-exposure

Mice were exposed to 10^9 CFU of bacterial cells resuspended in PBS. 100 μ L of bacterial cell suspension was pipetted on to the backs of anaesthetised mice and distributed across the dorsal skin using a sterile cotton swab.

Oral Pre-exposure

Mice were fed 10^8 CFU of bacterial cells resuspended in PBS in a 25 μ L volume every other day, for five total feedings. To avoid the stress and potential for damage from oral gavage, mice were

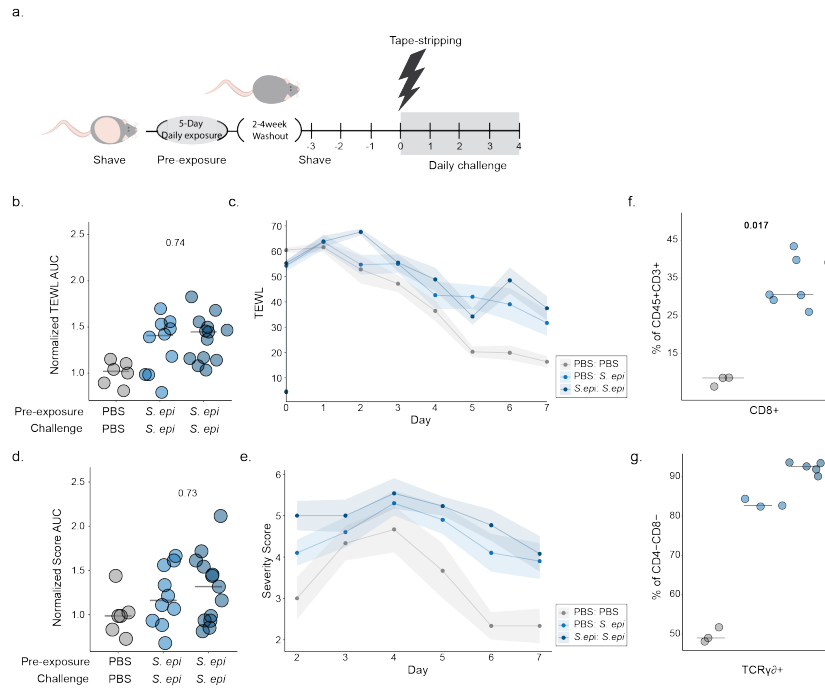


Figure 3: Pre-exposure to *S. epidermidis* does not improve healing in a Staphylococcus-naive mouse model. (a) diagrammatic representation of pre-exposure in ASF mice (b) Normalised TEWL AUC for both primary and secondary exposure showing no significant differences between groups. Throughout, points represent individual mice and lines represent median values. (c) Daily TEWL values. (d) Normalized severity score AUC for both primary and secondary exposure showing no significant differences between groups. (e) Daily severity score values. (f) CD8+ T-cells as a percentage of CD45+CD3+ T-cells (g) gd-T cells as a percentage of CD45+CD3+CD4-CD8- T-cells

restrained by scruffing and bacterial cell suspension was gently pipetted into the oral cavity.

References

1. Kandler, O., Stetter, K.-O. & Köhl, R. *Lactobacillus reuteri* sp. nov., a new species of heterofermentative lactobacilli. *Zentralblatt Für Bakteriologie: I. Abt. Originale C: Allgemeine, Angewandte Und Ökologische Mikrobiologie* **1**, 264–269 (1980).
2. Jacobsen, C. *et al.* Screening of Probiotic Activities of Forty-Seven Strains of *Lactobacillus* Spp. by in Vitro Techniques and Evaluation of the Colonization Ability of Five Selected Strains in Humans. en. *Applied and Environmental Microbiology* **65**, 4949–56 (1999).
3. Jones, M. L., Martoni, C. J., Pietro, E., Simon, R. R. & Prakash, S. Evaluation of Clinical Safety and Tolerance of a *Lactobacillus Reuteri* NCIMB 30242 Supplement Capsule: A Randomized Control Trial. en. *Regulatory Toxicology and Pharmacology: RTP* **63**, 313–20 (2012).
4. Toba, T., Samant, S., Yoshioka, E. & Itoh, T. Reuterin 6, a New Bacteriocin Produced by *Lactobacillus Reuteri* LA 6. en. *Letters in Applied Microbiology* **13**, 281–86 (1991).
5. Mu, Q., Tavella, V. J. & Luo, X. M. *Role of Lactobacillus Reuteri in Human Health and Diseases* en. *Frontiers in Microbiology* **9** (April): 315828. 2018.
6. Khmaladze, I., Butler, É., Fabre, S. & Gillbro, J. M. *Lactobacillus Reuteri* DSM 17938—A Comparative Study on the Effect of Probiotics and Lysates on Human Skin. en. *Experimental Dermatology* **28**, 822–28 (2019).
7. Kang, H.-J. *et al.* Probiotics-Derived Metabolite Ameliorates Skin Allergy by Promoting Differentiation of FOXP3 Regulatory T Cells. en. *The Journal of Allergy and Clinical Immunology* **147**, 1517–21 (2021).
8. Liu, Y., Fatheree, N. Y., Dingle, B. M., Tran, D. Q. & Rhoads, J. M. *Lactobacillus Reuteri* DSM 17938 Changes the Frequency of Foxp3+ Regulatory T Cells in the Intestine and Mesenteric Lymph Node in Experimental Necrotizing Enterocolitis. en. *PloS One* **8**, 56547 (2013).
9. Poutahidis, T. *et al.* Microbial Symbionts Accelerate Wound Healing via the Neuropeptide Hormone Oxytocin. en. *PloS One* **8**, 78898 (2013).
10. Poutahidis, T. *et al.* Microbial Reprogramming Inhibits Western Diet-Associated Obesity. af. *PloS One* **8**, 68596 (2013).
11. Kwon, H.-K. *et al.* Generation of Regulatory Dendritic Cells and CD4+Foxp3+ T Cells by Probiotics Administration Suppresses Immune Disorders. en. *Proceedings of the National Academy of Sciences of the United States of America* **107**, 2159–64 (2010).
12. Gerber, P. A. *et al.* The Top Skin-Associated Genes: A Comparative Analysis of Human and Mouse Skin Transcriptomes. en. *Biological Chemistry* **395**, 577–91 (2014).
13. Skaar, E. P. *Biogeography of the Genus Staphylococci on Human Skin* en. in *Proceedings of the National Academy of Sciences of the United States of America* (2023).
14. Battaglia, M. & Garrett-Sinha, L. A. *Staphylococcus Xylosus* and *Staphylococcus Aureus* as Commensals and Pathogens on Murine Skin. en. *Laboratory Animal Research* **39**, 18 (2023).
15. Leech, J. *et al.* Toxin-Triggered Interleukin-1 Receptor Signaling Enables Early-Life Discrimination of Pathogenic versus Commensal Skin Bacteria. en. *Cell Host Microbe* **809** (Dec. 2019).
16. Dewhirst, F. *et al.* Phylogeny of the Defined Murine Microbiota: Altered Schaedler Flora. en. *Applied and Environmental Microbiology* **65**, 3287–92 (1999).
17. Naik, S. *et al.* Compartmentalized Control of Skin Immunity by Resident Commensals. en. *Science* **337**, 1115–19 (2012).
18. Harrison, O. J. *et al.* Commensal-Specific T Cell Plasticity Promotes Rapid Tissue Adaptation to Injury. en. *Science* **363**. <https://doi.org/10.1126/science.aat6280>. (2019).
19. Linehan, J. L. *et al.* Non-Classical Immunity Controls Microbiota Impact on Skin Immunity and Tissue Repair. en. *Cell* **172**, 784–96 18 (2018).